

**FLASH PHOTOLYSIS GENERATION AND REACTIVITIES
OF BIPHENYLYLNITRENIUM IONS AND
PHENYLCYCLOHEXADIENYL CATIONS**

by

Dali Ren

A thesis submitted in conformity with the requirements for
the degree of Doctor of Philosophy
Department of Chemistry
University of Toronto

© Copyright by Dali Ren (1998)



**National Library
of Canada**

**Acquisitions and
Bibliographic Services**

**395 Wellington Street
Ottawa ON K1A 0N4
Canada**

**Bibliothèque nationale
du Canada**

**Acquisitions et
services bibliographiques**

**395, rue Wellington
Ottawa ON K1A 0N4
Canada**

Your file Votre référence

Our file Notre référence

The author has granted a non-exclusive licence allowing the National Library of Canada to reproduce, loan, distribute or sell copies of this thesis in microform, paper or electronic formats.

The author retains ownership of the copyright in this thesis. Neither the thesis nor substantial extracts from it may be printed or otherwise reproduced without the author's permission.

L'auteur a accordé une licence non exclusive permettant à la Bibliothèque nationale du Canada de reproduire, prêter, distribuer ou vendre des copies de cette thèse sous la forme de microfiche/film, de reproduction sur papier ou sur format électronique.

L'auteur conserve la propriété du droit d'auteur qui protège cette thèse. Ni la thèse ni des extraits substantiels de celle-ci ne doivent être imprimés ou autrement reproduits sans son autorisation.

0-612-35297-8

To My Mother

Flash Photolysis Generation and Reactivities of Biphenylnitrenium Ions and Phenylcyclohexadienyl Cations

Dali Ren, Ph.D. (1998)

Department of Chemistry, University of Toronto

Abstract

A series of substituted 4-azidobiphenyls have been subjected to flash photolysis irradiation in 20% acetonitrile:water. The corresponding 4-biphenylnitrenium ions are observed and first-order rate constants for their reactions with solvent (k_w) have been measured. The plot of the solvent reactivities for the X' -substituted derivatives *versus* σ^+ exhibit a poor correlation, with the points for the para π -electron donors deviating in the direction of requiring a more negative σ^+ value. The data are more satisfactorily fit to the two-parameter Yukawa-Tsuno equation; the parameter r^+ obtained for this fit is 2.8. This is similar to the situation that has been previously observed with benzylic-type carbenium ions. The conclusion is made that in their reaction with water, 4-biphenylnitrenium ions behave like benzyl cations bearing two additional stabilizing vinyl groups, i.e. as if they had the structure $\text{Ar-C}^+(\text{C}=\text{C})_2$.

The nitrenium ions are quenched by azide ion, 2'-deoxyguanosine (dG), and ethyl vinyl ether and second-order rate constants k_{Nu} for these reactions are measured. The plots of k_{Nu} *versus* k_w indicate that these quenching reactions approach the diffusion limit for the first two nucleophiles. The ratios k_{dG}/k_w for most of these nitrenium ions are larger than 10^3 M^{-1} , indicating a high selectivity for the nucleoside.

A 6,6-dimethyl-3-phenylcyclohexadienyl cation (**45**) has been generated in the ground state from three precursors in 20% acetonitrile:water: in the solvolysis of 6,6-dimethyl-3-phenylcyclohexa-2,4-dien-1-yl acetate (**46**) or from

the isomeric alcohols 4,4-dimethyl-1-phenylcyclohexa-2,5-dien-1-ol (**61**) and 6,6-dimethyl-1-phenylcyclohexa-2,4-dien-1-ol (**62**) under acidic conditions. Although attempts to detect the cation by flash photolysis of **46** and **61** were unsuccessful, a cation-like transient (**71**, $k_s = 6.92 \times 10^4 \text{ s}^{-1}$, $k_{az} = 5 \times 10^9 \text{ M}^{-1}\text{s}^{-1}$) has been observed by employing 4,4-dimethyl-1-(3',5'-dimethoxyphenyl)cyclohexa-2,5-dien-1-ol (**47**) as precursor. The overall analysis shows that the conjugated alcohol **62** is both the kinetic and thermodynamic product of the addition of water to **45**. These results are compared with ones for the 4-biphenylnitrenium ion (**15**), in terms of its cyclohexadienyl cation resonance contributors. **45** is slightly more stable than **15** in aqueous solutions. The two differ significantly in site preference of water addition as the kinetic product with **15** is the unconjugated alcohol. It is suggested that the electronegative nitrogen of **15** results in greater fraction of the positive charge being localized at the remote para carbon, so that is the site where water preferentially reacts.

Acknowledgments

I would like to thank my supervisor, Professor Robert A. McClelland, for his guidance, encouragement, and help throughout this project.

I would like to thank all members of our group during my stay in the university: Eddie Low, Pratima Ramlall, Thuy Van Pham, Addrian Davidse, Toufan Parman Low, Earl Macknight, John Matejovic, Mary-Jo Kahley, Cathy Love, Abid Ahmed, and Cristina Sanchez. We are a loving group just like a family. You guys made life in this lab warm and enjoyable and I love all of you.

I would also like to thank Dr. Timothy A. Gadosy who performed the 2'-deoxyguanosine quenching experiments, and Dina Ghobrial who carried out some HPLC and UV-Vis experiments of the cyclohexadienyl cations.

Thanks also go to Mr. Nick Plavac for the 400 MHz NMR spectra he ran for me and Dr. Alex Young for running the numerous MS spectra during the length of this project. I would also like to thank Dr. Vladimir Popic for his help in laser flash photolysis.

Special thanks to Henry Wang, who has been a close friend to me and my family all these years in Toronto, for letting me use his apartment as my writing place.

I would like to thank my mom for her willing to suffer one more Canada winter to take care of my son Jonah so that I can be worry free in the final days of the project. And finally I want to thank my wife Vivian for putting up with me during the period of writing the thesis and also for her perfect computer technical support.

Table of Contents

List of Tables

List of Figures

<u>Introduction</u>	1
1. The Electronic Structure, Formation, and Reactions of Arylnitrenium Ions	1
1.1. The electronic structure	1
1.2. Formation and reactions	3
2. Arylnitrenium Ions and Carcinogenicity of Aromatic Amines	7
2.1. Carcinogenicity and metabolic activation of aromatic amines	7
2.2. Nitrenium ions as reactive intermediates formed in the solvolysis of ester derivatives of carcinogenic N-arylhydroxylamines	10
3. Laser Flash Photolysis (LFP) Study of Arylnitrenium Ions	15
3.1. LFP generation of arylnitrenium ions	16
3.2. Reactivity of nitrenium ions toward water and added nucleophiles	23
4. Nitrenium Ions or Iminocyclohexadienyl Cations	28
5. Scope of the Project	30

<u>Results and Discussion</u>	32
Section 1. LFP Study of Substituted 4-Biphenylnitrenium Ions	32
1.1. Preparation of 4-azidobiaryls	32
1.2. Laser flash photolysis of 4-azidobiaryls	40
1.3. Flash photolysis of 4-azido-4'-(N,N-dimethylamino)biphenyl	51
1.4. Reactivity of X'-substituted-4-biphenylnitrenium ions toward solvent and added nucleophiles	54
1.4.1. Absolute rate constants for water and substituent effect on solvent reactivity	54
1.4.2. Reactivity toward other nucleophiles	61
(1) Azide ion	61
(2) Guanine	64
(3) Ethyl vinyl ether	71
1.5. Nitrenium ions and carcinogenicity of aromatic amines	74
Section 2. Generation of 6,6-Dimethyl-3-phenylcyclohexadienyl Cations and Comparison with the Carbenium Forms of 4-Biphenylnitrenium Ion	75
2.1. Preparation of precursors	75
2.2. Formation of the 6,6-dimethyl-3-phenylcyclohexadienyl cation in aqueous solutions	82
2.2.1. Solvolysis of the acetate 46	83
2.2.2. Acid catalyzed reactions of the alcohols 61 and 62	84

2.3. Generation of 6,6-dimethyl-3-phenylcyclohexadienyl cation by Laser flash photolysis	91
2.3.1. Laser flash photolysis of the alcohol 47	91
2.3.2. Comparison with 4-biphenylnitrenium ion	97
<u>Experimental</u>	103
1. Materials	103
2. General methods	103
2.1. Laser flash photolysis	103
2.2. HPLC	107
2.3. UV spectroscopic studies	107
2.4. NMR and Mass spectroscopy	107
3. Syntheses	108
3.1. Synthesis of 4-azidobiaryl compounds	108
3.1.1. Preparation of aryltin compounds	108
3.1.2. Preparation of arylboronic acids	109
3.1.3. Synthesis of 4-aminobiaryls	110
(1) By the coupling of aryltin compounds with 4-nitrophenyl triflate	110
(2) By the coupling of arylboronic acids with 4- bromoaniline	112
3.1.4. Synthesis of 4-azidobiaryls	114

3.2. Synthesis of precursors for the cyclohexadienyl cations	116
4. LFP measurements of second-order rate constants for reactions of nitrenium ions with added nucleophiles	119
4.1. Azide ion	120
4.2. Ethyl vinyl ether	129
<u>References</u>	137

List of Tables

Table 1.	Absolute rate constants for nitrenium ions reacting with solvent and azide ion	19
Table 2.	Selectivities and absolute rate constants for the reaction of nitrenium ions with 2'-deoxyguanosine (dG) and 2'-deoxyguanosine-5'-phosphate	25
Table 3.	Absolute rate constants for the reaction of carbenium ions and nitrenium ions with vinyl ethers	26
Table 4.	High resolution EI mass spectrum peaks for 4-azidobiaryls	37
Table 5.	Absorption maxima and cation:non-cation ratios expressed as relative optical densities for 4-biphenylnitrenium ions 44 in 20% acetonitrile:water	47
Table 6.	Rate constants k_w and k_{az} for nitrenium ions 44 at 20°C in 20% and 40% acetonitrile:water	50
Table 7.	A comparison of the rate constants k_w for selected triarylmethyl cations and 4-biphenylnitrenium ions	53
Table 8.	Parameters for two-parameter analysis of rate constants for solvent addition to benzylic-type cations 53-55 and nitrenium ions 44	58
Table 9.	Absolute rate constants for nitrenium ions 44 reacting with 2'-deoxyguanosine (dG) in 20% acetonitrile:water	65
Table 10.	Percentages of nitrenium ions that react with 2'-deoxyguanosine to form the C8 adducts in 1 mM aqueous solution of the nucleoside	70

Table 11.	Absolute rate constants for nitrenium ions 44 reacting with ethyl vinyl ether in 20% acetonitrile:water	72
Table 12.	Observed rate constants for decay of the transient at 440 nm generated upon irradiation of the alcohol 47 in 20% acetonitrile:water in the presence of azide ion	96
Table 13.	The values of k_w and k_{az} for the cyclohexadienyl cation 71 , and <i>meta</i> -methoxy-substituted 4-biphenylnitrenium ions and triphenylmethyl cations	98
Table 14.	Absolute rate constants and equilibrium constants for reactions of the cyclohexadienyl cation 45	99
Table 15.	Observed first-order rate constants for the decay of 4'-methoxy-4-biphenylnitrenium ion in the presence of azide ion	120
Table 16.	Observed first-order rate constants for the decay of 4'-methyl-4-biphenylnitrenium ion in the presence of azide ion	121
Table 17.	Observed first-order rate constants for the decay of 4'-fluoro-4-biphenylnitrenium ion in the presence of azide ion	122
Table 18.	Observed first-order rate constants for the decay of 3'-methyl-4-biphenylnitrenium ion in the presence of azide ion	123
Table 19.	Observed first-order rate constants for the decay of 3'-methoxy-4-biphenylnitrenium ion in the presence of azide ion	124

Table 20.	Observed first-order rate constants for the decay of 4'-chloro-4-biphenylnitrenium ion in the presence of azide ion	125
Table 21.	Observed first-order rate constants for the decay of 3'-chloro-4-biphenylnitrenium ion in the presence of azide ion	126
Table 22.	Observed first-order rate constants for the decay of 3',5'-dimethoxy-4-biphenylnitrenium ion in the presence of azide ion	127
Table 23.	Observed first-order rate constants for the decay of 2,6-dimethyl-4-biphenylnitrenium ion in the presence of azide ion	128
Table 24.	Observed first-order rate constants for the decay of 4'-methoxy-4-biphenylnitrenium ion in the presence of ethyl vinyl ether	129
Table 25.	Observed first-order rate constants for the decay of 4'-methyl-4-biphenylnitrenium ion in the presence of ethyl vinyl ether	130
Table 26.	Observed first-order rate constants for the decay of 4'-fluoro-4-biphenylnitrenium ion in the presence of ethyl vinyl ether	131
Table 27.	Observed first-order rate constants for the decay of 3'-methyl-4-biphenylnitrenium ion in the presence of ethyl vinyl ether	132

Table 28.	Observed first-order rate constants for the decay of 3'-methoxy-4-biphenylnitrenium ion in the presence of ethyl vinyl ether	133
Table 29.	Observed first-order rate constants for the decay of 4'-chloro-4-biphenylnitrenium ion in the presence of ethyl vinyl ether	134
Table 30.	Observed first-order rate constants for the decay of 3'-chloro-4-biphenylnitrenium ion in the presence of ethyl vinyl ether	135
Table 31.	Observed first-order rate constants for the decay of 2,6-dimethyl-4-biphenylnitrenium ion in the presence of ethyl vinyl ether	136

List of Figures

Figure 1.	Singlet and triplet nitrenium ions	2
Figure 2.	Transient spectra obtained upon 248-nm irradiation of 13a in 0.5 M NaClO ₄ aqueous solution containing 5% acetonitrile.	18
Figure 3.	Transient spectra of the 4-biphenylnitrenium ion obtained by irradiation of 50 μM 4-azidobiphenyl in 1:1 acetate buffer (2 mM) in 20% acetonitrile: water	22
Figure 4.	500 MHz ¹ H NMR for 4-amino-4'-fluorobiphenyl	38
Figure 5.	500 MHz ¹ H NMR for 4-azido-4'-fluorobiphenyl	39
Figure 6.	Transient spectra generated upon 248-nm irradiation of 4-azido-4'-methoxybiphenyl in 40% acetonitrile:water	42
Figure 7.	Transient spectra generated upon 248-nm irradiation of 4-azido-3'-methoxybiphenyl in 20% acetonitrile:water	42
Figure 8.	Transient spectra generated upon 248-nm irradiation of 4-azido-4'-methylbiphenyl in 20% acetonitrile:water	43
Figure 9.	Transient spectra generated upon 248-nm irradiation of 4-azido-3'-methylbiphenyl in 20% acetonitrile:water	43
Figure 10.	Transient spectra generated upon 248-nm irradiation of 4-azido-3,5-dimethylbiphenyl in 20% acetonitrile:water	44
Figure 11.	Transient spectra generated upon 248-nm irradiation of 4-azido-4'-fluorobiphenyl in 20% acetonitrile:water	44
Figure 12.	Transient spectra generated upon 248-nm irradiation of 4-azido-4'-chlorobiphenyl in 20% acetonitrile:water	45

Figure 13. Transient spectra generated upon 248-nm irradiation of 4-azido-3'-chlorobiphenyl in 20% acetonitrile:water	45
Figure 14. Time-resolved transient spectra generated upon 248-nm irradiation of 4-azido-3'-chlorobiphenyl in 20% acetonitrile:water	46
Figure 15. Transient spectra generated upon 248-nm irradiation of 4-azido-4'-(N,N-dimethyl)biphenyl in 20% acetonitrile:water	53
Figure 16. Linear free energy correlation for X'-substituted-4-biphenylnitrenium ions 44	59
Figure 17. Linear correlation of $\log k_w$ for the nitrenium ions 44 and appropriately substituted triarylmethyl cations ($\text{XC}_6\text{H}_4\text{C}^+\text{Ph}_2$)	60
Figure 18. Variation in k_{az} as a function of the rate constants k_s for decay of nitrenium ions, diarylmethyl and triarylmethyl cations in the same solvent	63
Figure 19. Variation in k_{dG} and k_{az} in 20% acetonitrile for nitrenium ions as a function of k_w for decay in the same solvent	66
Figure 20. Correlation of $\log k_2(\text{CH}_2=\text{CHOEt})$ and $\log k_w$ for the nitrenium ions 44 .	73
Figure 21. ^1H NMR spectrum of 4,4-dimethyl-1-phenylcyclohexa-2,5-dien-1-ol (61)	79
Figure 22. ^1H NMR spectrum of 6,6-dimethyl-3-phenylcyclohexa-2,4-dien-1-ol (62)	80
Figure 23. ^1H NMR spectrum of 6,6-dimethyl-3-phenylcyclohexa-2,4-dien-1-yl acetate (46)	81

Figure 24.	The correlation of $\log k_{\text{on}}$ of acetate 46 with the solvent polarity parameter Y .	84
Figure 25.	UV spectra observed with 4,4-dimethyl-1-phenylcyclohexa-2,5-dien-1-ol (61) (8×10^{-5} M) in acetic acid buffers (pH 5-6) in 20% acetonitrile:water	88
Figure 26.	HPLC Chromatogram and product identifications for acid catalyzed reactions of the unconjugated alcohol 61 in 20% acetonitrile	89
Figure 27.	Fraction of starting material 61 , and the two products 62 and 64 for a solution of the unconjugated alcohol 61 in 20% acetonitrile	90
Figure 28.	Transient absorption spectra obtained by 248-nm irradiation of 0.2 mM solution of the alcohol 47 in 20% acetonitrile:water	94
Figure 29.	The change of optical density at 440 nm as a function of time upon irradiation of the alcohol 47 at 248 nm in 20% acetonitrile:water	95
Figure 30.	The dependence of the observed rate constant for decay of the transient at 440 nm as a function of the concentration of sodium azide	96
Figure 31.	Comparison of rate constants (s^{-1} , 20-25°C) for the addition of water to cyclohexadienyl cations	100
Figure 32.	Free energy changes for the isomerization of cyclohexadienols. Calculated values are based on the AM1 method	101

Figure 33.	Schematic diagram of nanosecond laser flash photolysis apparatus.	105
Figure 34.	A typical trace of the exponential decay for a transient at 460 nm	106
Figure 35.	Trace of the signal after laser flash	106
Figure 36.	Relationship between the observed first-order rate constants for the decay of 4'-methoxy-4-biphenylnitrenium ion and the concentration of azide ion	120
Figure 37.	Relationship between the observed first-order rate constants for the decay of 4'-methyl-4-biphenylnitrenium ion and the concentration of azide ion	121
Figure 38.	Relationship between the observed first-order rate constants for the decay of 4'-fluoro-4-biphenylnitrenium ion and the concentration of azide ion	122
Figure 39.	Relationship between the observed first-order rate constants for the decay of 3'-methyl-4-biphenylnitrenium ion and the concentration of azide ion	123
Figure 40.	Relationship between the observed first-order rate constants for the decay of 3'-methoxy-4-biphenylnitrenium ion and the concentration of azide ion	124
Figure 41.	Relationship between the observed first-order rate constants for the decay of 4'-chloro-4-biphenylnitrenium ion and the concentration of azide ion	125
Figure 42.	Relationship between the observed first-order rate constants for the decay of 3'-chloro-4-biphenylnitrenium ion and the concentration of azide ion	126

Figure 43.	Relationship between the observed first-order rate constants for decay of 3',5'-dimethoxy-4-biphenylnitrenium ion and the concentration of azide ion	127
Figure 44.	Relationship between the observed first-order rate constants for decay of 2,6-dimethyl-4-biphenylnitrenium ion and the concentration of azide ion	128
Figure 45.	Relationship between the observed first-order rate constants for the decay of 4'-methoxy-4-biphenylnitrenium ion and the concentration of ethyl vinyl ether	129
Figure 46.	Relationship between the observed first-order rate constants for the decay of 4'-methyl-4-biphenylnitrenium ion and the concentration of ethyl vinyl ether	130
Figure 47.	Relationship between the observed first-order rate constants for the decay of 4'-fluoro-4-biphenylnitrenium ion and the concentration of ethyl vinyl ether	131
Figure 48.	Relationship between the observed first-order rate constants for the decay of 3'-methyl-4-biphenylnitrenium ion and the concentration of ethyl vinyl ether	132
Figure 49.	Relationship between the observed first-order rate constants for the decay of 3'-methoxy-4-biphenylnitrenium ion and the concentration of ethyl vinyl ether	133
Figure 50.	Relationship between the observed first-order rate constants for the decay of 4'-chloro-4-biphenylnitrenium ion and the concentration of ethyl vinyl ether	134
Figure 51.	Relationship between the observed first-order rate constants for the decay of 3'-chloro-4-biphenylnitrenium ion and the concentration of ethyl vinyl ether	135

Figure 52. Relationship between the observed first-order rate constants for the decay of 2,6-dimethyl-4-biphenylnitrenium ion and the concentration of ethyl vinyl ether

136

INTRODUCTION

The past two decades have seen a great amount of activity in the study of the chemistry of nitrenium ions. The interest in this area is mainly due to the important role of these species in the carcinogenic process of aromatic amines and amides.¹ It has been generally accepted that nitrenium ions are formed in the metabolism of aromatic amines, and that these reactive intermediates are responsible for the initiation of carcinogenesis by reacting with nucleophilic residues of critical cellular components (e.g., nucleic acid and proteins).¹⁻⁵ While the genetic consequences of such reactions are extremely complex and only poorly understood,^{1,3} it seems reasonable to expect that the reactivities of different aryl nitrenium ions will be reflected in some way in their biological activities.¹ Studies of the reactivity of nitrenium ions may thus be very valuable for understanding arylamine carcinogenesis and, possibly, for developing new anti-cancer drugs.

1. The Electronic Structure, Formation and Reactions of Aryl Nitrenium Ions

1.1. The Electronic Structure of Aryl Nitrenium Ions

Nitrenium ions⁶⁻¹⁰ are cationic intermediates that contain a divalent, positively charged nitrogen. Nitrenium ions are isoelectronic with carbenes and nitrenes. Like these neutral electron species, nitrenium ions have two non-bonding electrons on the nitrogen atom. These electrons could be spin paired or unpaired, and consequently, nitrenium ions can exist either as singlets or triplets (Figure 1).

Both theory^{11,12} and sophisticated gas phase experiments¹³ indicate that the simplest nitrenium ion, NH_2^+ , is a ground state triplet with a singlet-triplet energy gap of ca. +30 kcal/mol. However, for phenyl- and most simple aryl nitrenium ions

semiempirical,¹⁴⁻¹⁷ *ab initio*,^{15,18,19} and density functional theory (DFT)¹⁹ all predict a singlet ground state. The DFT calculations predict the singlet phenylnitrenium ion is 17.7 kcal/mol more stable than the triplet ion, and the *ab initio* calculations give qualitatively similar values. Both singlet and triplet arylnitrenium ions are stabilized through transfer of π -electron density from the phenyl substituent to the nitrogen atom, but this effect is more manifest in the singlet than it is in the triplet since the p orbital in the singlet state is empty and hence serves as a better π -acceptor. It can then be predicted that π -donor substituents on the aromatic ring should further stabilize the singlet relative to the triplet. Likewise π -acceptors should stabilize the triplet relative to the singlet.¹⁵

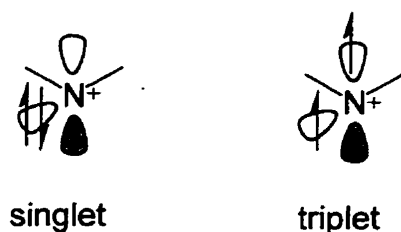
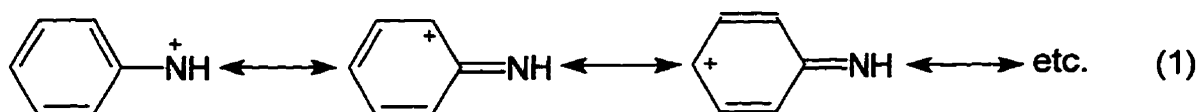


Figure 1. Singlet and triplet nitrenium ions.

Based on the above predictions, the Falvey group has generated a ground state triplet nitrenium ion — the *p*-nitrophenyl nitrenium ion by laser flash photolysis of an anthranilium salt substituted by an electron-withdrawing nitro group.²⁰ An experimental method has also been suggested to distinguish singlet and triplet: singlet nitrenium ions react with nucleophiles to give adducts, while triplet nitrenium ions react with hydrogen atom donors to give amines. It seems that the majority of arylnitrenium ions are singlets because they do react with nucleophiles to form adducts.

The greater electronegativity of nitrogen compared with carbon suggests that there should be considerable charge delocalization to the aromatic ring. In an MNDO study by Ford and Scribner,¹⁴ phenylnitrenium ion was calculated to be

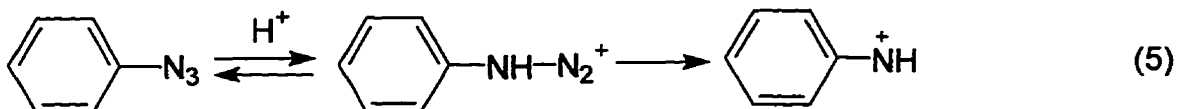
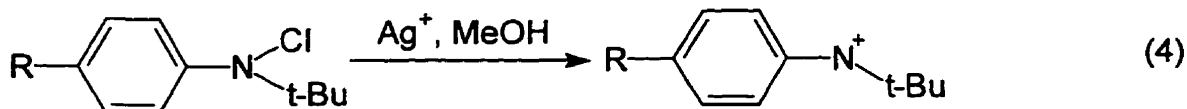
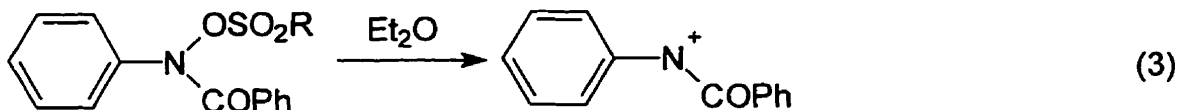
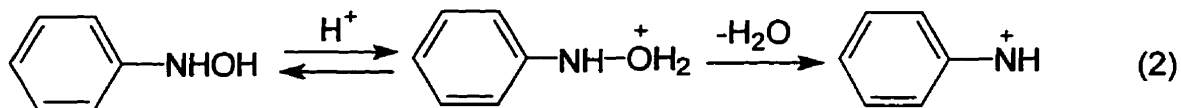
planar with an N-H bond angle of 116.9° and with the positive charge delocalized very extensively to the *ortho* and the *para* positions, mainly the latter. This calculation suggested that the nitrogen atom carries less than 20% of the charge in the ground state. These results indicate that there are significant contributions from carbenium resonance structures.



1.2. Formation and Reactions of Arylnitrenium Ions

Nitrenium ions have been generated in the ground state mainly by heterolytic cleavage of an N-X bond.

Examples of such reactions are those involving protonated N-arylhydroxylamines (eq. 2),^{10,21-23} esters of N-arylhydroxylamines (eq. 3), N-haloamines (eq. 4),^{24,25} and protonated aryl azides (eq. 5).²⁶⁻³¹



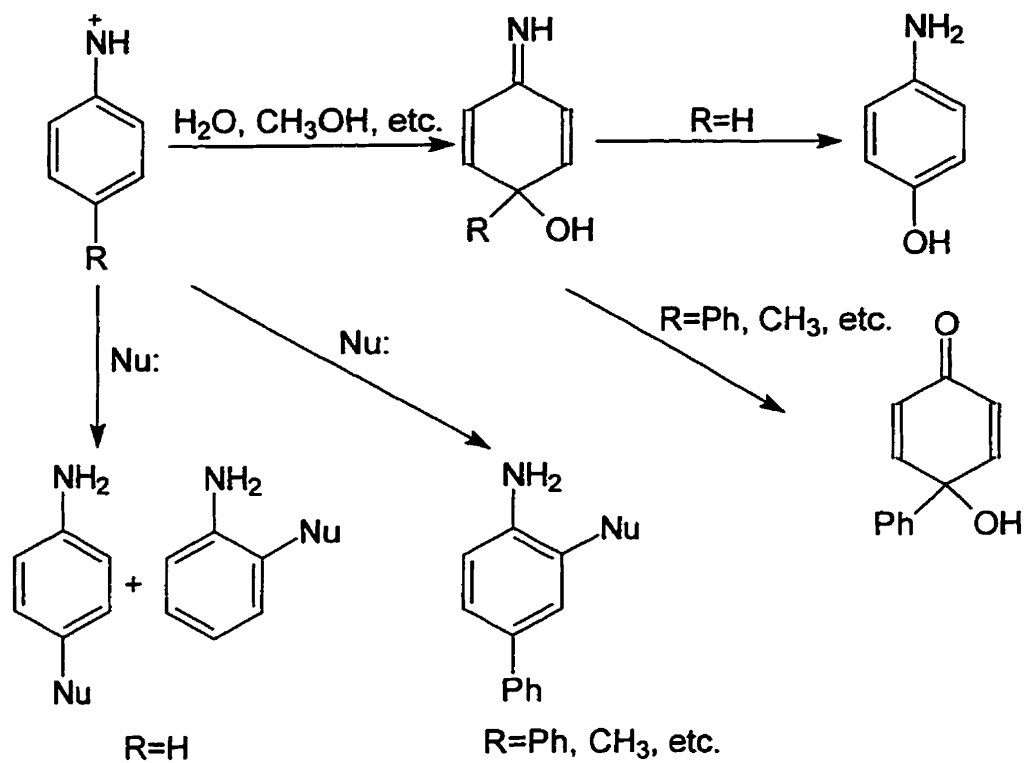
Various criteria were employed to establish the presence of the nitrenium ion intermediates. These included the analysis of final reaction products, especially in the presence of trapping nucleophiles, and the observation of large negative ρ values in kinetic studies.²¹⁻³⁰ There were also reports of aryl nitrenium ion lifetimes determined by competition kinetics experiments, indicating that free aryl nitrenium ions are formed as intermediates in these reactions.^{32,33}

Reactions of aryl nitrenium ions with nucleophiles are more complicated than those of the analogous carbocations. Whereas aryl carbenium ions normally react with nucleophiles at the carbon external to the ring, aryl nitrenium ions react with many nucleophiles preferentially at ring positions *ortho* and *para* to the nitrogen. This is usually attributed to the extensive charge delocalization from the nitrogen into the phenyl ring which makes the ring susceptible to nucleophilic attack.^{24,25} Substitution at the nitrogen is also observed, for example, when aromatic hydrocarbons or alkenes react with aryl nitrenium ions in specific media.

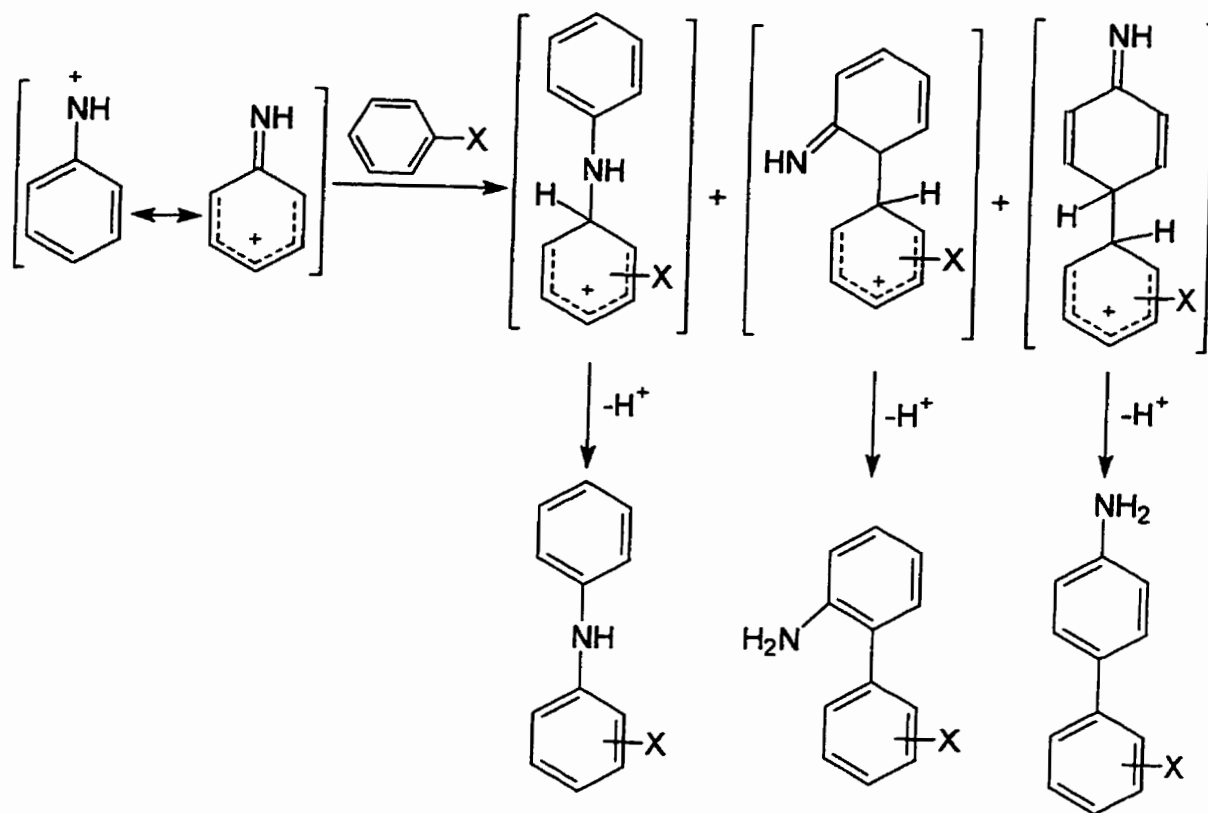
As shown in Scheme 1, solvent nucleophiles such as water and methanol react mainly with the *para* carbon.^{6,9,24} In cases where there is no *para* substituent ($R = H$), rapid tautomerization gives *p*-substituted anilines. In cases such as the 4-biphenyl system where this tautomerization is blocked, the imine can be observed but it is not stable. Several reactions occur, including imine hydrolysis and migration of R or OH to an adjacent carbon. External nucleophiles such as chloride and azide react at both *ortho* and *para* positions, except when the *para* position is blocked, where the reaction occurs exclusively at the *ortho* position.

Carbon nucleophiles such as alkenes and aromatic hydrocarbons can react with aryl nitrenium ions at both the external nitrogen and at the carbons in the ring. For example, aryl nitrenium ions formed from aryl azide in the presence of trifluoroacetic acid (TFA) or trifluoromethanesulfonic acid (TFSA) react with aromatic compounds to give both diarylamines (N-substitution products) and aminobiphenyls (C-substitution products),²⁷⁻³¹ as shown in Scheme 2. The product ratios are dependent on the nature of the acid.

Scheme 1



Scheme 2

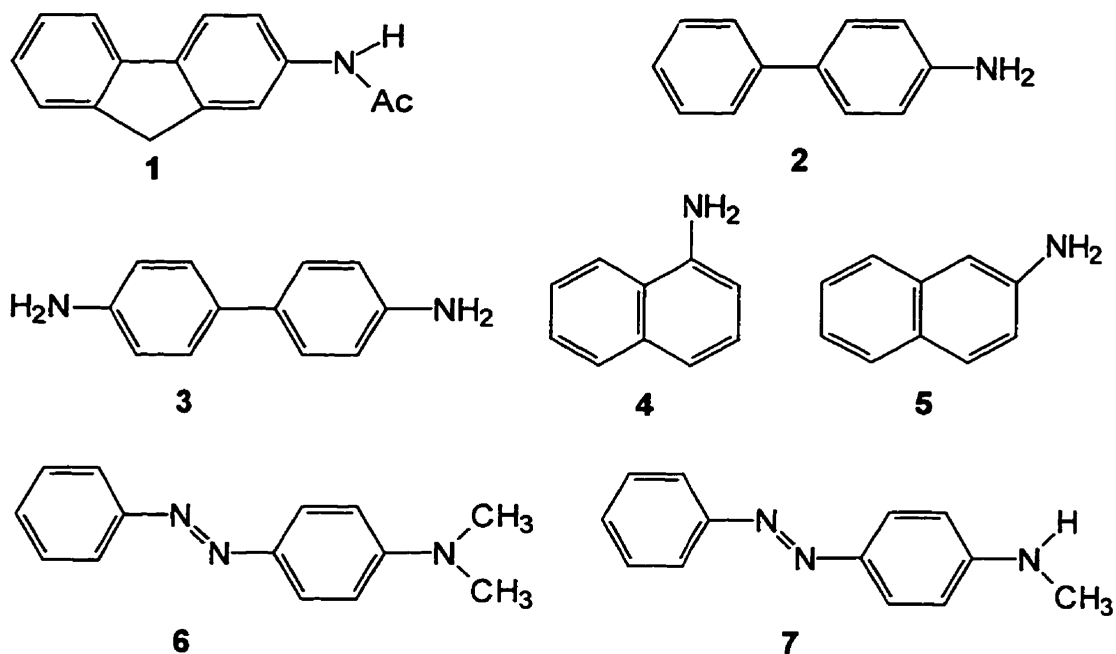


2. Arylnitrenium Ions and Carcinogenicity of Aromatic Amines

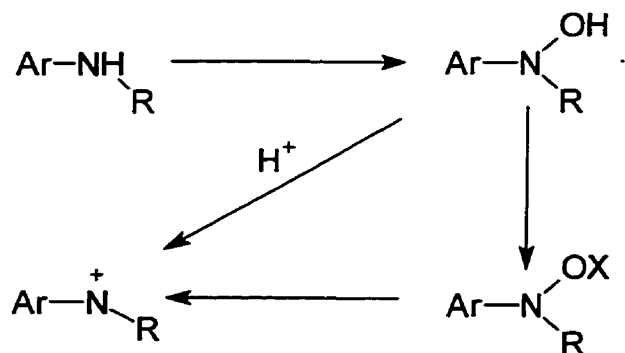
2.1. Carcinogenicity and Metabolic Activation of Aromatic Amines

Aromatic amines and amides constitute an extremely important class of chemical carcinogens. They are valuable chemicals in many areas of industry and research, especially as intermediates in the dyestuff and pharmaceutical industries.³ A number of these compounds have been identified as carcinogens both in animal experiments and in humans. Aromatic amines usually induce tumors at organs such as liver, intestine, or urinary bladder.¹ Compounds such as 4-aminobiphenyl (2), benzidine (3), 1-naphthylamine (4), and 2-naphthylamine (5) are all known to induce bladder cancer in humans. The aminoazo dyes such as N,N-dimethyl-4-aminoazobenzene (6) and N-methyl-4-aminoazobenzene are hepatocarcinogens.^{1,3-5} Structures of these compounds and that of the model compound 2-acetylaminofluorene (1) are shown in Scheme 3. The carcinogenicity of these compounds is partly dependent on their structures and two factors are important: (1) the type of aromatic system, and (2) substituents on the amino nitrogen and on the aromatic rings.^{1,3}

Studies on a variety of chemical carcinogens have demonstrated that their ultimate carcinogenic forms are strong electrophiles, formed, with most chemical carcinogens, as a result of biological metabolism.⁴ Aromatic amine carcinogens, too, need metabolic activation; the proposed pathways are shown in Scheme 4.¹ A prerequisite for carcinogenicity for this group of compounds is N-hydroxylation; this reaction may be followed by esterification of the hydroxyl group in some but not all cases. The ester intermediate is not stable and breaks down to a nitrenium ion electrophile that interacts with the tissues.³⁴ Acidic tissue may convert the hydroxylamine directly to the nitrenium ion, through an H⁺-catalyzed cleavage.



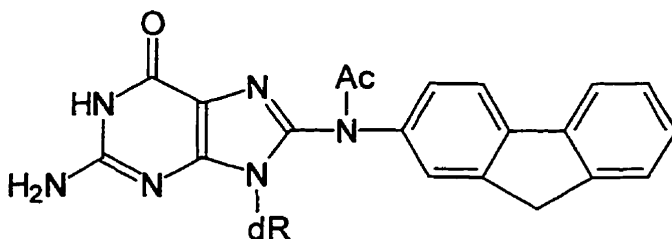
Scheme 3. 1, 2-acetylaminofluorene; 2, 4-aminobiphenyl; 3, benzidine; 4, 1-naphthylamine; 5, 2-naphthylamine; 6, N,N-dimethyl-4-aminoazobenzene; 7, N-methyl-4-aminoazobenzene.



Scheme 4. Metabolic pathways of aromatic amines. Ar = aryl group, R = H or COCH_3 , X = COCH_3 , SO_3^- , etc.

The N-oxidation is carried out by cytochrome P-450 and flavin-containing monooxygenase in liver microsomes.³⁵ This N-hydroxylation step is of unique importance in the activation of an aromatic amine to its ultimate carcinogenic form, since derivatives of the N-hydroxy compounds have sufficient chemical reactivity to react nonenzymically with cellular constituents.

The N-arylhydroxylamines are converted to ultimate carcinogens either through conjugation with sulfuric acid, acetic acid, or glucuronic acid or sometimes through protonation under acidic conditions. Evidence that esters of N-arylhydroxylamines and N-hydroxamic acids are the reactive and ultimate carcinogenic metabolites came from the discovery that these esters can react nonenzymatically under physiological conditions with cellular constituents such as protein or nucleic acids. The products of such reactions are covalently bonded adducts identical to the adducts released from the tissues of animals given the parent carcinogens.³⁶⁻³⁸ A prominent type of aromatic amine binding to DNA involves the N-substitution at C-8 of the guanine residues of DNA.³⁹ For example, approximately 80% of the residues containing 2-acetylaminofluorene in rat liver DNA have been identified as N-2-(8-deoxyguanosyl)acetylaminofluorene (**8**). Analogous adducts are found in model studies in which the esters of N-arylhydroxylamines undergo solvolysis in the presence of guanine derivatives.^{40,41}



8 (dR = 2'-deoxyribose)

2.2. Nitrenium ions as reactive intermediates formed in the solvolysis of ester derivatives of carcinogenic N-arylhydroxylamines

From a study of the kinetics of the decomposition of N-acetoxy-N-arylacetamides in aqueous media, Scribner et al. proposed a mechanism involving heterolytic cleavage of the N-O bond to produce a nitrenium ion as a reactive intermediate. This electrophile was suggested to attack DNA or its nucleophilic constituents to form covalently bonded adducts.⁴² This mechanism was consistent with the structures of adducts formed. However, direct evidence was lacking.

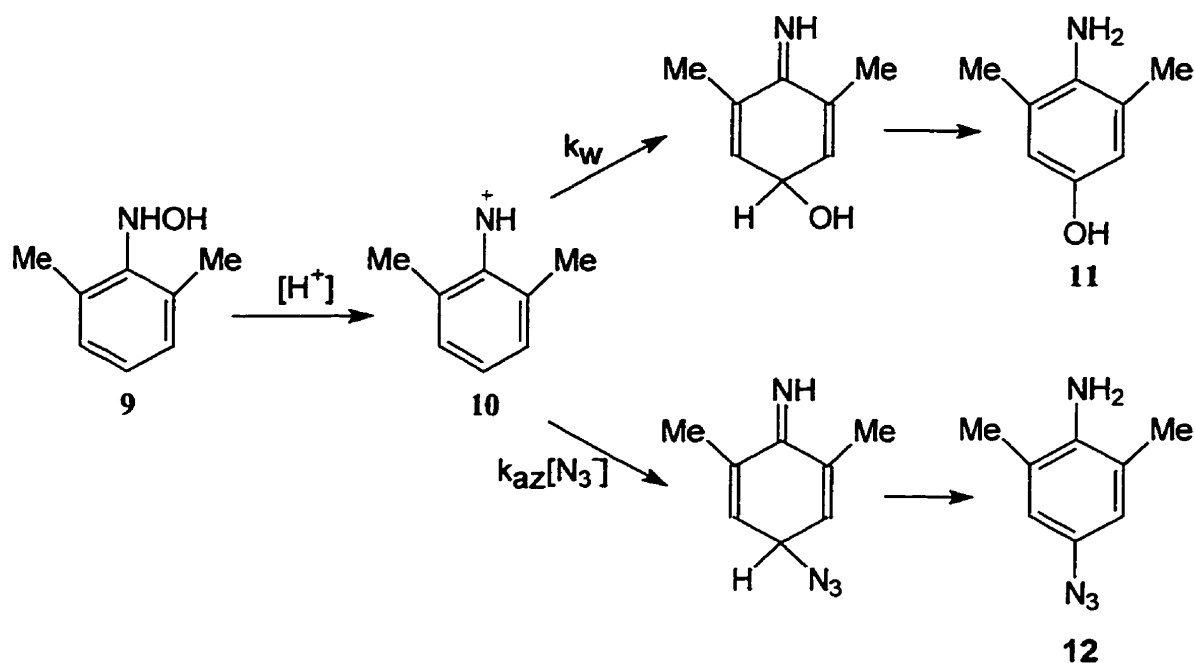
This hypothesis stimulated a number of studies of the solvolysis of N-arylhydroxylamine esters and related reactions seeking evidence for the intermediacy of the arylnitrenium ions and probing their chemistry. It is now well established that a number of these esters generate reactive nitrenium ions by rate-determining N-O bond cleavage during their hydrolysis reactions.^{33,41-46} Significant advances have been made in determining nitrenium ion lifetimes in aqueous solution,^{32,33} in understanding the effect of ion pairing,^{47,48} and in characterizing reactivity and selectivity toward nucleophiles, especially DNA-related nucleophiles such as 2'-deoxyguanosine.^{49,50}

One of the critical issues in evaluating the proposal that nitrenium ions react with DNA to initiate the carcinogenic process is the lifetime of the electrophile in the aqueous solvent where it is formed. Nitrenium ions can serve as intermediates for efficient reactions with DNA and other cellular nucleophiles only if they are trapped by water at a slow enough rate in a largely aqueous cellular environment so that these nucleophiles can effectively compete.

Fishbein and McClelland reported the first experiment which estimated the lifetime of an arylnitrenium ion, thus providing definite evidence of the existence of a free nitrenium ion as a reactive intermediate.^{32,47} The lifetime of the 2,6-dimethylphenylnitrenium ion formed in an acid-catalyzed Bamberger rearrangement was determined by application of the "azide clock" method. This

required measurement of the quantity of k_{az}/k_s , the ratio of the second-order rate constant for trapping of the cation by N_3^- and the pseudo-first-order rate constant for trapping by solvent. In the actual experiment a known mutagen, N-(2,6-dimethylphenyl)hydroxylamine (9), reacted in a dilute acid solution in the presence of azide ion (Scheme 5).

Scheme 5

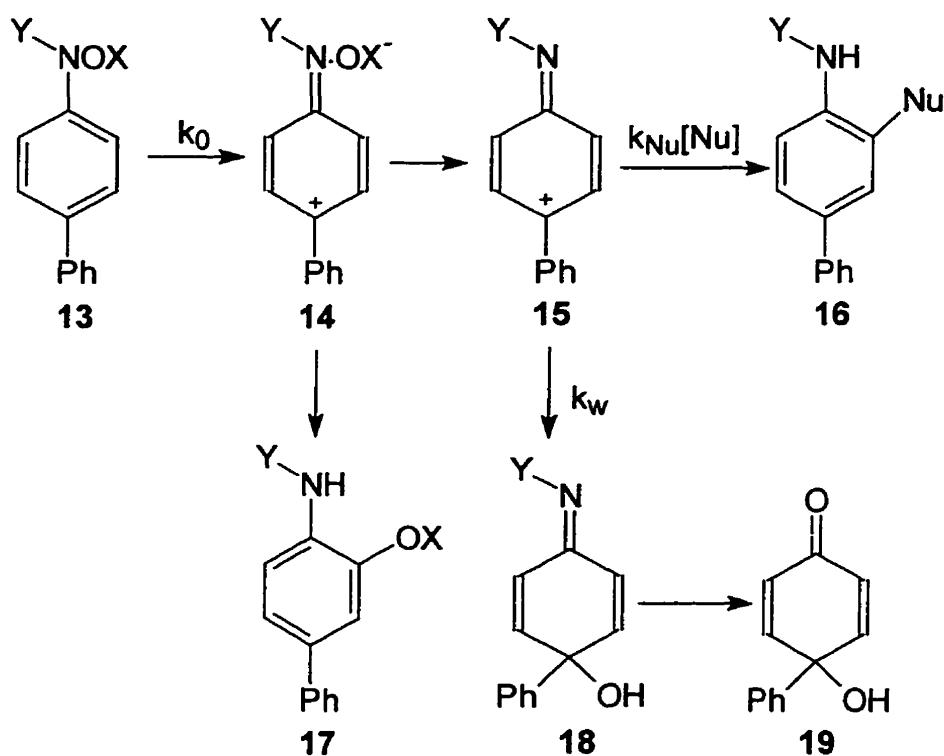


Two products were observed, the Bamberger rearrangement product 4-hydroxy-2,6-dimethylaniline (11) and the azide adduct 4-azido-2,6-dimethylaniline (12). The latter formed in increasing amount with increasing concentration of azide. However, there was no increase in the decay rate of the hydroxylamine. This provided the first evidence for the formation of a free nitrenium ion (10) in a rate-determining step, followed by a product-determining step involving partitioning between the solvent and the added nucleophile. The product data were fit by the standard equation for competition kinetics providing the ratio $k_{az}/k_w = 7.5 \text{ M}^{-1}$. With the assumption widely employed for carbenium ions that azide

reacts at $\sim 5 \times 10^9 \text{ M}^{-1}\text{s}^{-1}$, the diffusion limit, the lifetime ($1/k_w$) of the nitrenium ion **10** was calculated as 1.4 ns. While this number does indicate that **10** can exist as a free cation in water, its lifetime is very short, suggesting that this intermediate at least would be unlikely to survive long enough to react with DNA.

Novak and coworkers applied the trapping kinetics method to the ester derivatives of N-(4-biphenyl)hydroxylamines **13a** and **13b**.^{33,48} The addition of nucleophiles Cl^- and N_3^- caused a marked decrease in the yields of all hydrolysis products derived from **13**, except the rearrangement products **17**, without any change in the hydrolysis rate.

Scheme 6



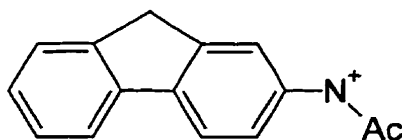
a: Y = Ac, X = SO_3^-

Nu = Cl^- , N_3^-

b: Y = H, X = COtBu

Novak explained the trapping behavior in terms of Scheme 6. The esters **13a** and **13b** decompose *via* rate-determining N-O bond heterolysis to generate the contact ion pair **14**. This ion pair can undergo diffusional separation to generate the free ion **15**, or internal return with rearrangement to yield **17** (after aromatization). All other products are derived from nucleophilic attack of solvent or other species on **15**.

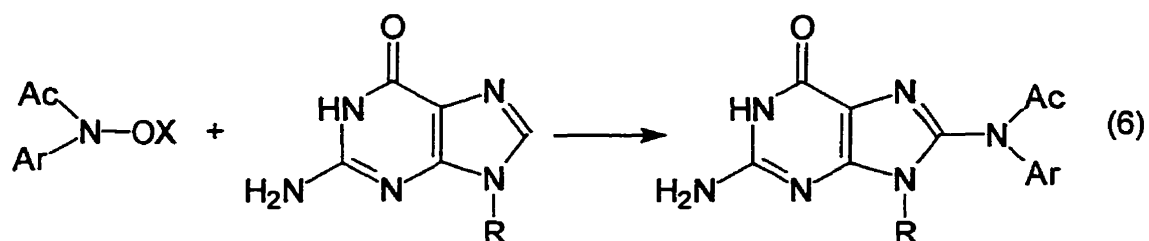
The azide/solvent ratios, k_{az}/k_w , are $1.02 \times 10^3 \text{ M}^{-1}$ for **15a**, and $2.9 \times 10^3 \text{ M}^{-1}$ for **15b**, respectively. If k_{az} is at the diffusion controlled limit of $5 \times 10^9 \text{ M}^{-1}\text{s}^{-1}$, k_w for **15a** is $4.9 \times 10^6 \text{ s}^{-1}$, and k_w for **15b** is $1.7 \times 10^6 \text{ s}^{-1}$. Novak and McClelland later obtained a k_{az}/k_w ratio of $6.2 \times 10^4 \text{ M}^{-1}$ for trapping of the N-acetyl-2-fluorenylnitrenium ion (**20**).⁵¹ With k_{az} assumed to be $5 \times 10^9 \text{ M}^{-1}\text{s}^{-1}$, k_w for this cation is $8.1 \times 10^4 \text{ s}^{-1}$. These results indicate that the 4-biphenyl- and 2-fluorenylnitrenium ions are longer-lived species, possibly of sufficient lifetime to react with biological targets, such as the bases of DNA, in an aqueous environment.



20

Novak provided more definite evidence that nitrenium ions **15a** and **20** could be responsible for the carcinogenic effects of the parent esters by showing that these nitrenium ions are efficiently trapped by 2'-deoxyguanosine in aqueous solutions.⁵⁰ Solvolysis of N-acetyl derivatives **13a** or **21** in the presence of 2'-deoxyguanosine (dG) resulted in the formation of significant amounts of the C-8 adducts **8** or **22** (eq 6), e.g. >95% of **8** from **21** and 75% of **22** from **13a** in 10 mM dG. In the meantime the rate constants for the disappearance of **13a** or **21** were independent of the concentration of dG, showing that free nitrenium ions **15a** and

20 are formed in the rate-determining step, followed by partitioning between dG and solvent.



13a, Ar = 4-biphenyl, X = SO₃⁻

8, Ar = 2-fluorenyl

21, Ar = 2-fluorenyl, X = COtBu

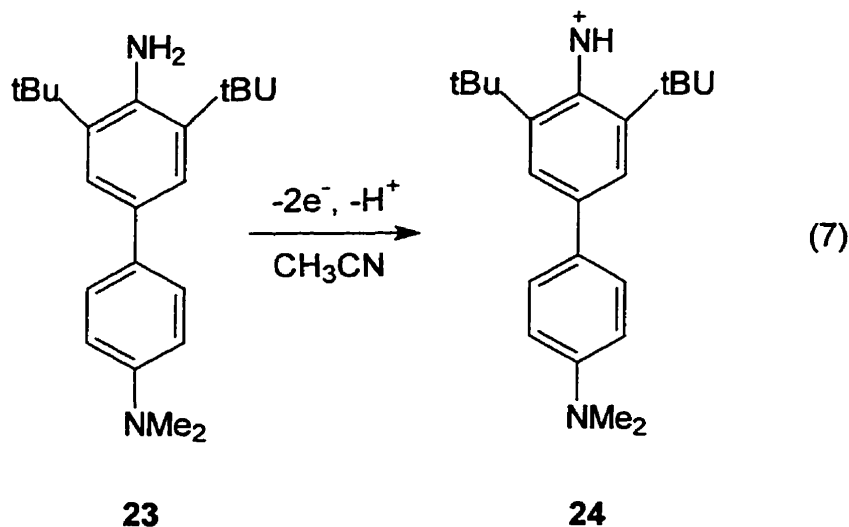
22, Ar = 4-biphenyl

R = 2'-deoxyribose

The partitioning ratios k_{dG}/k_w were calculated as 290 M⁻¹ and 8000 M⁻¹ for the nitrenium ions **15a** and **20**, respectively. These ratios indicate a high selectivity of these nitrenium ions for the nucleoside. This selectivity could explain the carcinogenicity of N-(2-fluorenyl)hydroxylamine and N-(4-biphenyl)hydroxylamine derivatives.

3. Laser Flash Photolysis (LFP) Study of Arylnitrenium Ions

As stated before, the fact that nitrenium ions are formed at intermediate stages has usually been established by product and kinetic studies. Reports of the direct observation of nitrenium ions have been very limited. Attempts to observe such ions under super-acid conditions have generally failed.^{52,53} There are three reports of relatively stabilized nitrenium ions being produced by electrochemical two-electron oxidation/deprotonation of the corresponding amines in acetonitrile. These include diarylnitrenium ions bearing stabilizing *o*- and *p*-methoxy substituents such as the bis-(4-methoxyphenyl)nitrenium ion,^{54, 55} and the 2,6-di-*t*-butyl-4'-(*N,N*-dimethylamino)-4-biphenylnitrenium ion **24**.⁵⁶ The diarylnitrenium ions are not stable, however, and were only characterized by UV-visible absorption spectra. The 4-biphenylnitrenium ion **24** was sufficiently persistent for its NMR spectrum to be recorded.



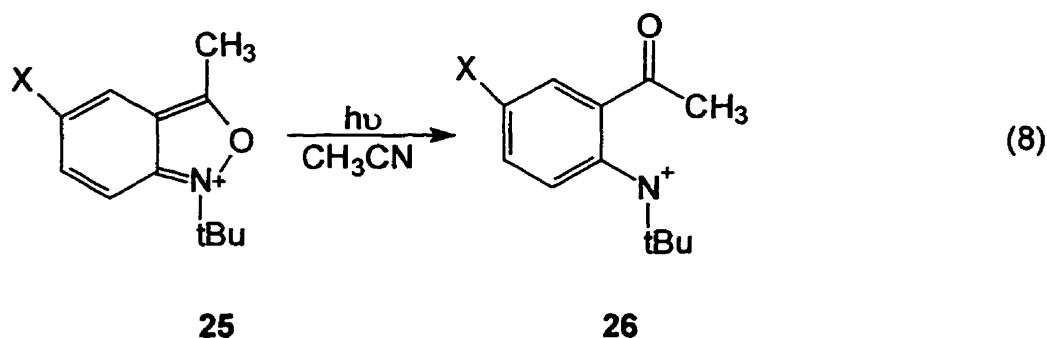
Flash photolysis is an alternative method for the direct study of intermediate cations, and there have been a number of investigations on carbenium ions using this technique.⁵⁷ This method offers some significant advantages over solvolytic generation of cations. First, ambiguities from competing concerted decomposition

reactions (S_N2 vs S_N1) are avoided, since the S_N1 intermediate is actually observed. Second, the photochemical generation allows for nitrenium ions to be spectroscopically characterized by using laser flash photolysis. This not only provides the structural information about the cation, but also means that detailed kinetic information can be obtained for the decay reactions.

There are three basic requirements for the LFP method to be successful for the study of a cationic intermediate such as a nitrenium ion.^{57,58} (a) There must be a photochemical reaction generating the desired cation. (b) The cation must be observable with the monitoring method. (c) The cation must have a sufficient lifetime to be detected. The azide-trapping experiments discussed in the previous section imply that at least some aryl nitrenium ions should be sufficiently long-lived to be observed. There should also be a significant absorbance in the ultraviolet or visual spectral range, due to the extensive delocalization. What had been missing were the photochemical methods.

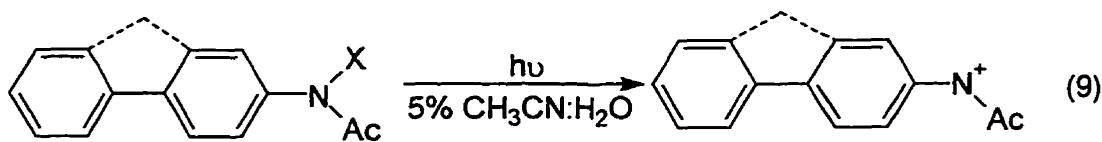
3.1. LFP generation of aryl nitrenium ions

The first direct observation of an aryl nitrenium ion with LFP was reported by Falvey and coworkers in 1993.⁵⁹ Upon 10 ns irradiation of anthranilium ions **25a** and **25b** at 308 nm in acetonitrile, transients with $\lambda_{max} \approx 390$ nm were observed. The signals decayed with first-order kinetics, with lifetimes ($1/k_{decay}$) of 131 and 137 ns for **25a** and **25b**, respectively. The transients were assigned to the corresponding nitrenium ions **26** produced by heterolytic ring-opening of the five-membered ring (eq. 8). The Falvey group has more recently reported detailed studies of the electrophilicity of this system and the spin multiplicity of the nitrenium ion.^{20, 60}



a: X = Br, b: X = Cl

Shortly after the first Falvey report, McClelland and Novak reported the observation of nitrenium ions **15a** and **20** on irradiation of N-acetyl derivatives **13a**, **21** and **27** in aqueous acetonitrile (eq. 9). The precursor compounds employed in these experiments were the same as the ones employed by the Novak group in their competition kinetics studies.⁵¹



13a, 4-biphenyl, X = OSO₃⁻

15a, 4-biphenyl

21, 2-fluorenyl, X = OCOtBu

20, 2-fluorenyl

27, 4-biphenyl, X = Cl⁻

Pulsed laser (248 nm, 20 ns) irradiation of the precursors gave transient spectra with λ_{max} in the vicinity of 450-460 nm, plus a weaker absorbance at 300-350 nm. The absorbance at higher wavelength decayed with excellent exponential kinetics; the absorbance at lower wavelength showed little decay at times up to 100 μ s. The transient absorption spectra obtained with **13a** are shown in Figure 2.

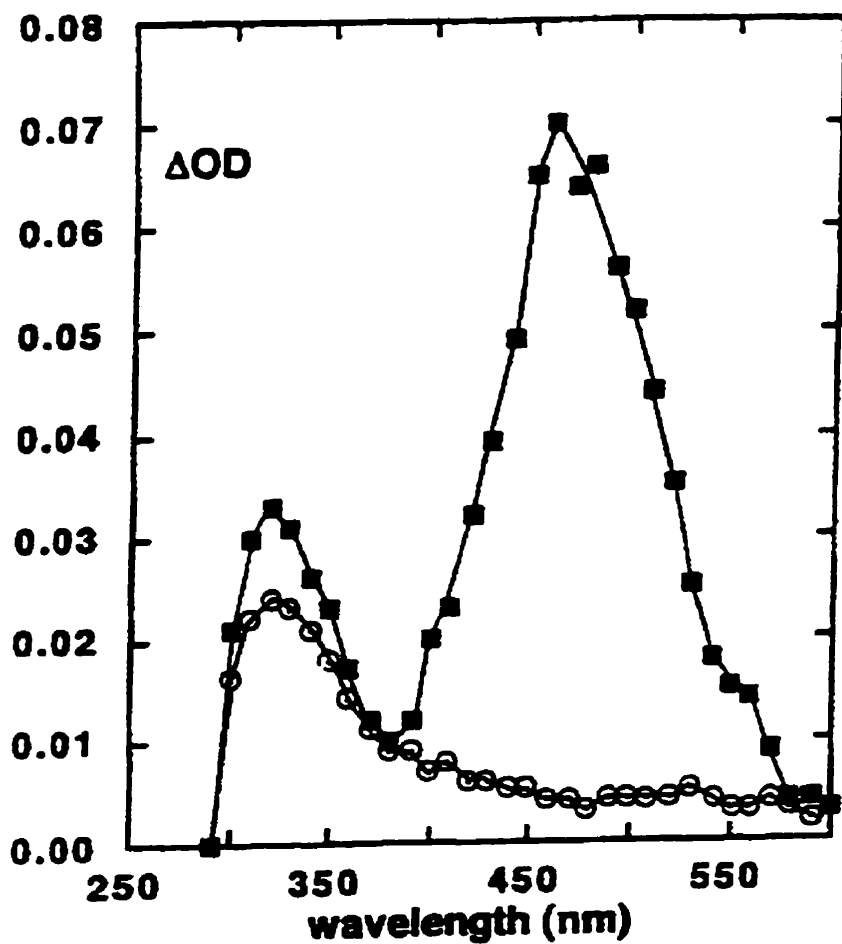


Figure 2. Transient absorption spectra obtained upon 248-nm irradiation of 13a in 0.5 M NaClO₄ aqueous solution containing 5% acetonitrile. Closed squares, immediately after laser pulse; open circles, after 5 μs .⁵¹

The transient species at 450–460 nm were assigned to the corresponding nitrenium ions **15a** and **20** based on the following evidence: (1) A product study showed that irradiation resulted in products similar to those obtained from ground state solvolysis. (2) The 450 nm absorbances showed the decay characteristics of a cationic intermediate, being quenched effectively by azide ion, but unaffected by oxygen, a radical and triplet trap. (3) With both cations, the ratios k_{az}/k_w obtained directly with LFP were, within experimental error, the same as ones obtained through product analysis of solvolysis reactions by the Novak group³³ (see Table 1). This latter observation is important since it also demonstrates that the transient is identical with the ground state intermediate.

Table 1. Absolute rate constants for nitrenium ions reacting with solvent and azide ion (20°C, ionic strength 0.5 M, adjusted with NaClO₄).

Nitrenium ion	k_w (s ⁻¹)	k_{az} (M ⁻¹ s ⁻¹)	k_{az}/k_w , ^a M ⁻¹	k_{az}/k_w , ^b M ⁻¹
N-Acetyl-4-biphenyl (15a) ^c	5.9 x 10 ⁶	5.1 x 10 ⁹	8.6 x 10 ²	1.02 x 10 ^{3e}
4-Biphenyl (15b) ^d	1.8 x 10 ⁶	5.0 x 10 ⁹	2.8 x 10 ³	2.9 x 10 ^{3e}
N-Acetyl-2-fluorenyl (20) ^c	7.7 x 10 ⁴	4.2 x 10 ⁹	5.6 x 10 ⁴	6.2 x 10 ^{4c}
2-Fluorenyl (32) ^d	3.4 x 10 ⁴	4.0 x 10 ⁹	1.2 x 10 ⁵	

^a Ratio of absolute rate constants.

^b Obtained from ground state solvolysis by method of competition kinetics.

^c Ref. 51.

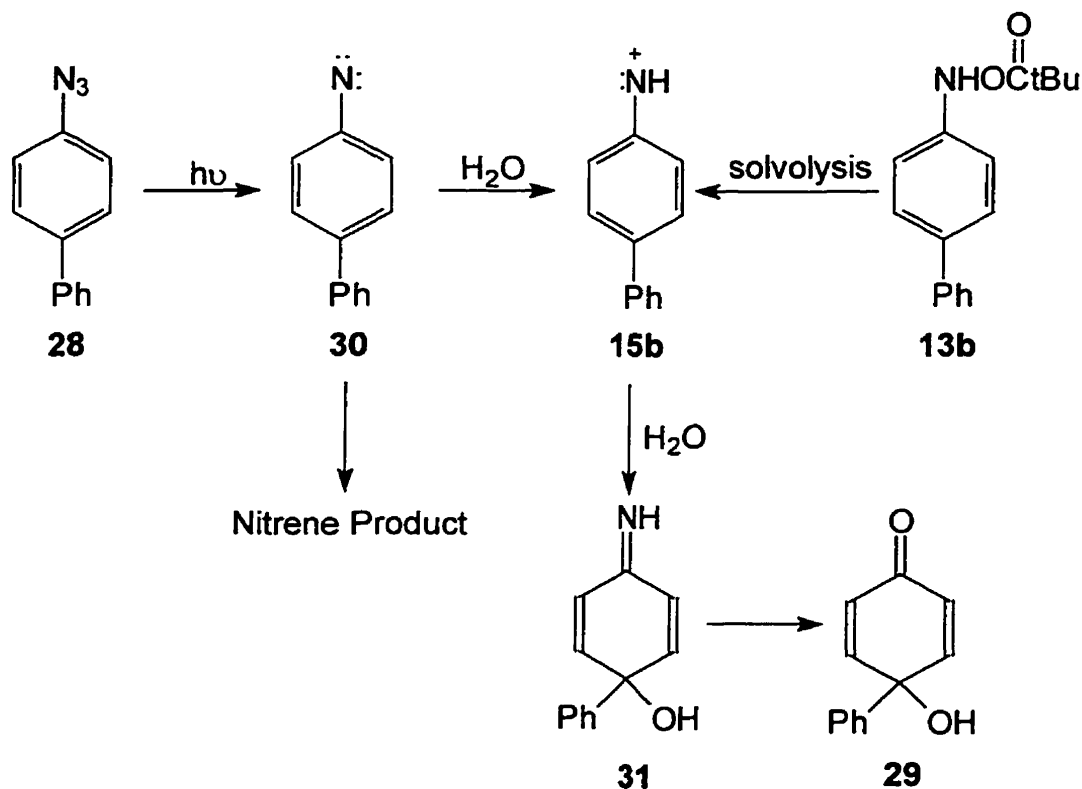
^d Ref. 61.

^e Ref. 33.

Both the Falvey approach and the initial McClelland approach involved photoheterolysis—the heterolytic cleavage in the excited state of a nitrogen-leaving group bond. However, precursors that can be used to generate nitrenium ions by such an approach are limited. This is especially true for precursors that lack the N-acetyl group, because of the ground state solvolytic lability of such compounds. Later on McClelland developed a different approach employing aryl azides as precursors involving the protonation of photogenerated nitrenes.⁶¹

Irradiation of 4-biphenyl azide **28** at 300 nm for 30-90 s in 20% acetonitrile:water gave 4-hydroxy-4-phenyl-2,5-cyclohexadienone **29** as the major product. This is the same product as the one obtained in the solvolysis of the O-pivalate of 4-biphenylhydroxylamine **13b**.

Scheme 7



The proposed mechanism for the reaction is shown in Scheme 7. The irradiation of the azide **28** results in formation of a singlet nitrene **30**. This species is a strong base, and thus the predominant reaction that follows is protonation with water as the proton donor. Competing reactions are intersystem crossing to the triplet nitrene and ring expansion to an azepine. The singlet nitrenium ion **15b** formed from the protonation of the singlet nitrene reacts with water at the position *para* to the nitrogen to give the imine **31**, which eventually hydrolyzes to the cyclohexadienone **29**.

Laser flash photolysis of 4-biphenyl azide at 248nm or 308 nm revealed a strong transient with λ_{max} at 460 nm (Figure 3). This spectrum is very similar to the one assigned to the N-acetyl analog **15a** generated by photoheterolysis of **13a**. The transient decays with exponential kinetics, is quenched by nucleophiles but unaffected by oxygen. And again, the $k_{\text{az}}/k_{\text{w}}$ ratio measured by LFP is in excellent agreement with the one obtained by the competition kinetics method in the solvolysis of the pivalate **13b** (see Table 1). All this evidence demonstrates that the transient with λ_{max} at 460 nm is the ground state nitrenium ion **15b**.

A similar, longer-lived transient is observed with 2-azidofluorene, and it is assigned to the 2-fluorenylnitrenium ion (**32**). Although product evidence was lacking with this system, the similarity with the spectrum for the 4-biphenylnitrenium ion (**15b**), the efficient quenching by azide ion, and the close match to the spectrum of the N-acetyl-2-fluorenylnitrenium ion (**20**) all point to this assignment.

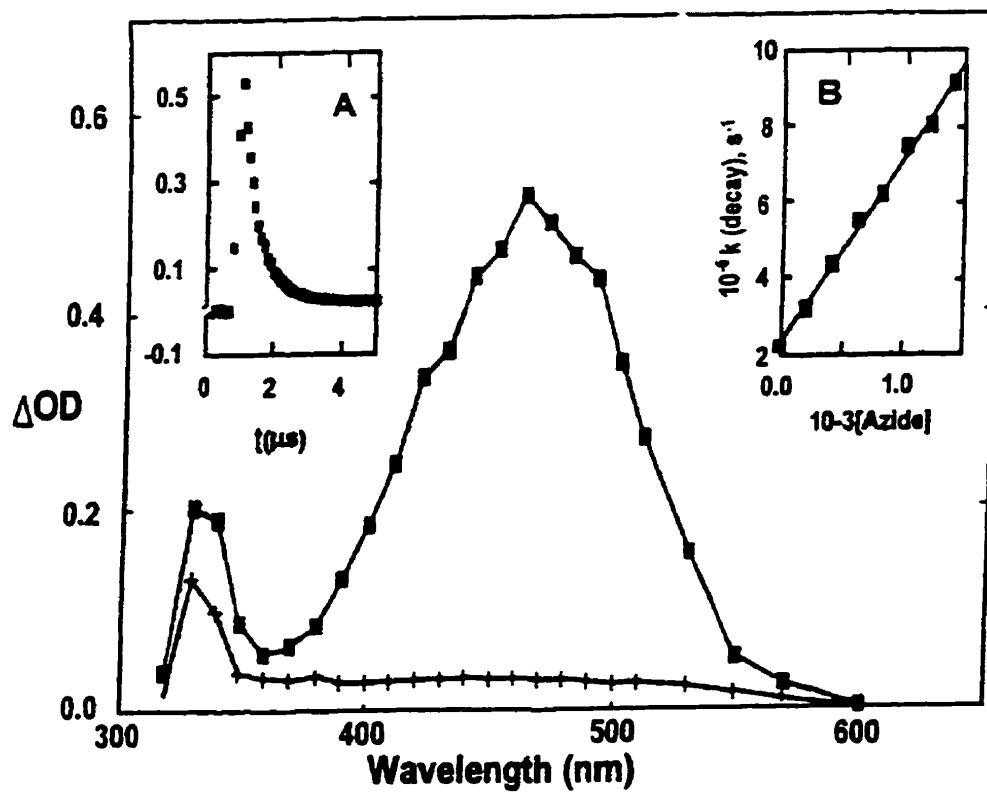


Figure 3. Transient spectrum of the 4-biphenylnitrenium ion obtained by irradiation of 50 μm 4-azidobiphenyl in 1:1 acetate buffer (2 mM) in 20% acetonitrile:water.⁶¹

3.2. Reactivities of arylnitrenium ions toward water and added nucleophiles

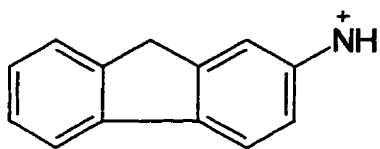
With LFP, rate constants for nitrenium ions reacting with water and with added nucleophiles are measured directly. The rate constants for the nitrenium ions **15a**, **15b**, **20**, and **32** have shown that nitrenium ions are surprisingly different from their carbenium ion analogs both in terms of their lifetimes in water,^{51,61} and their reactivities toward guanine derivatives and π -nucleophiles.^{57,58}

3.2.1. Lifetimes in water

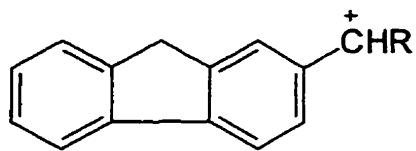
From the absolute rate constants k_w in Table 1, it can be seen that these nitrenium ions do indeed have reasonably long lifetimes in water. On the other hand, the estimated lifetimes for the parent phenylnitrenium ion and its 2,6-dimethyl derivative are much shorter, 0.2 and 1.4 ns, respectively.³² Thus the addition of the *p*-phenyl group results in a kinetic stabilization much greater than expected, for example, on the basis of the σ^+ substituent constant.⁶² This effect is especially pronounced when the entire system is forced to be planar. As seen from the comparisons in Table 1, 2-fluorenylnitrenium ions are about two orders of magnitude longer-lived than their 4-biphenyl analogs. On the other hand, substitution of N-H by N-acetyl group has only a small effect. For a given aryl group the rate constants k_w for the NH and NAc derivatives differ only by a factor of ~ 3 .^{51,61}

The remarkable kinetic stability of the 4-biphenyl- and 2-fluorenylnitrenium ions is further illustrated through a comparison with the carbenium ion analogs.⁵¹ As one example, the 2-fluorenylnitrenium ion **32** has a lifetime of 30 μ s. This is five orders of magnitude longer than the lifetime of the benzyl analog **34** (whose rate constant has been estimated from that for **33**, based on the effect of replacing phenyl with H in other carbenium ions). McClelland attributed the kinetic stability of nitrenium ions to the activation barrier associated with water attack on the ring carbons. This addition to the ring disrupts aromaticity and may

significantly raise the intrinsic activation energy. A similar activation barrier does not exist for the carbenium ions because they normally undergo attack at the external carbon and thus do not lose aromatic stabilization in the product.^{32,33}



32, $k_w = 3.4 \times 10^4 \text{ s}^{-1}$



33, R = Ph, $k_w = 1.5 \times 10^7 \text{ s}^{-1}$

34, R = H, $k_w \sim 10^9 \text{ s}^{-1}$ (estimated)

3.2.2. Azide ion

Azide ion has been extensively used as a “clock” for obtaining absolute rate constants from selectivities measured by competition kinetics. The assumption is made that this nucleophile reacts with short-lived cations at a constant, diffusion-limited rate constant, with an assignment of $5 \times 10^9 \text{ M}^{-1}\text{s}^{-1}$ for that limit. This approach was originally applied to reactivities of carbenium ions,^{63,64} and still sees considerable use in this regard.⁶⁵ Laser flash photolysis has provided evidence that this assumption is valid through the direct measurements of the absolute rate constants k_{az} .⁵⁷

Azide ion has also been employed as a “clock” to probe reactivities of arylnitrenium ions. Like water, azide ion reacts with nitrenium ions at a ring carbon, and the products are azido-substituted aromatic compounds. The k_{az} measured directly with LFP for 4-biphenyl- and 2-fluorenylnitrenium ions are listed in Table 1. Although the cations have quite different k_w , the k_{az} values are all of the order $4\text{-}5 \times 10^9 \text{ M}^{-1}\text{s}^{-1}$. Thus, it would appear that azide ion reacts with nitrenium ions at the diffusion limit or at least very close to this limit.

3.2.3. Guanine derivatives

Nitrenium ions are effectively quenched by guanine derivatives. As seen in Table 2, second-order rate constants for the quenching by 2'-deoxyguanosine and its 5'-monophosphate derivative measured by LFP are in the range of $1 - 2 \times 10^9 \text{ M}^{-1}\text{s}^{-1}$. The $k_{\text{dG}}/k_{\text{w}}$ ratio measured for N-acetyl-4-biphenylnitrenium ion by LFP is in excellent agreement with the number obtained in competition experiments, showing that the quenching represents the reaction of nitrenium ions at C-8 of guanine.⁵⁸

Table 2. Selectivities and absolute rate constants for the reaction of nitrenium ions and 2'-deoxyguanosine (dG) and 2'-deoxyguanosine-5'-phosphate (dGmp) (20°C, ionic strength 0.5 M, adjusted with NaClO₄)

Nitrenium ion	$k_{\text{dG}}/k_{\text{w}}$ ^a	$k_{\text{dG}}/k_{\text{w}}$ ^b	k_{dG} (M ⁻¹ s ⁻¹) ^c	k_{dGmp} (M ⁻¹ s ⁻¹) ^c
N-Acetyl-4-biphenyl (15a)	290	330	1.9×10^9	1.3×10^9
4-Biphenyl (15b)	1060	1170	2.1×10^9	1.8×10^9
N-Acetyl-2-fluorenyl (20)	8000	5500	4.2×10^8 ^d	4.5×10^8

^a Competition kinetics.^{50, 93}

^b Ratio calculated from absolute rate constants by LFP.⁵⁸

^c Absolute rate constants by LFP.⁵⁸

^d Unpublished result.⁶⁶

The rate constants k_{dG} indicate that the reaction of deoxyguanosine with these nitrenium ions is fast, in fact, approaching the diffusion limit. Both this high reactivity and the position of attachment of the electrophiles contrast with results for analogous carbenium ions. For example, the *p*-methoxybenzyl cation reacts at the heterocycle's external NH₂ group and does so very inefficiently. LFP

experiments with diarylmethyl cations in the presence of dG and dGmp show no rate acceleration, under conditions where the nitrenium ions are very effectively quenched.

Table 3. Absolute rate constants for the reactions of carbenium ions and nitrenium ions with vinyl ethers.

Cation	$k_2(\text{H}_2\text{O})^a$	$k_2(\text{CH}_2=\text{CHOEt})^a$	$k_2(\text{CH}_2=\text{CHOEt})/k_2(\text{H}_2\text{O})$
$(4\text{-ClC}_6\text{H}_4)_2\text{CH}^+{}^b$	1.7×10^{8c}	1.7×10^8	1.0
$(4\text{-CH}_3\text{C}_6\text{H}_4)_2\text{CH}^+{}^b$	4.3×10^{6c}	6.3×10^8	1.5
N-Acetyl-4-biphenyl ^d	2.1×10^{5e}	2.3×10^8	1.1×10^3
4-Biphenyl ^d	6.8×10^{4e}	2.2×10^8	3.2×10^3
2-Fluorenyl ^d	2.5×10^{2e}	1.4×10^7	5.6×10^4

^a Unit $\text{M}^{-1}\text{s}^{-1}$.

^b Ref. 67; solvent is 100% acetonitrile.

^c True bimolecular rate constant.

^d Ref. 58; solvent is acetonitrile-water (20:80).

^e Obtained by dividing the rate constant for decay in the solvent by the concentration of water (ca 44 M).

3.2.4. Vinyl ethers

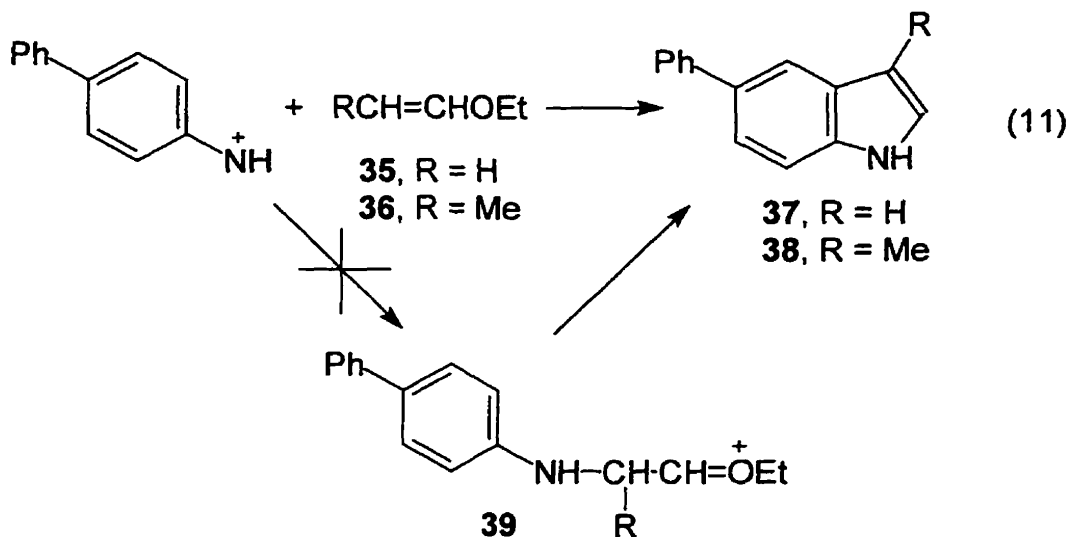
Different patterns of reactivity are also observed for the reactions of π -nucleophile vinyl ethers with nitrenium ions and carbenium ions.⁵⁸ As shown in Table 3, vinyl ethers are very effective quenchers for nitrenium ions in water. Concentrations as low as 0.01 M of a vinyl ether result in significant accelerations of the decay of the nitrenium ions. Selectivities ($k_2(\text{EtOCH}=\text{CH}_2)/k_2(\text{H}_2\text{O})$) are 10^3 –

10⁵. On the other hand, with diarylcarbenium ions in 100% acetonitrile, ethyl vinyl ether shows a reactivity almost the same as that of water.⁶⁷ In a wholly aqueous solution, the enol ether would only be able to quench 2% of the cation even at an enol ether concentration of 1 M.

The products are also interesting. Carbenium ions react with alkenes in Markovnikov fashion,⁶⁸ and with vinyl ethers would give intermediate oxocarbo-cations:



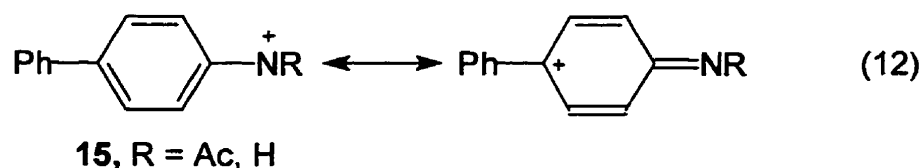
With the nitrenium ion **15b**, the products with two vinyl ethers, **35** and **36**, have been identified as the indoles **37** and **38** respectively.⁵⁸



This reaction is regio-specific with **38**. Although the mechanism is uncertain, the regiochemistry rules out the formation of the oxocarbo-cation **39** through initial N-C bond formation.

4. Nitrenium Ion or Iminocyclohexadienyl Cation

As has been mentioned previously, there is theoretical evidence that arylnitrenium ions have little positive charge on the nitrogen, but instead most of the positive charge is delocalized to the ring carbon (especially the *para* carbon). In other words, an arylnitrenium ion is perhaps better viewed as the carbenium ion resonance contributor — a cyclohexadienyl cation bearing an imine substituent (eq 12).



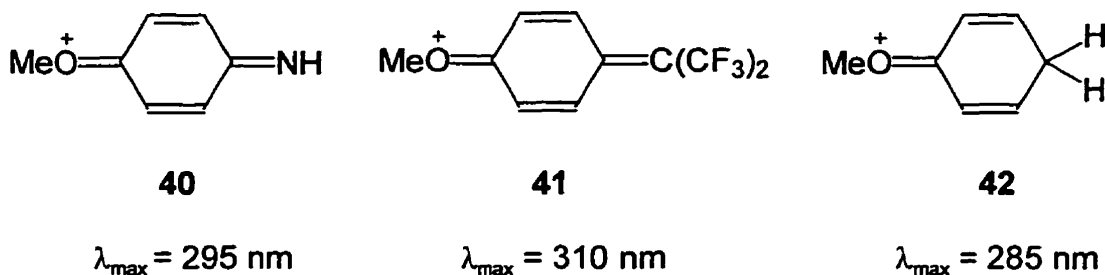
There are in fact several pieces of experimental evidence in favor of such a suggestion:

(1) In both the 2-fluorenyl- and 4-biphenylnitrenium ions, there is no effect on λ_{\max} of the cation when changing the group R on nitrogen from H to acetyl.^{51,61} Moreover, that change results in only a 3-fold increase in rate constant, despite the fact that a strongly electron-withdrawing substituent has been introduced.^{33,51,61,62}

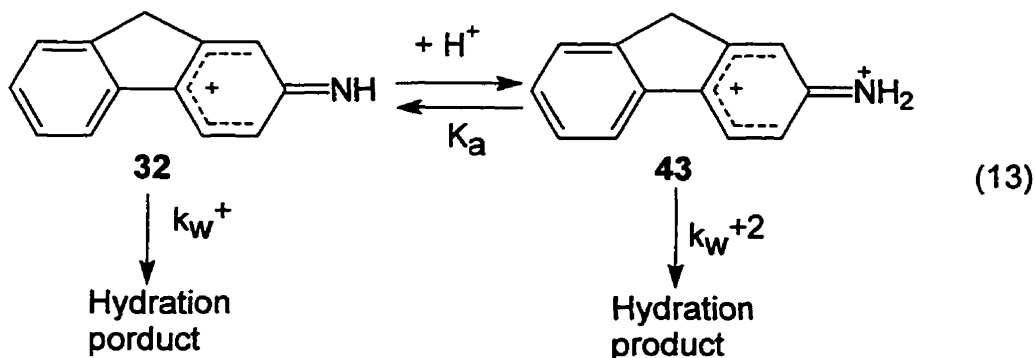
(2) Novak and coworkers have obtained aqueous lifetimes of a series *p*-substituted phenylnitrenium ions using the “azide clock” method. However, these lifetimes correlate poorly with σ^+ .⁶² In other words, the interaction of the *para* substituents with the positive charge is different in phenylnitrenium ions as compared to phenylcarbenium ions.

(3) Reacting with azide ion at the diffusion limit is of course characteristic of most carbenium ions.

(4) The *p*-methoxyphenylnitrenium ion **40** has been observed by irradiation of the precursor azide, with λ_{\max} at 295 nm.⁶⁹ This is similar to the λ_{\max} of both cation **41**,⁷⁰ and cation **42**.⁷¹ The cation **41** was observed with flash photolysis while **42** was generated by protonation of anisole in concentrated acid. All these cations are best viewed as O-methylated 2,5-cyclohexadienones.



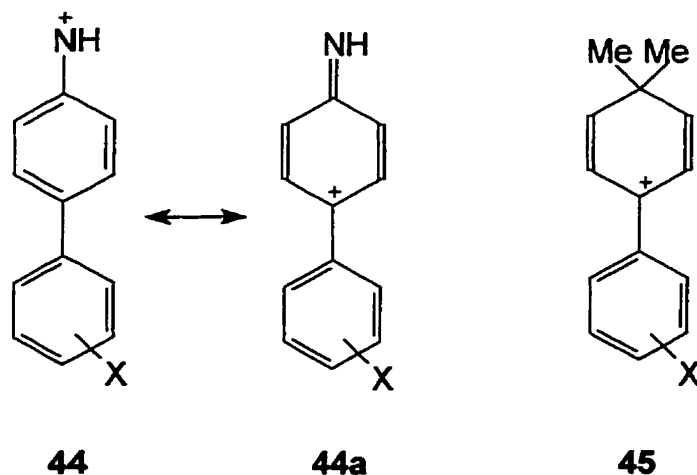
(5) The LFP studies with 4-biphenyl- and 2-fluorenylnitrenium ions have revealed that the decay is accelerated by dilute solutions of H^+ . The rate constants then approach a plateau in more concentrated acids (e.g., 1 M HClO_4).⁷² The data can be fit by the kinetic model of eq. 13, where the nitrenium ion **32** is in equilibrium with dication **43**. The acidity constant K_a of the dication in the 2-fluorenyl system obtained from the kinetic fit is 0.25. (The value is 0.8 for 4-biphenyl). In terms of this protonation, **32** is behaving as an imine with a nearby positive charge that reduces basicity.



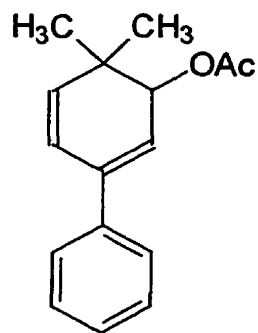
5. Scope of the Project

The main objective of this project was further to investigate the proposal that the 4-biphenylnitrenium ion is better regarded as an iminocyclohexadienyl cation. This was done in two ways: (1) The effect of substituents in the remote phenyl ring of 4-biphenylnitrenium ions (**44**) on the reactivity of these ions was studied. If 4-biphenylnitrenium ions indeed mainly exist in the form of an iminocyclohexadienyl cation (**44a**), then substituents in the phenyl ring attached at C-4 should have significant effect on the reactivity. (2) An analogous 4,4-dimethylcyclohexadienyl cation (**45**) was generated by LFP, to provide a comparison of the spectroscopic and kinetic properties of the carbenium ion and nitrenium ion **44a**. The imino group of the latter is replaced by two methyl groups, which are required to block the immediate aromatization through loss of H⁺. On the basis of studies on similar systems, migration of one of the methyl groups had been expected to be a competing pathway. This does occur, but it is a minor process compared with solvent addition.

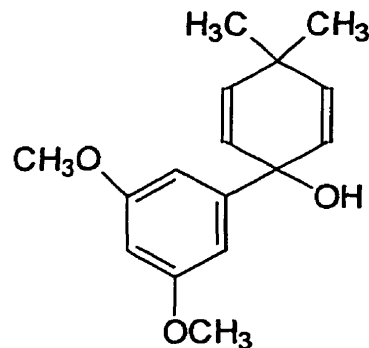
A further consequence of this work was the generation of a series of structurally similar nitrenium ions **44** of quite different lifetimes in water. This series was then studied with azide ion, ethyl vinyl ether, and 2'-deoxyguanosine in order to probe structure-activity relations with these nucleophiles.



A general route for the syntheses of 4-biaryllyl azides was developed. These azides were used as the precursors to generate the corresponding nitrenium ions by LFP. Transient spectra and rate constants of these nitrenium ions reacting with various nucleophiles were obtained. Two precursors were synthesized for the generation of the 4,4-dimethylcyclohexadienyl cation **45**, 6,6-dimethyl-1-phenylcyclohexa-2,4-dien-1-yl acetate (**46**) and 4,4-dimethyl-1-(3',5'-dimethoxyphenyl)cyclohexa-2,5-dien-1-ol (**47**). The former did form the dimethylcyclohexadienyl cation in its solvolysis in water, but attempts to observe this cation by LFP failed. However, the 4,4-dimethylcyclohexadienyl cation was generated by LFP from the latter in 20% acetonitrile:water.



46



47

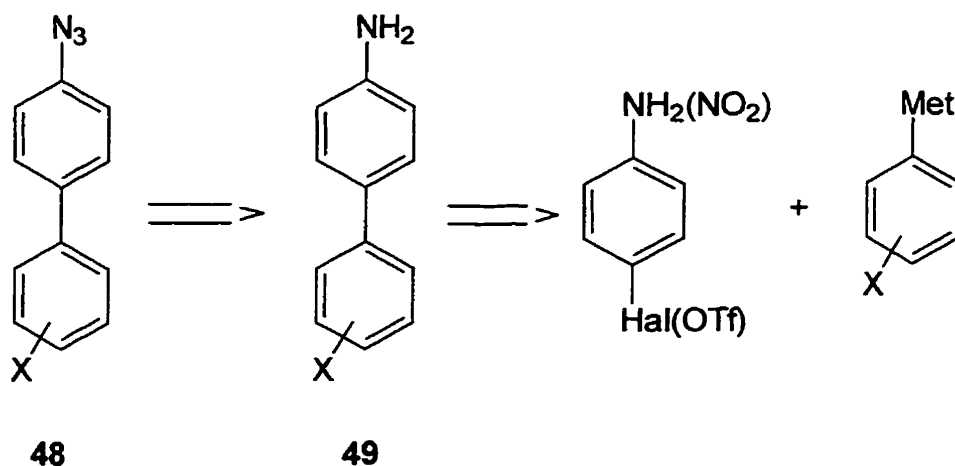
Results and Discussion

Section 1. LFP Study of Substituted 4-Biphenylnitrenium Ions

1.1. Preparation of 4-azidobiaryls

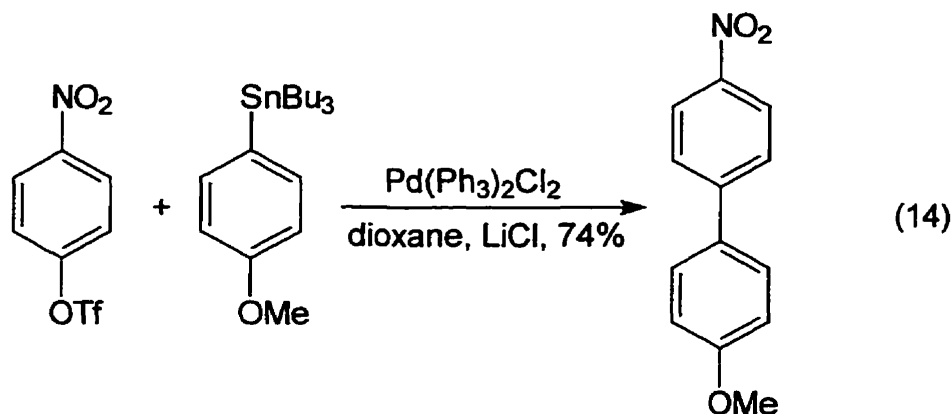
The most generally and widely used method to prepare aryl azides is diazotization of the corresponding anilines followed by addition of sodium azide. The precursors for 4-azidobiaryls, 4-aminobiaryls, could be prepared from aryl coupling reactions of *p*-nitro- or *p*-amino-substituted phenyl halides or related electrophiles (such as phenyl triflates) with appropriately substituted arylmetallic compounds (Scheme 8). Thus the key step for the preparation involves the regioselective formation of the biaryl skeleton.

Scheme 8

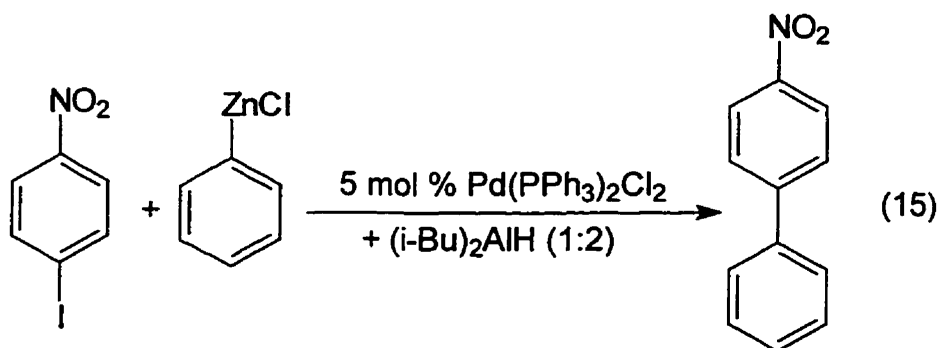


Although there are many methods of forming biphenyls using aryl-aryl bond-forming reactions, the number become more limited when one of the coupling components contains a nitro or amino substituent. One literature

example is the coupling of aryltin reagents with nitro-substituted aryl iodides or aryl triflates catalyzed by a palladium complex (eq. 14).^{73,74} This reaction works well with the only drawbacks being that the purification of aryltin reagents is rather troublesome and organotin compounds are highly toxic.



Another solution to this problem is the palladium-catalyzed coupling of arylzinc reagents with aryl halides developed by Negishi et al. In this way phenylzinc chloride (1.4 equiv) was coupled with *p*-iodonitrobenzene (1.0 equiv) to give 4-nitrobiphenyl in 74% isolated yield (eq. 15).⁷⁵ However, if applied as a general method for the syntheses of biphenyls, the preparation of substituted phenylzinc chlorides could be a problem.



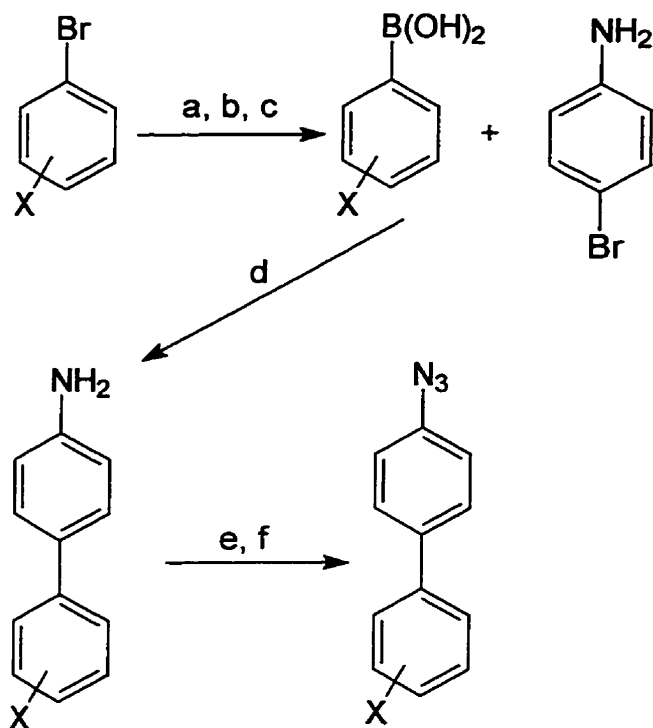
The most versatile and successful approach to unsymmetrical biphenyls is the coupling reaction of arylboronic acids with aryl halides, the so-called Suzuki reaction.^{76,77} Suzuki coupling offers several advantages over the above-mentioned methods. First, arylboronic acids are readily available by reaction of arylmagnesium halides with trimethyl borate.^{78,79} Second, the coupling is largely unaffected by water. Third, the byproducts are nontoxic. Fourth and most importantly, a broad range of functionality can be tolerated. Although there were few precedents in literatures, we found that *p*-bromoaniline could be used directly in the coupling reaction without protecting the amino group. The results are quite satisfactory with isolated yields of 4-aminobiphenyls between 50-80% depending on substituents in the phenyl ring of the boronic acids. Therefore an additional deprotection or reduction step could be avoided, compared to using amino-protected *p*-bromoaniline or *p*-bromonitrobenzene for the coupling, respectively.

General procedures for the conversion of aromatic amines to the corresponding azides have been developed by Smith and coworkers,⁸⁰ the method of choice mainly being determined by the basicity of the amine involved and the solubility of its salts. The more basic amines are converted to sulfate salts first and diazotized with sodium nitrite in aqueous solutions (Procedure A). Weakly basic amines are diazotized with amyl nitrite in an acetic acid-concentrated sulfuric acid mixture (Procedure B). In both procedures aqueous sodium azide is subsequently added. Since most 4-aminobiphenyls are hardly soluble in aqueous solutions even in the presence of strong sulfuric acid, the diazotization was carried out in an acetic acid-concentrated sulfuric acid mixture, as in Smith's Procedure B. One modification was made with sodium nitrite being used in place of amyl nitrite. This did not affect the results.

The general procedure for the syntheses of 4-azidobiphenyls is illustrated in Scheme 9. A Grignard reagent prepared from the appropriately substituted bromobenzene was reacted with trimethyl borate, followed by hydrolysis to afford the corresponding arylboronic acid.⁷⁹ The coupling of the arylboronic acids with *p*-

bromoaniline gave the 4-aminobiaryls, which were then converted to the azides by the method described above.

Scheme 9



a. Mg, ether or THF, reflux, ; b. $B(OCH_3)_3$, ether, $-78^\circ C$; c. H_3O^+ , $0^\circ C$;

d. $Pd(PPh_3)_4$, Na_2CO_3 (2 M, aq.), benzene, reflux;

e. H_2SO_4 /acetic acid, Na_2NO_2 , $0-5^\circ C$; f. NaN_3 .

X = 4-MeO, 3-MeO, 4-MeS, 4-Me, 3-Me, 4-Cl, 3-Cl, 4-F, 4-CF₃, etc.

Generally, 4-biphenyl azides with substituents on either phenyl ring can be readily synthesized by this procedure with overall yields of 30-50%. All the products were characterized by 500 MHz 1H NMR and high resolution mass spectroscopy. The effect of the azido group on the chemical shifts of protons in the phenyl rings is similar to that of halo groups. That is, the azide substituent has

a negative inductive effect that causes the protons in the phenyl ring to absorb downfield. This is demonstrated by the comparison of the NMR of 4-biphenyl azides and the corresponding amines, for example, that of 4-amino-4'-methylbiphenyl and 4-azido-4'-methylbiphenyl (Figures 4 and 5). As for the mass spectroscopy, most literature papers have reported only observations of the peak at M-28 corresponding to loss of a nitrogen molecule.⁸¹ However, we were able to observe the molecular peak of all 4-biaryl azides we prepared, although the peak is usually much weaker than the peak at M-28. The high resolution mass spectrum of both the molecular peaks and the M-28 peaks for some representative azides are shown in Table 4.

Table 4. High resolution EI mass spectrum peaks for 4-azidobiphenyls.

X'	Molecular peak		M ⁺ -28	
	Experimental	Calculated	Experimental	Calculated
4'-OMe	225.0891	225.0902	197.0837	197.0841
3'-OMe	225.0897	225.0902	197.0839	197.0841
3',5'-(OMe) ₂	255.1015	255.1008	227.0953	227.0946
4'-Me	209.0951	209.0953	181.0885	181.0891
3'-Me	209.0957	209.0953	181.0896	181.0891
4'-Cl	229.0409	229.0407	201.0343	201.0345
3'-Cl	229.0411	229.0407	201.0341	201.0345
4'-F	213.0694	213.0702	185.0630	185.0641
4'-CF ₃	263.0668	263.0670	235.0612	235.0609
3,5-Me ₂	223.1107	223.1109	Not measured	
4'-NMe ₂	238.1222	238.1218	Not measured	

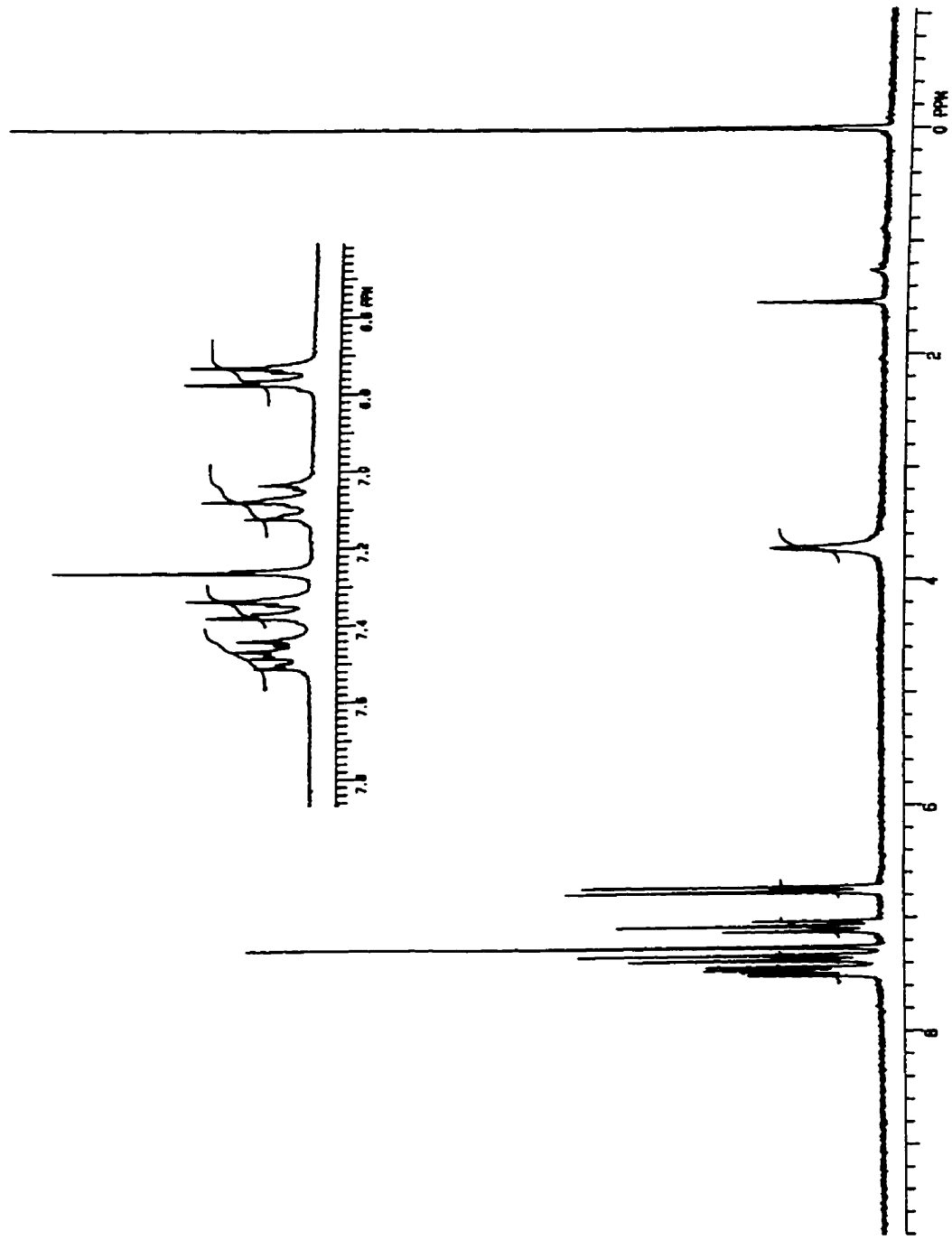


Figure 4. 500 MHz ¹H NMR for 4-amino-4'-fluorobiphenyl.

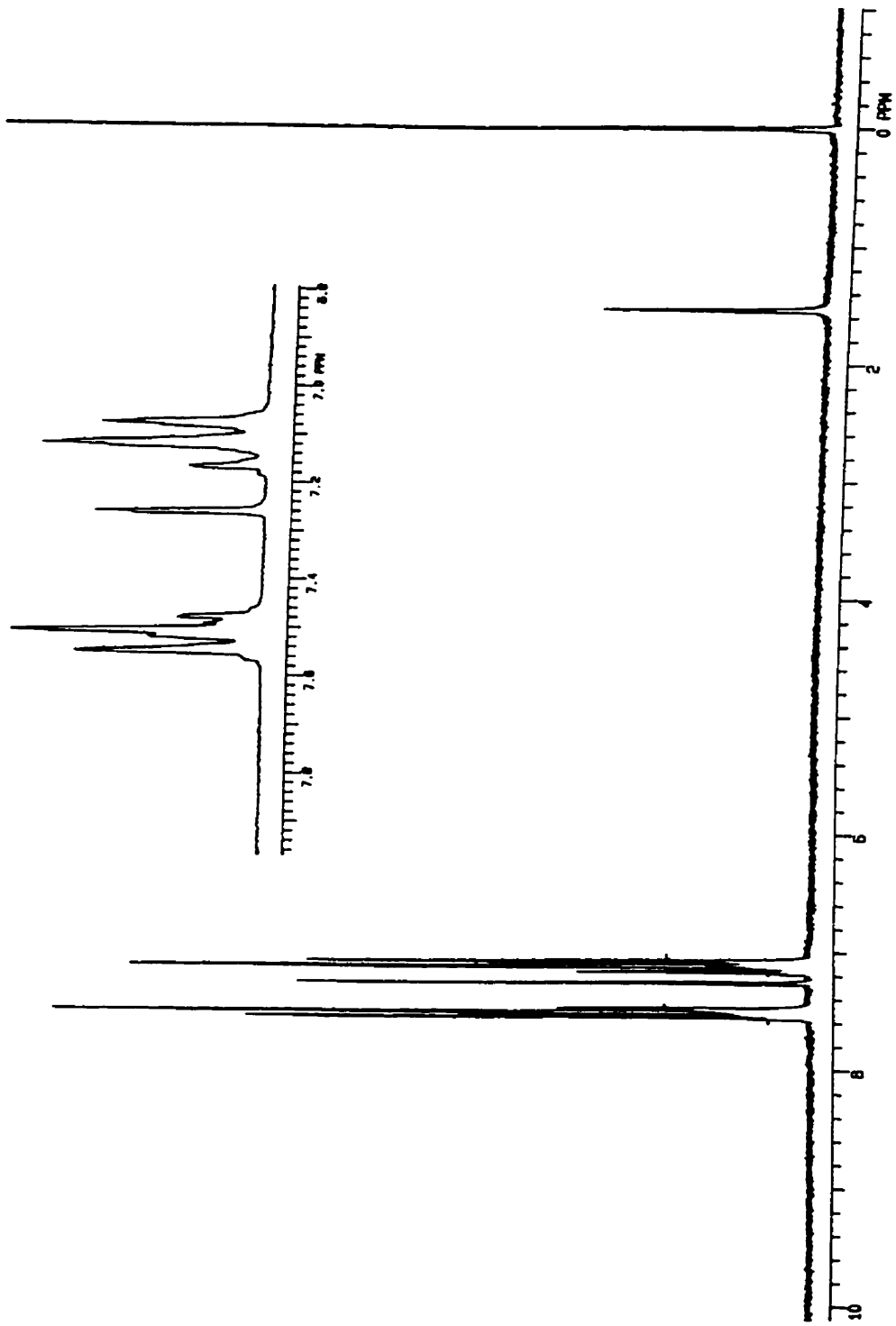
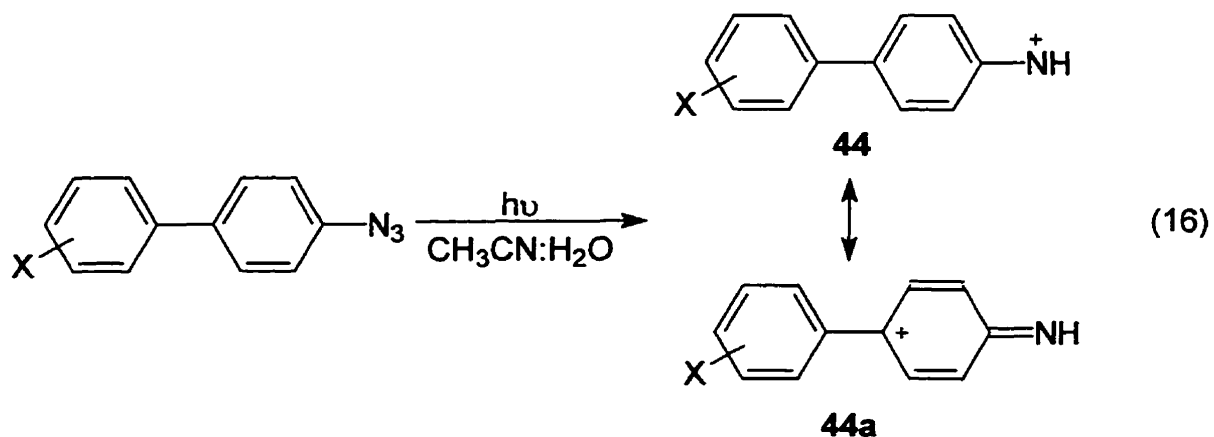


Figure 5. 500 MHz ^1H NMR for 4-azido-4'-fluorobiphenyl.

1.2. Laser Flash Photolysis of 4-Azidobiaryls

The X'-substituted-4-azidobiphenyls were subjected to laser flash photolysis to generate the corresponding nitrenium ions **44**, in the same manner as the parent. The substituents chosen for this study are given in Table 5.

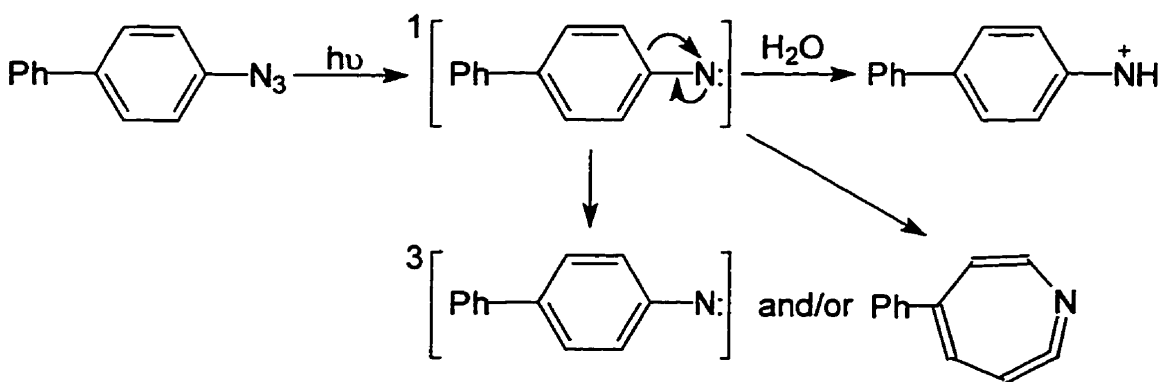


Flash photolysis experiments were carried out with laser irradiation at 248 nm in a 20% acetonitrile:water solution. The acetonitrile was required to dissolve the precursors. Laser irradiation of these azides produced good transient spectra with the exception of 4-azido-4'-(trifluoromethyl)biphenyl where there is very rapid decay of the nitrenium ion transient. As shown in Figures 6-13, these spectra are qualitatively similar to that obtained with the parent 4-azidobiphenyl as precursor. Like the parent, two transients with different kinetic patterns were observed with each precursor, one absorbing in the 400-500 nm region, and a second at 300-350 nm. The transient with λ_{max} in the region from 400 to 500 nm decays with first-order kinetics. At the end of the decay there is little residual absorbance above 400 nm, as illustrated by the time-resolved transient absorption spectra obtained at different times after laser irradiation of the 3'-Cl compound (Figure 14). The second peak does not decay over 100 μs . The λ_{max} for these transient spectra, and the ratios of the optical density of the first transient to that of the second one are given in Table 5.

The transients with λ_{max} at 450-500 nm are readily identified as the appropriate arylnitrenium ions **44** based upon the similarity of their spectroscopic and kinetic behavior to that of the parent 4-biphenylnitrenium ion. This assignment is further supported by the fact that these transients are effectively quenched by azide ion, with second order rate constants similar to the value obtained for the parent (see Table 6). Quenching by azide ion is of course characteristic of cationic intermediates. As stated before, in the case of the parent there is excellent agreement between the $k_{\text{az}}/k_{\text{w}}$ ratio obtained with flash photolysis and the value obtained by product analysis for a ground state solvolysis reaction.⁶¹

The identity of the non-decaying transient below 400 nm is uncertain. Absorbance in this region is also seen with the parent system. With this system, product analysis reveals that there is only an 84% yield of nitrenium ion on irradiation in 20% acetonitrile.⁶¹ The latter observation indicates that the protonation forming the nitrenium ion is not the only fate of the singlet nitrene. We assume that the absorbance below 400 nm represents some species forming in the competing reaction(s). Based on extensive literature studies,⁸² possibilities are a triplet nitrene or a ring-expanded 1,2-didehydroazepine.

Scheme 10



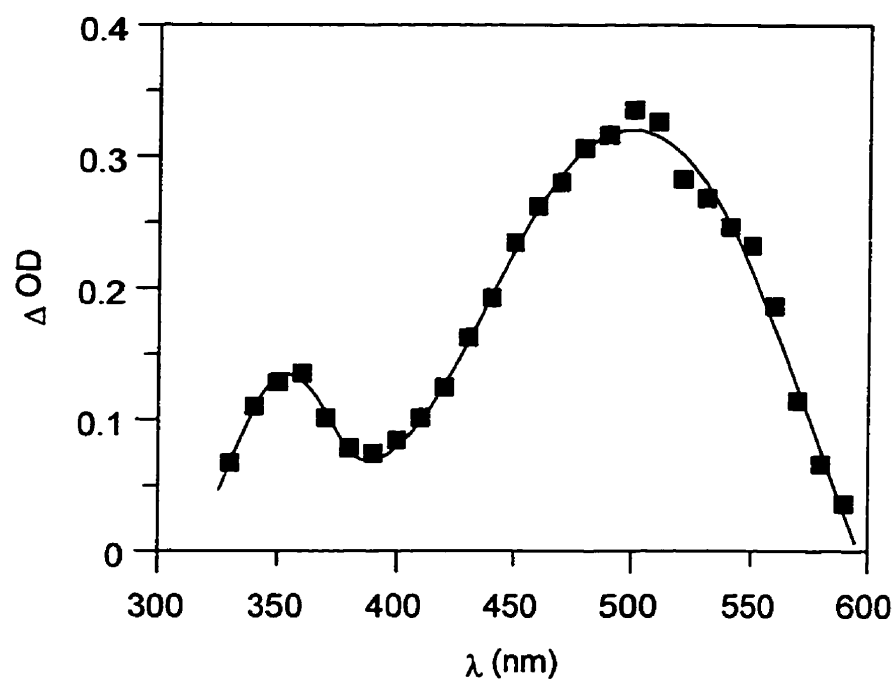


Figure 6. Transient spectra generated upon 248-nm irradiation of **4-azido-4'-methoxybiphenyl** in 40% acetonitrile:water.

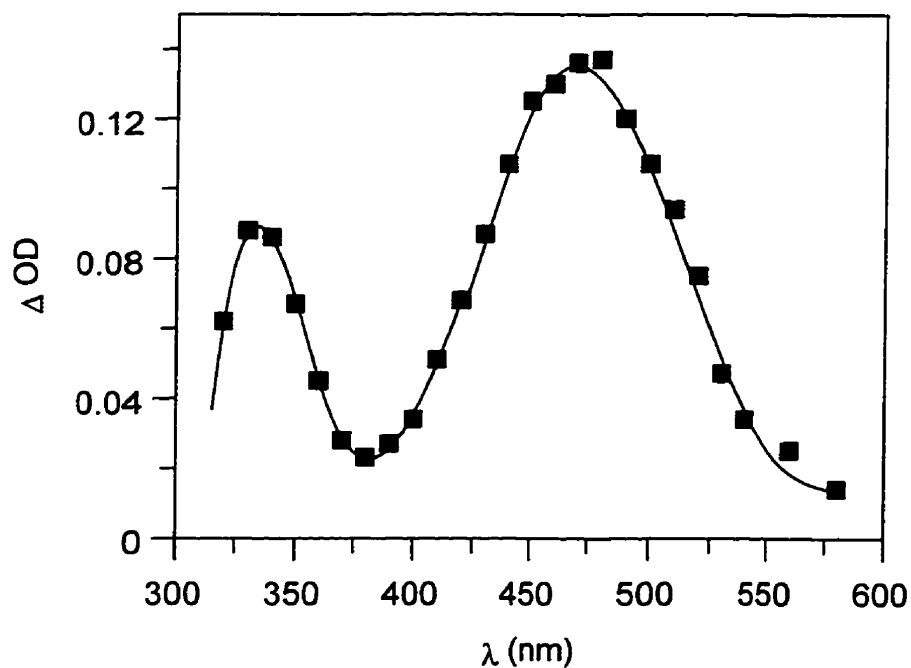


Figure 7. Transient spectra generated upon 248-nm irradiation of **4-azido-3'-methoxybiphenyl** in 20% acetonitrile:water.

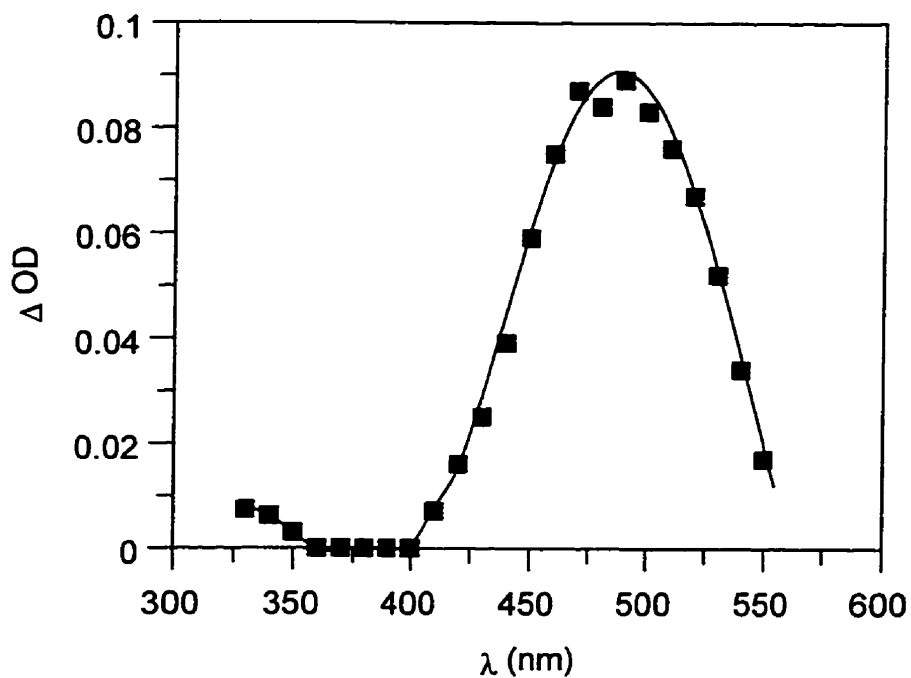


Figure 8. Transient spectra generated upon 248-nm irradiation of **4-azido-4'-methylbiphenyl** in 20% acetonitrile:water.

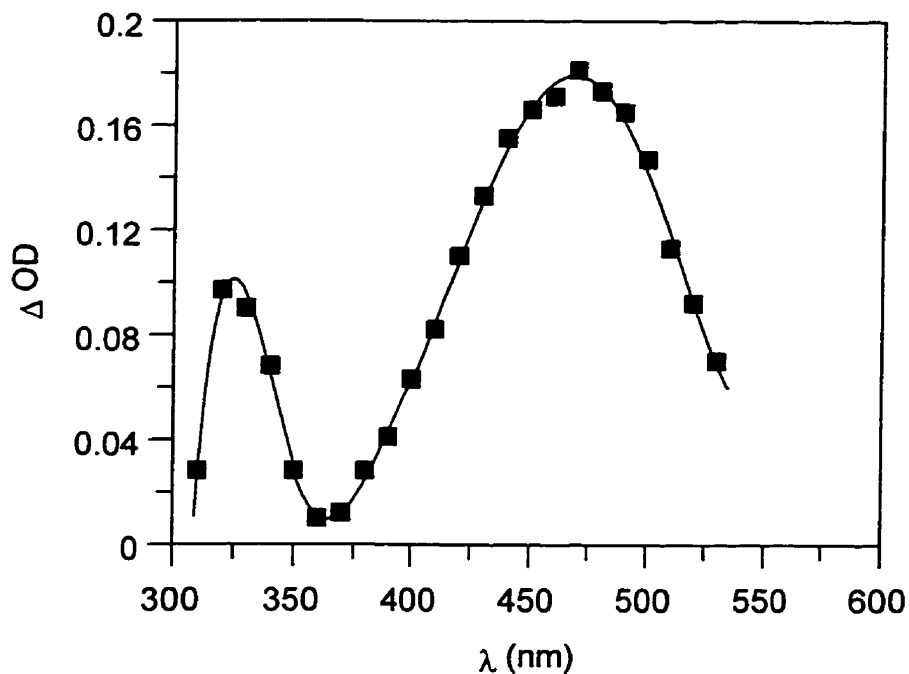


Figure 9. Transient spectra generated upon 248-nm irradiation of **4-azido-3'-methylbiphenyl** in 20% acetonitrile:water.

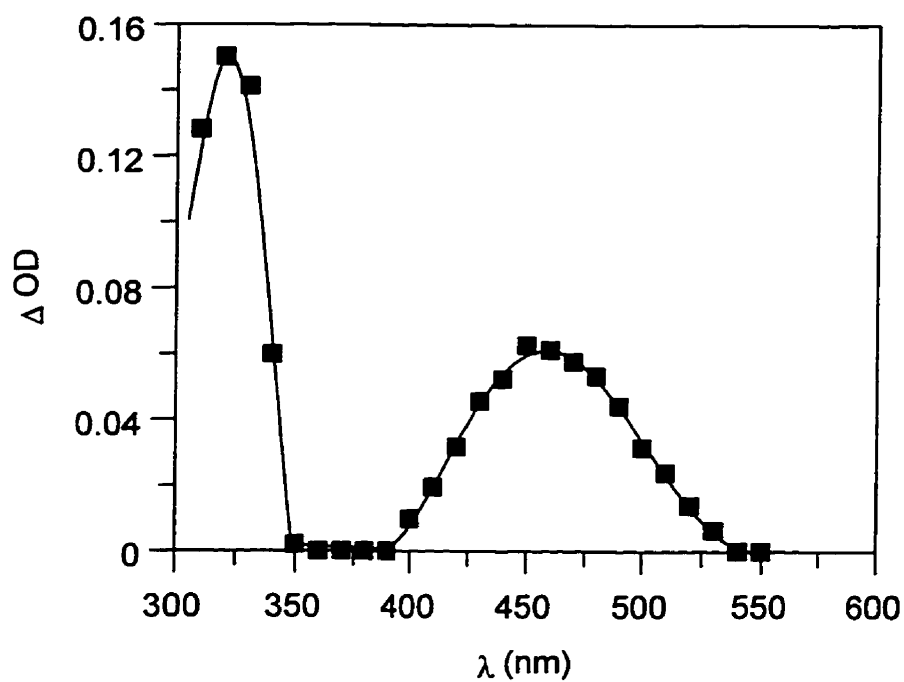


Figure 10. Transient spectra generated upon 248-nm irradiation of **4-azido-3,5-dimethylbiphenyl** in 20% acetonitrile:water.

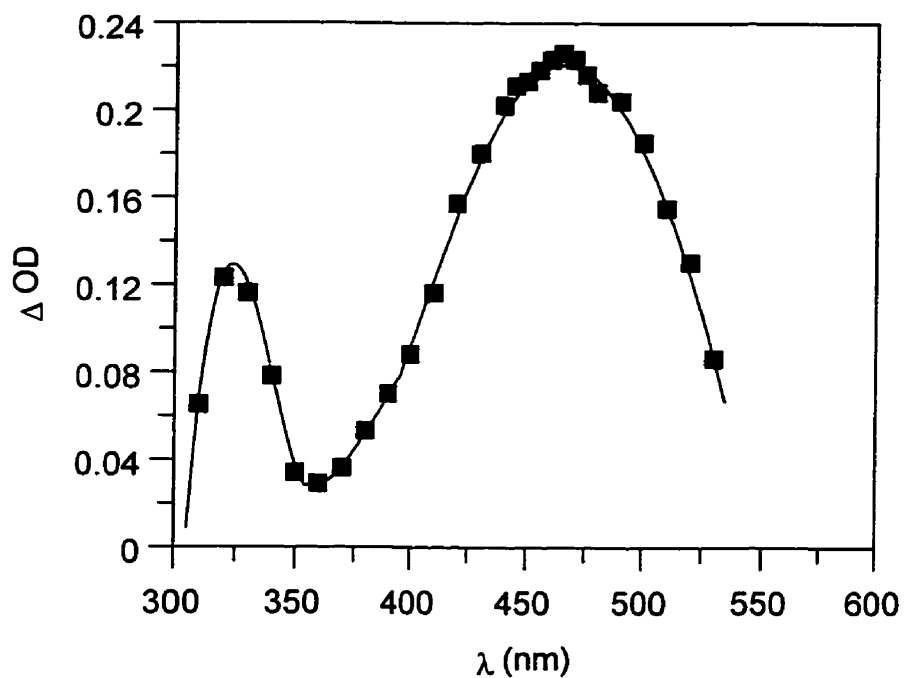


Figure 11. Transient spectra generated upon 248-nm irradiation of **4-azido-4'-fluorobiphenyl** in 20% acetonitrile:water.

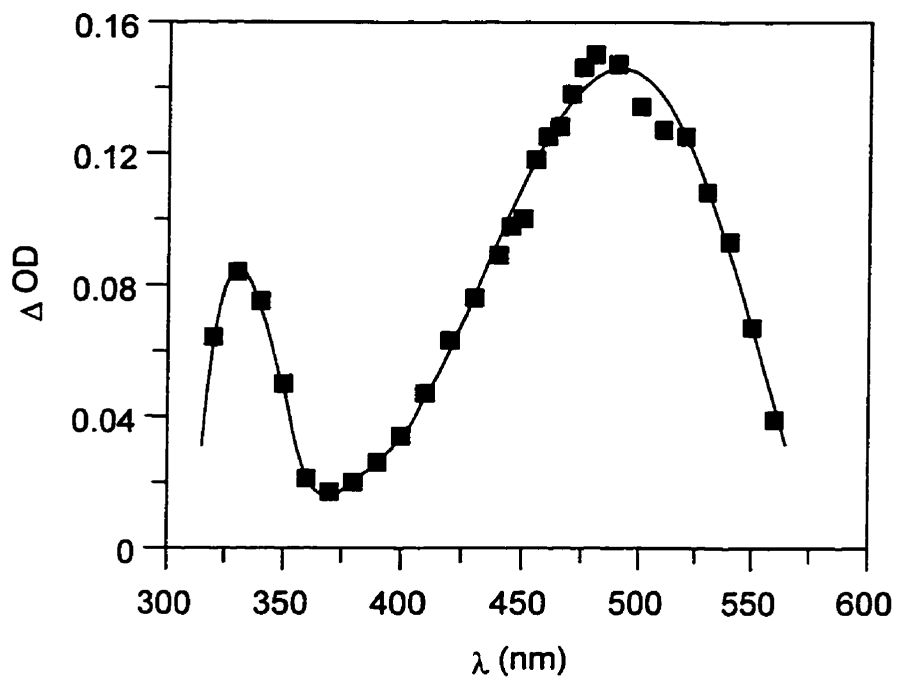


Figure 12. Transient spectra generated upon 248-nm irradiation of **4-azido-4'-chlorobiphenyl** in 20% acetonitrile:water.

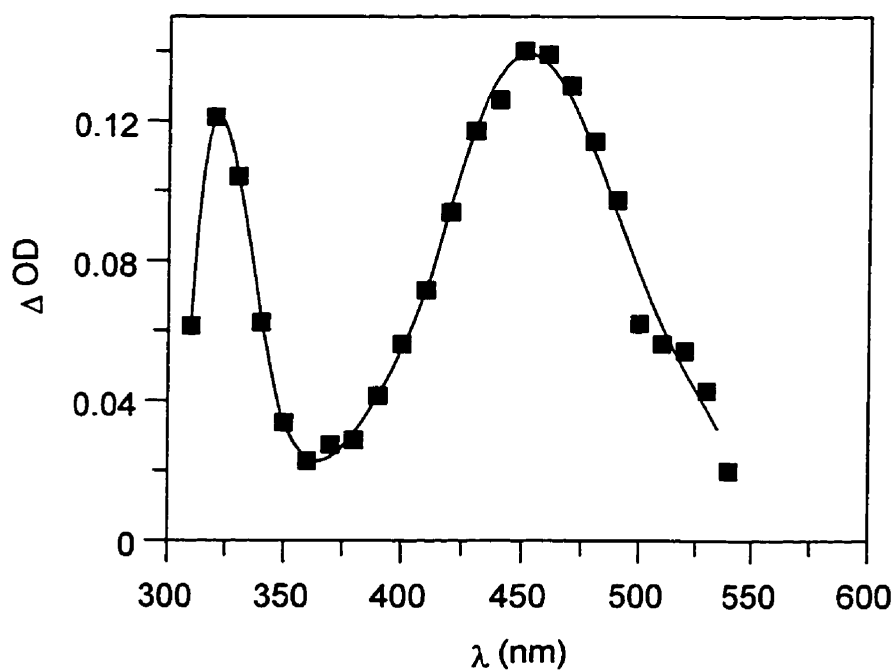


Figure 13. Transient spectra generated upon 248-nm irradiation of **4-azido-3'-chlorobiphenyl** in 20% acetonitrile:water.

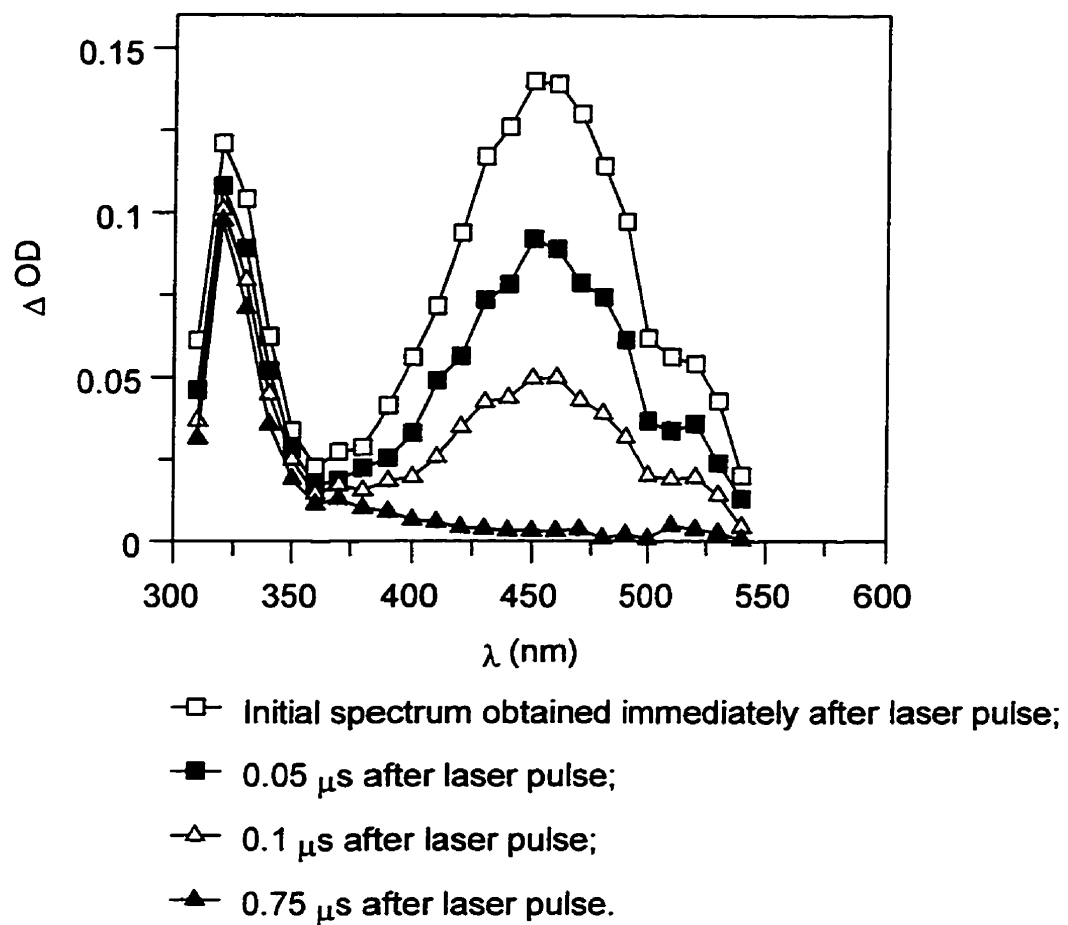
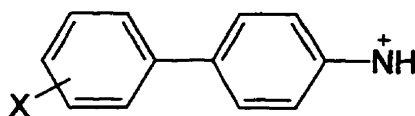


Figure 14. Time-resolved transient spectra generated upon 248-nm irradiation of 4-azido-3'-chlorobiphenyl in 20% acetonitrile:water.

Table 5. Absorption maxima and cation:non-cation ratios expressed as relative optical densities for X'-substituted-4-biphenylnitrenium ions (**44**) in 20% acetonitrile :water.



X	λ_{\max} (nm)	$[\text{OD}]_1/[\text{OD}]_2^a$
4'-OMe	500	2.3
4'-Me	490	12
4'-F	470	1.87
3'-Me	470	1.87
3'-OMe	475	1.54
4'-Cl	480	1.90
2,6-Me ₂	460	0.42
None	460	
3'-Cl	450	1.25
4'-CF ₃	450-470 ^b	

^a $[\text{OD}]_1$ refers to λ_{\max} of the transient at 450-500 nm, $[\text{OD}]_2$ refers to λ_{\max} of the transient at 300-350 nm.

^b Very rapid decay prevented accurate determination of absorption spectrum.

The relative amounts of the nitrenium ion and the noncationic species can be approximately expressed as ratios of optical densities, as given in Table 5. It is noteworthy that the substituent position in the phenyl ring has an effect on these ratios, with the ratio for *para*-substituted compounds apparently greater than that for the corresponding *meta*-substituted analogues. The trend suggests that substitution at the *para* position of the phenyl ring favors the formation of the nitrenium ion. This is most prominent in the case of 4-azido-4'-methylbiphenyl (Figure 8), which gave a large cation signal with little non-cationic species (compare with the 3'-methyl analogue in Figure 9). On the other hand, laser irradiation of 4-azido-3,5-dimethylbiphenyl gave a much greater signal at 300-350 nm than the transient at 400-500 nm (Figure 10).

As seen in Table 5, the substituents do have a small effect on the λ_{max} of the nitrenium ions. In general, λ_{max} increases with greater electron donation. This trend is similar to that observed in benzylic-type cations. For example, the λ_{max} (in acetonitrile) for diarylmethyl cations 4-X-C₆H₄C⁺HPh are 425 nm (X = CF₃), 435 (H), 436 (F), 456 (Cl), 450 (Me), and 455 (MeO).⁸³ Similarly, cumyl cations 4-X-C₆H₄C⁺(CH₃)₂ in (CF₃)₂CHOH have λ_{max} at 325 nm (X = H), 340 (4-Me), and 360 (4-MeO).⁸⁴ While it is risky to base structural conclusions on absorption maxima, the similar behavior is at least consistent with the idea that there is a significant benzylic-type interaction between the ring bearing the substituent and the positive charge.

Also worth noting is the λ_{max} at 502 nm of the persistent 4-biphenylnitrenium ion **24** obtained by anodic oxidation of the corresponding aniline derivative in acetonitrile.⁵⁶ This cation is obviously analogous to **44** except for the additional t-butyl groups ortho to the formal nitrenium ion center. While the effect of these groups is unknown, the λ_{max} for **24** clearly falls within the same pattern that was observed with **44**. One interesting feature with **24** is that the t-butyl groups exhibit non-equivalent signals in the ¹H NMR spectrum. This clearly points

to a non-linear $-N^+H$ moiety, whose geometry is fixed on the NMR time scale by extensive charge delocalization, such as shown in structure **24a**.

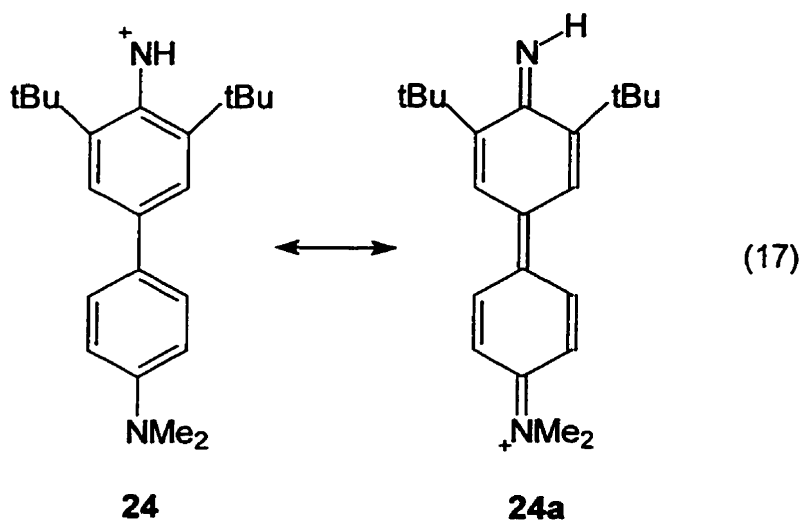
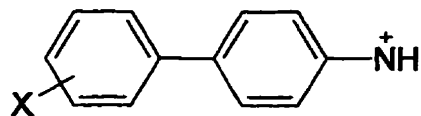


Table 6. Rate constants k_w and k_{az} for X'-substituted-4-biphenylnitrenium ions **44** at 20°C in 20% or 40% acetonitrile:water at zero ionic strength.



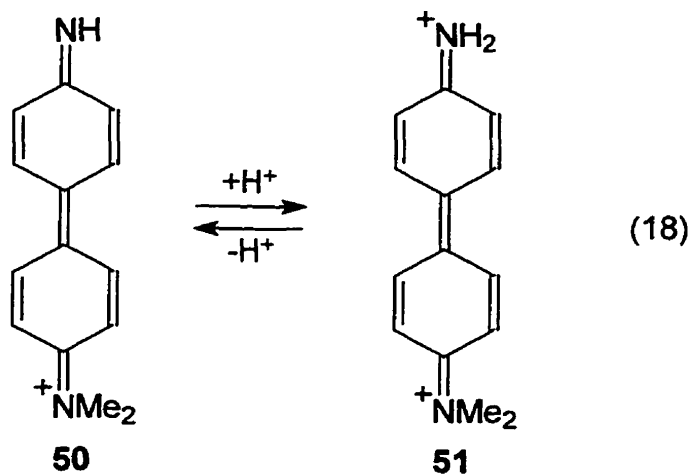
X'	k_w , s ⁻¹ (20%)	k_w , s ⁻¹ (40%)	k_{az} , M ⁻¹ s ⁻¹ (20%)	k_{az}/k_w , M ⁻¹
4'-OMe	$1.58 \pm 0.04 \times 10^3$	$1.95 \pm 0.06 \times 10^3$	6.12×10^9	3.87×10^6
4'-Me	$2.74 \pm 0.04 \times 10^5$	$3.04 \pm 0.05 \times 10^5$	9.16×10^9	3.34×10^4
4'-F	$1.32 \pm 0.02 \times 10^6$	$1.65 \pm 0.03 \times 10^6$	9.38×10^9	7.11×10^3
3'-Me	$1.50 \pm 0.02 \times 10^6$	$1.62 \pm 0.02 \times 10^6$	9.20×10^9	6.13×10^3
3'-OMe	$2.46 \pm 0.03 \times 10^6$	$2.54 \pm 0.04 \times 10^6$	7.85×10^9	3.19×10^3
4'-Cl	$2.53 \pm 0.01 \times 10^6$	$3.06 \pm 0.06 \times 10^6$	1.00×10^{10}	3.95×10^3
None	$2.70 \pm 0.04 \times 10^6$	$2.91 \pm 0.03 \times 10^6$	9.6×10^9	3.56×10^3
3'-Cl	$1.30 \pm 0.04 \times 10^7$	$1.41 \pm 0.04 \times 10^7$	1.02×10^{10}	7.85×10^2
4'-CF ₃	$3.77 \pm 0.10 \times 10^7$	$4.08 \pm 0.21 \times 10^7$	Not measured ^a	
2,6-Me ₂	$1.48 \pm 0.02 \times 10^5$	Not measured	8.44×10^9	5.70×10^4

^a Because of very rapid decay in solvent alone.

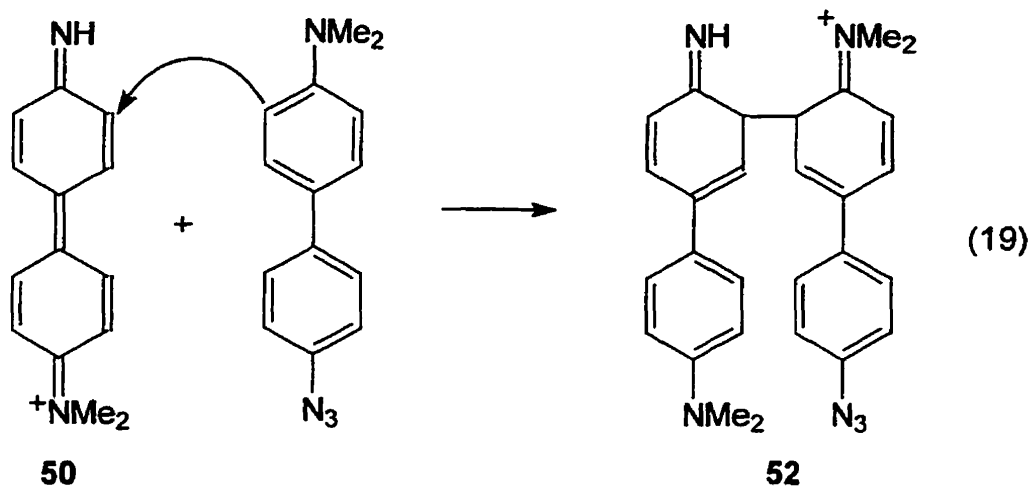
1.3. LFP Study of 4-Azido-4'-(N,N-dimethylamino)biphenyl

Besides the 4-biphenylnitrenium ions discussed above, preliminary studies were also carried out with the 4'-(N,N-dimethylamino) compound. As shown in Figure 15, irradiation of this compound at 248 nm in 20% acetonitrile gave a quite different transient absorption spectrum. First, there is an overlap between the transients and the precursor in the region of 300-360 nm, shown by the signal with negative optical density in this region. Second, there is not a single absorbance maximum between 400-500 nm. This may indicate that there is more than one transient. Two possible transients could form by the following routes.

(1) A dication (**51**) could be formed by protonation of the originally-formed nitrenium ion **50**:



(2) Nucleophilic attack of the unreacted 4-azido-4'-(N,N-dimethylamino)biphenyl, which is a very strong nucleophile, on the nitrenium ion **50**, would generate a second cation (**52**):



The transients are also very stable, not decaying on the second time-scale (by using conventional flash photolysis). This is not surprising on the basis of a comparison of the patterns of substituent effects on the values of k_w for 4-biphenylnitrenium ions and triarylmethyl cations. As shown in Table 7, for triarylmethyl cations, the k_w for the 4-methoxy cation is two orders of magnitude smaller than that for the parent, with the k_w for the 4-NMe₂ a further five orders of magnitude smaller.⁸⁵ With the 4-biphenylnitrenium ions, the 4-methoxy derivative is three orders of magnitude more stable than the parent. If the analogy to the triarylmethyl cations were to extend to 4-NMe₂, the k_w for this cation could be in the range of 10^{-3} - 10^{-4} s⁻¹.

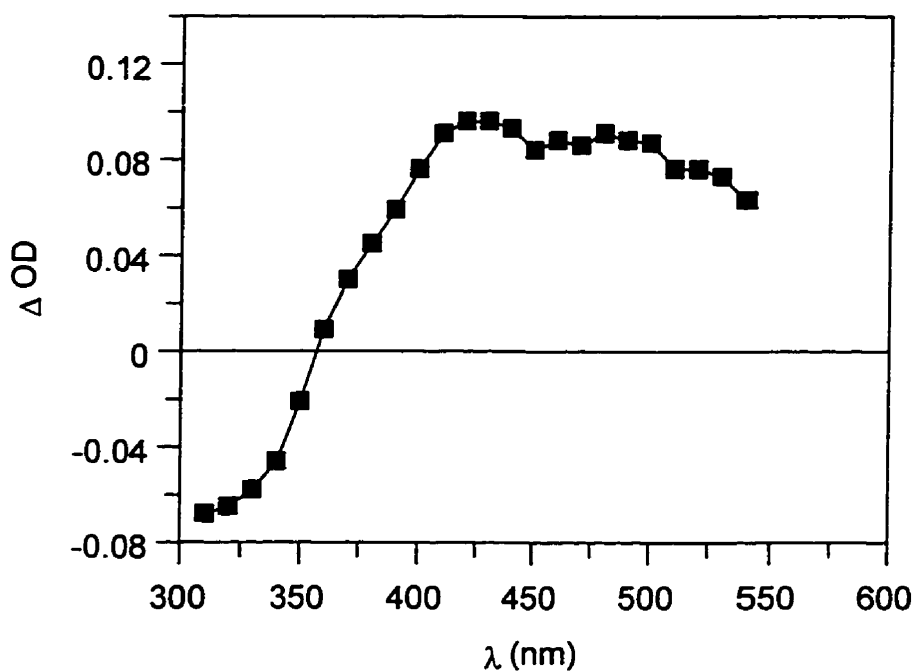


Figure 15. Transient spectrum obtained upon 248-nm irradiation of **4-azido-4'-(N,N-dimethylamino)biphenyl** in 20% acetonitrile:water.

Table 7. A comparison of the rate constants k_w for selected triarylmethyl cations and 4-biphenylnitreniums.

Substituents	k_w (Triphenylmethyl cation), ^a s ⁻¹	k_w (4-Biphenylnitrenium ion), s ⁻¹
None	1.5×10^5	2.7×10^6
4-MeO	1.4×10^3	1.6×10^3
4-NMe ₂	9×10^{-3}	ca. $10^{-3} - 10^{-4}$ (?)

^a Ref. 85.

1.4. Reactivities of X'-substituted-4-biphenylnitrenium ions toward Solvent and Added Nucleophiles

The decay of the nitrenium ions followed excellent exponential kinetics. Rate constants from replicate measurements agreed within $\pm 3\%$. Second-order rate constants for trapping of the nitrenium ions by added nucleophiles were obtained by irradiating precursor azides in the presence of an excess of these nucleophiles. The observed pseudo first-order rate constants of the decay were then plotted against the concentrations of the nucleophile. These plots were linear, and second-order rate constants were calculated as the slopes.

1.4.1. Absolute rate constants for water and substituent effect on solvent reactivities

Values of rate constants k_w for the entire set of nitrenium ions are given in Table 6. Although no study of solvent effect was attempted, k_w values were measured in 20% and 40% acetonitrile:water. A small increase ($\sim 10\%$) in k_w was observed in 40% acetonitrile. A similar increase in k_w was also observed with diaryl- and triarylmethyl cations.⁸⁵

Despite the fact that the change is taking place in the phenyl ring remote from the formal N^+ center, substituents have a pronounced effect on the lifetime of **44**. From the least reactive, 4'-methoxy, to the most reactive, 4'-trifluoromethyl, there is a change of over four orders of magnitude.

In attempting a quantitative correlation of the effect of aromatic substituents on the reactivities of 4-biphenylnitrenium ions, a single parameter Hammett plot was initially constructed by employing σ^+ as the substituent constants. As shown in Figure 16A, however, the correlation of $\log k_w$ with this parameter is poor, with points for the para π -electron donors, especially 4'-methoxy, deviating significantly from the correlation line based on the other substituents. Moreover, the deviations are in the unusual direction of requiring a more negative substituent parameter in

order for the points to fit on the line, indicating that σ^+ underestimates resonance effects of the π donors for the cation.

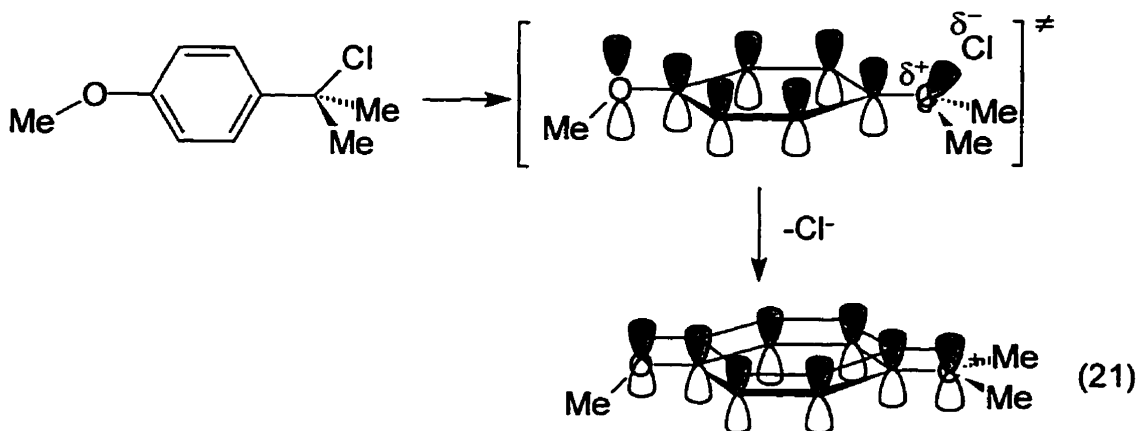
Similar behavior has been previously seen with benzylic-type cations **53-55** (see Table 7).^{64,85,86} More satisfactory fits can be obtained by correlating the data for these cations according to the two-parameter Yukawa-Tsuno equation (eq. 20).⁸⁷

$$\log(k_w/k_w^0) = \rho[\sigma + r^*(\sigma^+ - \sigma)] \quad (20)$$

This equation represents a modification of the Hammett equation. The original objective was to fit kinetic data for systems where the interactions with substituents lie between the σ and σ^+ scale. In other words, the r^* parameter was intended to range from 0 to 1. Obviously a correlation where $r^* = 0$ corresponds to a single parameter correlation against σ , while $r^* = 1$ represents a single parameter correlation against σ^+ . As shown in Table 8, a feature of the carbocation systems is that r^* values significantly greater than 1 are required to fit the data.

This behavior arises since the σ^+ scale considerably underestimates the resonance interaction of π electron donors in reactions involving fully formed cations. The σ^+ scale is based on rate constants for ionization of substituted cumyl chlorides. In the transition state for this reaction, the benzylic carbon has developed a significant positive charge, but it has not fully developed the sp^2 hybridization required for complete overlap with the aromatic π system (eq. 21). There is in fact good evidence that the resonance interaction lags behind C-Cl bond breaking.^{57,64} Thus the resonance interaction with a group such as *p*-methoxy is only fractionally developed in the transition state, while in the fully formed cation there is a full resonance interaction. Thus reactions that start at the cation require a substituent scale that provides a greater resonance interaction

than the σ^+ scale. In term of the Yukawa-Tsuno treatment, this manifests itself in r^+ values greater than unity.



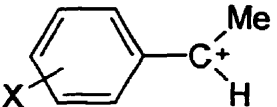
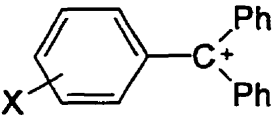
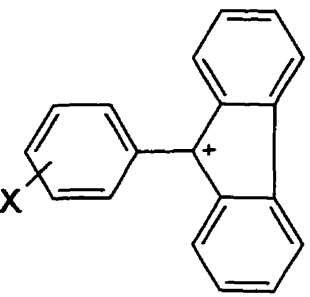
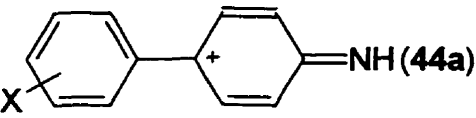
The Yukawa-Tsuno treatment was applied to the hydration of 4-biarylnitrenium ions, and the best fit was achieved for the experimental data with $r^+ = 2.8$. This fit is illustrated in Figure 16B; as shown in this figure, the methoxy substituent in a 4-biarylnitrenium ion behaves as if it has a “ σ ” constant of -1.7.

The ρ and r^+ parameters for the 4-biarylnitrenium ions are listed in Table 8 along with their product $r^+\rho$, which can be equated to a resonance ρ^+ value. Comparison with the values for **53-55** shows very clearly that substituents in the remote phenyl ring of a 4-biarylnitrenium ion interact with the positive charge very much as if this cation were a benzylic cation, i.e. as if the structure is **44a**. This conclusion is particularly evident when the “inherent” reactivities, the rate constants for the derivatives with $X = H$, are considered. The least stable and most reactive cation is the phenethyl cation, which has only one other stabilizing substituent, a methyl group, on the C^+ center. This system has the largest values of ρ and ρ^+ , indicating the greatest interaction with the aryl ring. The most stable and least reactive cation is the triphenylmethyl cation, which has two more phenyl groups on the C^+ center than the phenethyl cation. As expected, this system has

smaller values of ρ and ρ^* since there is less of a demand for stabilization by substitution in one ring. (The fluorenyl system **55** is not included in this comparison, since the 9-aryl ring is twisted considerably from coplanarity with the positively charged carbon, thus attenuating the substituent effect.) The 4-biphenylnitrenium ions written as **44a**, can be viewed as benzylic cations with two stabilizing vinyl substituents, i.e. $\text{Ar-C}^+(\text{C}=\text{C})_2$. The reactivity of this system lies intermediate between phenethyl and triphenylmethyl cations, albeit closer to the latter. The substituent effects are also intermediate, again closer to triphenylmethyl cations.

The similarity of the reactivity of biphenylnitrenium ion to that of triarylmethyl cations can be further illustrated by plotting $\log k_w$ data for one cation type versus the other. As shown in Figure 17, good linearity is observed. And again, the nitrenium ions are more sensitive to substituent change, as shown by the slope in Figure 17 being greater than one (1.51).

Table 8. Parameters from two-parameter analysis of rate constants for solvent addition to benzylic-type cations **53-55**^a and 4-biphenylnitrenium ions **44a**.

cation	ρ	$\rho^* = r^*\rho$	r^*	k_s (X = H), s ⁻¹
 (53)	+2.7	+6.1	2.3	$\sim 1 \times 10^{11}$ ^b
 (54)	+1.3	+4.7	3.6	1.5×10^5
 (55)	+1.3	+2.8	2.2	1.5×10^7
 (44a)	+1.8	+5.0	2.8	2.7×10^6

^a Data for **53** refer to 50:50 2,2,2-trifluoroethanol:water and are from ref. 64. Data for **54** refer to 1:2 acetonitrile:water and are from ref. 85. Data for **55** refer to 1:4 acetonitrile:water and are from ref. 86.

^b Estimate (ref. 64).

Figure 16. Linear free energy correlations. Figure 16A shows a single parameter correlation of $\log k_w$ versus the Hammett σ^+ substituent constants. The line in this figure (slope = 2.0) is the least-squares line calculated for the solid squares, representing the 4'-CF₃, 3'-Cl, 3'-MeO, 3'-Me, and unsubstituted cations. Figure 16B plots $\log k_w$ versus $\sigma + r^+(\sigma^+ - \sigma)$, where the value of $r^+ = 2.8$ has been obtained from application of the two parameter Yukawa-Tsuno equation. The line drawn in this figure (slope = 1.8) is the least-squares line for all points. Values of σ^+ and σ are taken from Ref. 88.

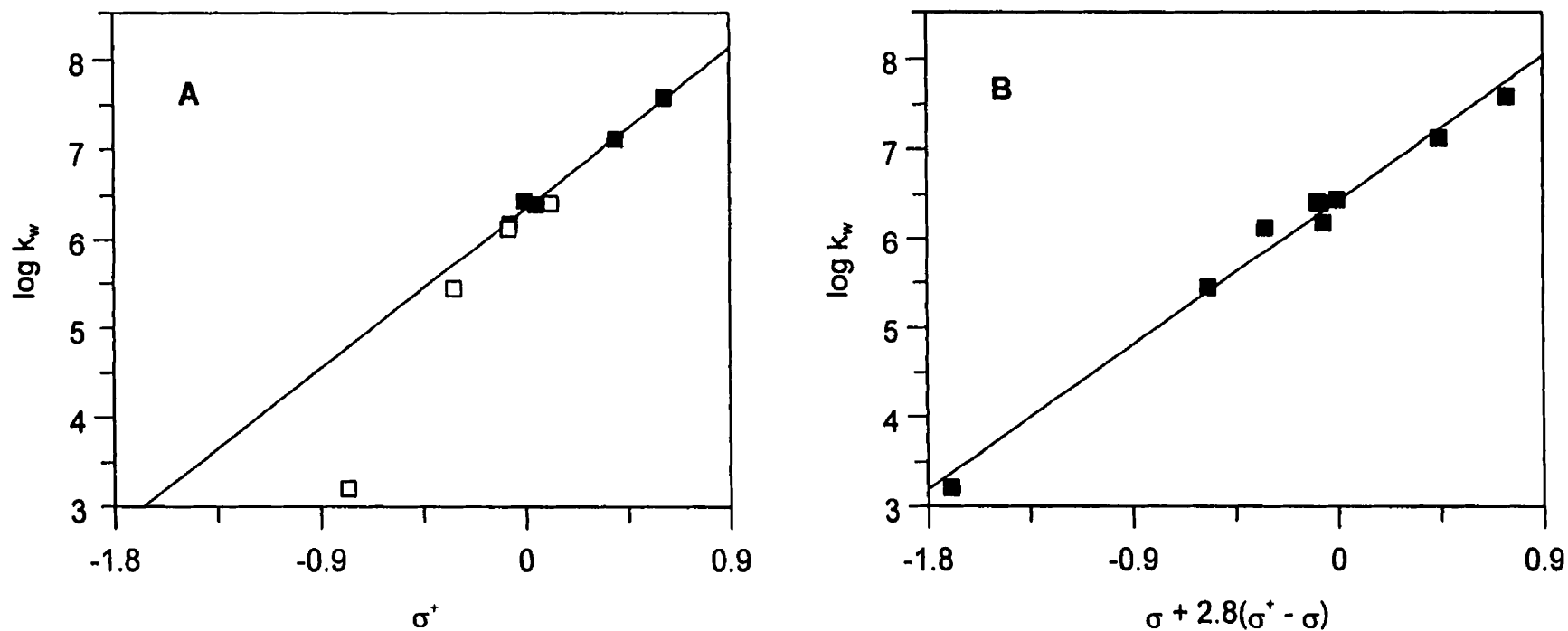
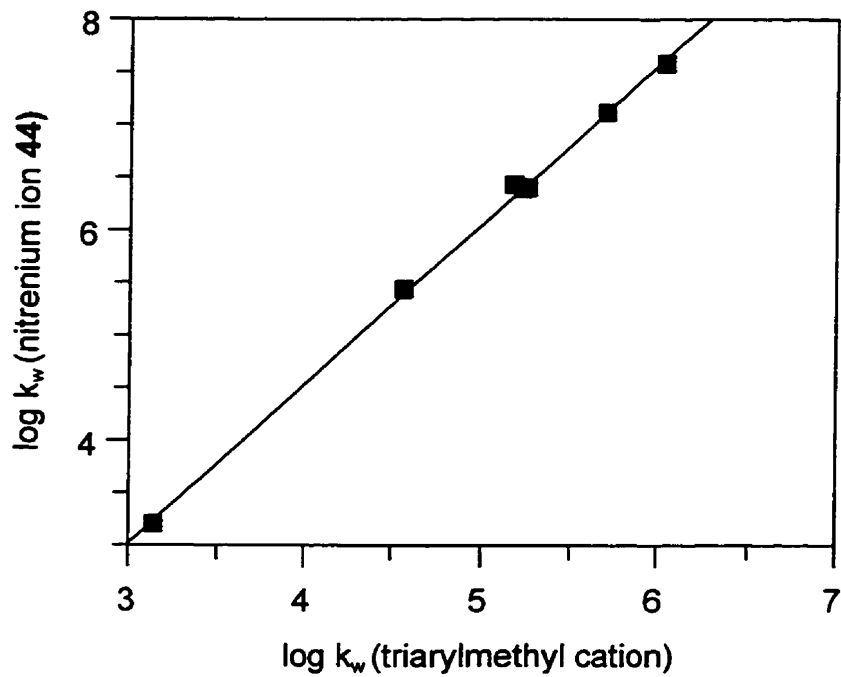


Figure 17. Linear correlation of $\log k_w$ for nitrenium ions **44** and appropriately substituted triarylmethyl cations ($\text{XC}_6\text{H}_4\text{C}^+\text{Ph}_2$). Rate constants for triarylmethyl cations are taken from Ref. 85.



1.4.2. Reactivity toward other Nucleophiles

(1) Azide ion

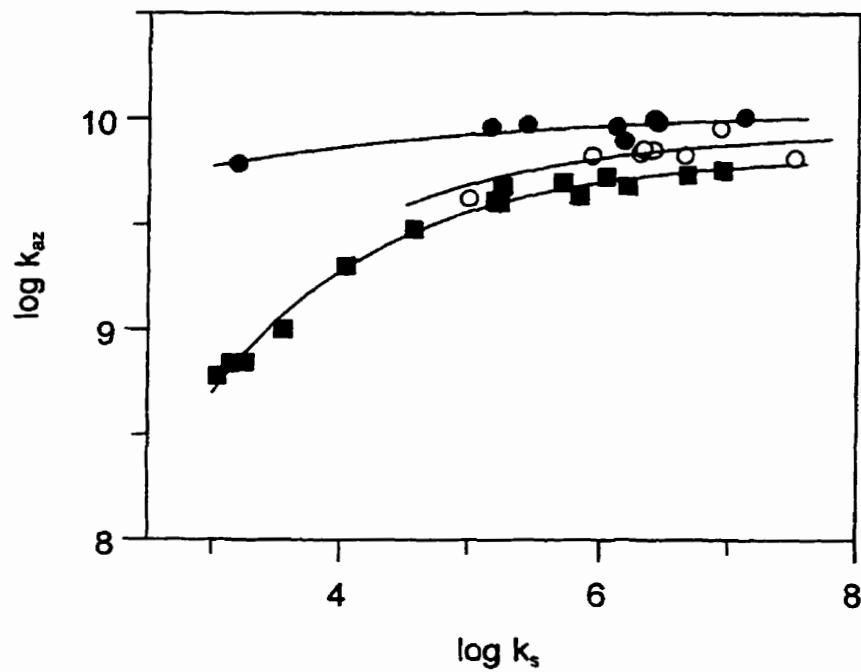
The absolute k_{az} values for the parent 4-biphenyl- and 2-fluorenylnitrenium ions **15a**, **15b**, **20**, and **33** have suggested that arylnitrenium ions react with azide ion at or near the diffusion limit. The data in Table 6 show that this is indeed the case. Despite a change of over four orders of magnitude in k_{w} , the values of k_{az} all lie within the range $6\text{-}10 \times 10^9 \text{ M}^{-1}\text{s}^{-1}$, with the majority in the range of $9\text{-}10 \times 10^9$. This is illustrated graphically in Figure 18, where the values of $\log k_{\text{az}}$ for **44** are plotted against the values of $\log k_{\text{w}}$ for the same cation. This figure also contains similar plots for two benzylic-type cations, a series of diarylmethyl cations in 20% acetonitrile:water and a series of triarylmethyl cations in 33% acetonitrile:water.^{89,90} The pattern of behavior with all these cation types is identical. As substituents in the aromatic ring are changed to more electron withdrawing (or less electron donating), the reactivity of the cation with water increases. This is of course expected, since the cation is becoming less stable. Starting with the most stable, least reactive, cation in each series, changing the substituent to more electron withdrawing also results in an increase in k_{az} . This increase however is much smaller than the change in k_{w} . Moreover, at the point where the cations have k_{w} of the order $10^4\text{-}10^5 \text{ s}^{-1}$, further destabilization results in no further increase in k_{az} , within experimental error. In other words, the rate constants k_{az} within each series become constant, independent of the aromatic substituent.

It can be noted that the rate constant calculated for a diffusion-controlled cation-anion encounter from the Debye-Smoluchowski equation in 30% acetonitrile:water is $\sim 1.5 \times 10^{10} \text{ M}^{-1}\text{s}^{-1}$.⁸⁹ As shown in Figure 18, the limiting k_{az} that are observed are smaller than this value. Moreover, there is a slight dependence on structural type. The nitrenium ions have a limit of $\sim 1 \times 10^{10} \text{ M}^{-1}\text{s}^{-1}$, diarylmethyl cations in the same solvent have a limit of $\sim 7 \times 10^9 \text{ M}^{-1}\text{s}^{-1}$, and triarylmethyl cations have a limit of $\sim 5 \times 10^9 \text{ M}^{-1}\text{s}^{-1}$. The smaller observed limit has been explained

through a model of nonproductive encounters. In other words, the anion and cation diffuse together, but cannot actually combine for steric reasons. The slightly higher limit for the arylnitrenium ions would suggest that there are fewer of these nonproductive encounters with this system, i.e. there is less steric hindrance.

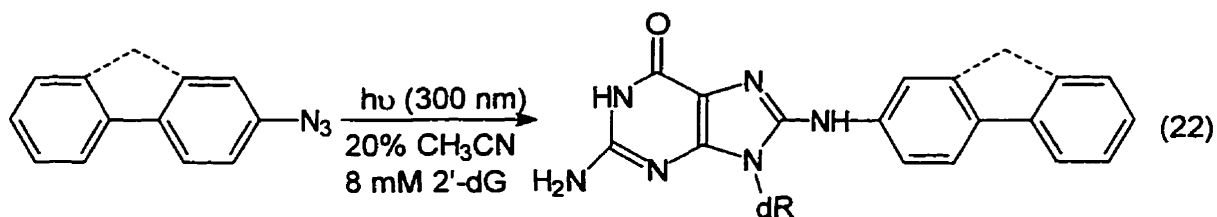
It should also be noted that the data in Table 6 and Figure 18 refer to solutions that have effectively zero ionic strength. Addition of salts can have significant effects on cation lifetime and azide reactivity.⁹¹ The k_w value for **15b** at 20% acetonitrile at zero ionic strength is measured as $2.7 \times 10^6 \text{ M}^{-1}\text{s}^{-1}$, a 50% increase as compared to the value of $1.8 \times 10^6 \text{ M}^{-1}\text{s}^{-1}$ upon addition of 0.5 M NaClO_4 . Whereas the limiting k_{az} for the 4-biphenylnitrenium ions is $\sim 5 \times 10^9 \text{ M}^{-1}\text{s}^{-1}$ in 20% acetonitrile containing 0.5 M NaClO_4 , the value in the absence of salts is $1 \times 10^{10} \text{ M}^{-1}\text{s}^{-1}$ (Table 6).

Figure 18. Variation in k_{az} ($M^{-1}s^{-1}$) as a function of the rate constants k_s (s^{-1}) for decay in the same solvent. Closed circles, 4-biarylnitrenium ions; open circles, diarylmethyl cations; closed squares, triarylmethyl cations.



(2) Guanine

The reactivity and selectivity of nitrenium ions toward guanine derivatives are important factors that may affect the carcinogenic potentials of ultimate carcinogen metabolites of aromatic amines. As seen in Table 2, data previously obtained for the 4-biphenyl and 2-fluorenylnitrenium ions **15a**, **15b**, and **20** show that the rate constants for the quenching with 2'-deoxyguanosine are very large, possibly approaching the diffusion limit. This quenching does represent the formation of the C8 adduct. As noted in the introduction, this is evidenced by the good agreement of k_{dG}/k_w ratios obtained with LFP and by product analysis. Product analyses carried out in our laboratories (McClelland and Kahley, unpublished) have recently shown that the C8 adduct is the only product derived from 2'-deoxyguanosine when 2-azidofluorene and 4-azidobiphenyl are irradiated in the presence of the nucleoside.



dR = 2'-deoxyribose.

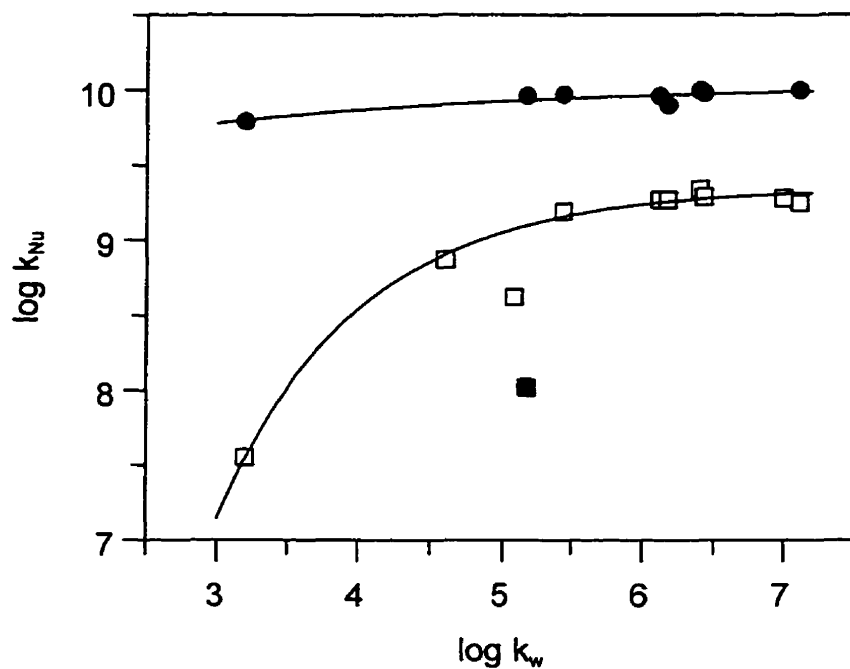
Yield \approx 75% in each case.

The availability of the series of structurally related aryl nitrenium ion **44** now provides the opportunity to probe the pattern of dG reactivity. The absolute rate constants are given in Table 9, along with k_{dG}/k_w ratios. Figure 19 shows a plot of $\log k_{dG}$ vs $\log k_w$ including data for all nitrenium ions. For comparative purpose the plot of $\log k_{az}$ vs $\log k_w$ is also shown.

Table 9. Absolute rate constants for nitrenium ions **44** reacting with 2'-deoxyguanosine (dG) in 20% acetonitrile:water at zero ionic strength.

X	$k_{dG}, M^{-1}s^{-1}$	$k_{dG}/k_w, M^{-1}$
4'-MeO	3.56×10^7	2.25×10^4
2,6-Me ₂	1.04×10^8	6.08×10^2
4'-Me	1.53×10^9	5.58×10^3
4'-F	1.88×10^9	1.42×10^3
3'-Me	1.88×10^9	1.25×10^3
4'-Cl	2.20×10^9	8.70×10^2
None	1.96×10^9	7.26×10^2
3'-Cl	1.76×10^9	1.35×10^2

Figure 19. Variation in k_{dG} ($M^{-1}s^{-1}$) and k_{az} ($M^{-1}s^{-1}$) in 20% acetonitrile:water for 4-biphenylnitrenium ions as a function of k_w (s^{-1}) for decay in the same solvent. Closed circles, $\log k_{az}$ vs $\log k_w$; open squares, $\log k_{dG}$ vs $\log k_w$. The points deviating from the line represent rate constants for 2,6-dimethyl-4-biphenylnitrenium ion (closed square) and N-acetyl-2-fluorenylnitrenium ion (open square).



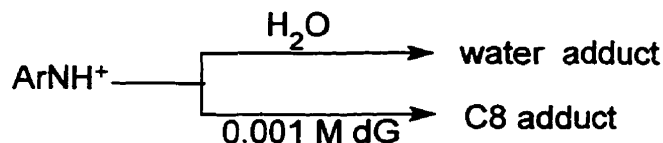
What is immediately apparent is that the k_{dG} data for the 4-biphenylnitrenium ions follow the same pattern as the k_{az} data. Thus the 4'-methoxy cation reacts with dG more slowly than the others, and so does the 4'-methyl cation, although here the difference is small. The remainder of the cations all react with the same rate constant, within experimental error. It would then appear that the reaction of dG with these nitrenium ions has reached a limit, with a rate constant of around $2 \times 10^9 \text{ M}^{-1}\text{s}^{-1}$. It can be argued that this represents a diffusion-limited rate constant. The value is 5 times smaller than the diffusion-limited rate constant for azide ion. This is a typical difference between the diffusion-limit for a cation-anion encounter and a cation-neutral encounter. The former situation benefits from electrostatic attraction when the reacting pair approach one another. This results in a greater number of encounters per unit time compared to the combination with the neutral nucleophile.

It is interesting to note that the 2,6-dimethyl derivative deviates from the plot. This cation has a similar k_w to the 4'-methyl compound, but reacts with dG 15 times slower. The details of the mechanism for the formation of the C8 guanine adduct have not been unambiguously established.^{92,93} Three possibilities are illustrated in Scheme 11. Reaction A involves straightforward electrophilic addition to C8 to give a resonance stabilized cation **56** that simply loses a proton to give the product. Reaction B involves initial addition of the nitrenium ion at N7 forming a cation **57** that could either rearrange to **56**, or lose the C8 proton to form **58**. The initial formation of an adduct such as **57** has been suggested in the literature.⁹² Reaction C also involves N7 but in this case reacting at the *ortho* position to give an adduct **59**. Cyclization to **60** connects the nitrogen of the nitrenium ion to C8. Deprotonation would then unzip the molecule to give the C8 adduct.

The slower reaction of the 2,6-dimethyl compound would appear to offer support for mechanism C, with steric crowding retarding the initial bond formation. However, the effect is quite small. Steric effects of a similar magnitude could also operate for the other two mechanisms. Interestingly also, the reaction of the 2,6-

dimethyl compound with ethyl vinyl ether is not unusually slow, despite the fact that in this case the reaction would appear to involve initial reaction at an *ortho* position (see next section). In conclusion, the effect with the 2,6-dimethyl compound is not sufficient to distinguish the mechanisms of Scheme 11.

Also interesting are the k_{dG}/k_w ratios that indicate very high selectivities of these nitrenium ions for 2'-deoxyguanosine. The data also imply that the more stable the 4-biphenylnitrenium ion, the more selective for 2'-deoxyguanosine. This can be shown by calculating the percentage of nitrenium ion that reacts with 2'-deoxyguanosine in an aqueous solution containing one millimolar of the nucleoside:



This percentage is calculated as below:

$$\% \text{ C8 adduct} = 100 \times \left(\frac{0.001k_{dG}}{k_w + 0.001k_{dG}} \right) \quad (23)$$

The numbers are given in Table 10. For the most stable and least reactive nitrenium ions such as the 4'-MeO and 2-fluorenyl which have k_{dG}/k_w of over 10^4 M^{-1} , ca. 95% of them would be quenched by 1 mM 2'-deoxyguanosine. On the other hand, for the most reactive nitrenium ions such as 3'-Cl, only ~12% will be quenched. For nitrenium ions with k_{dG}/k_w ratios of $>10^3 \text{ M}^{-1}$, a substantial amount (>50%) would be quenched.

Scheme 11. Possible mechanisms for the formation of the C8 adduct by reaction of nitrenium ion with 2'-deoxyguanosine.

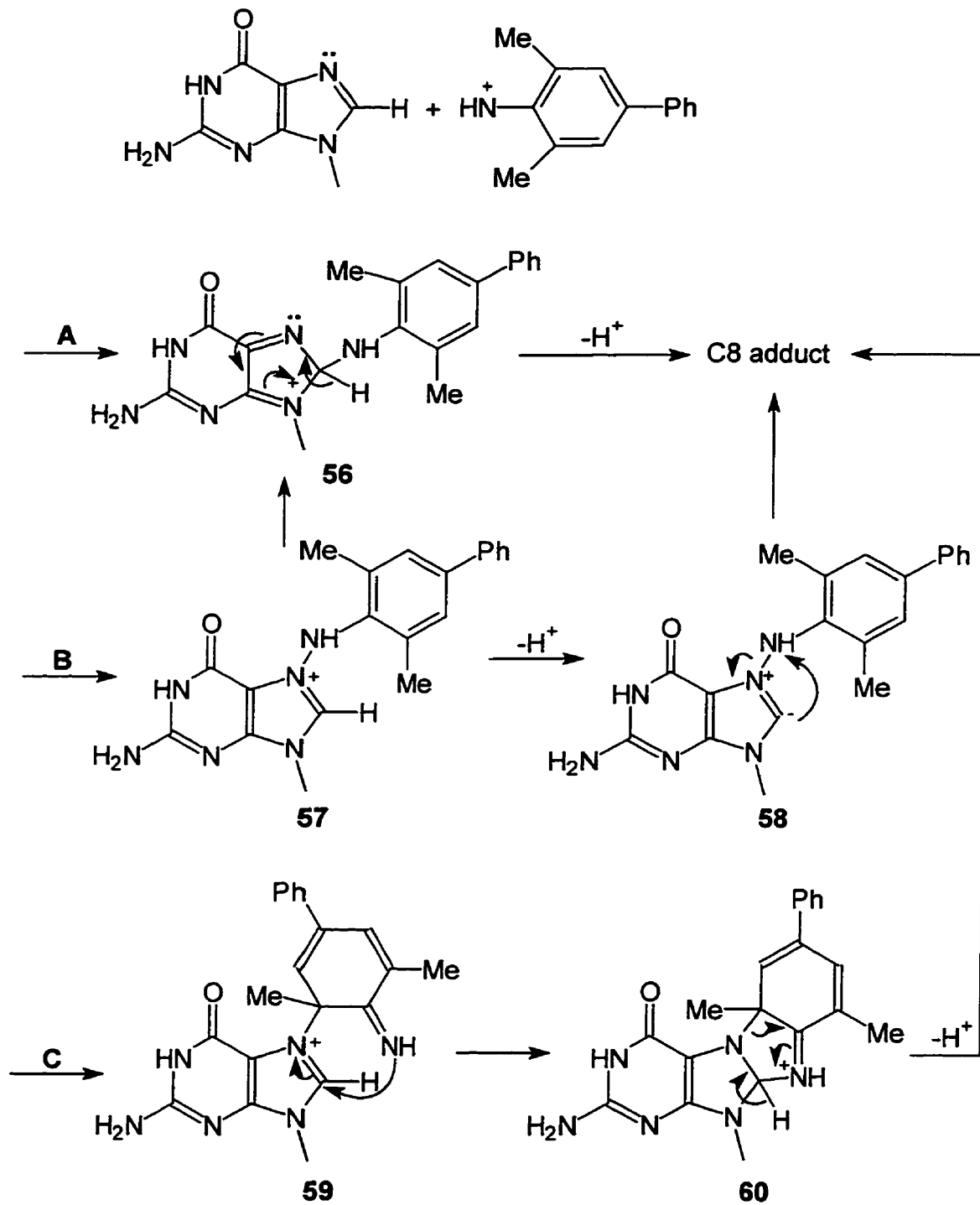


Table 10. Percentages of nitrenium ions that react with 2'-deoxyguanosine to form the C8 adducts in 1 mM aqueous solutions of the nucleoside (calculated from rate constants k_{dG} and k_w).

Substituent(s)	% C8 adduct
4'-MeO	95.7
2,6-Me ₂	41.3
4'-Me	84.9
4'-F	58.6
3'-Me	55.2
4'-Cl	46.6
None	42.0
3'-Cl	12.1
N-Ac ^a	16.0
N-Ac (2-fluorenyl) ^a	77.7
None (2-fluorenyl) ^a	94.9

^a Ref. 58 (ionic strength 0.5 M, adjusted with NaClO₄).

(3) Ethyl vinyl ether

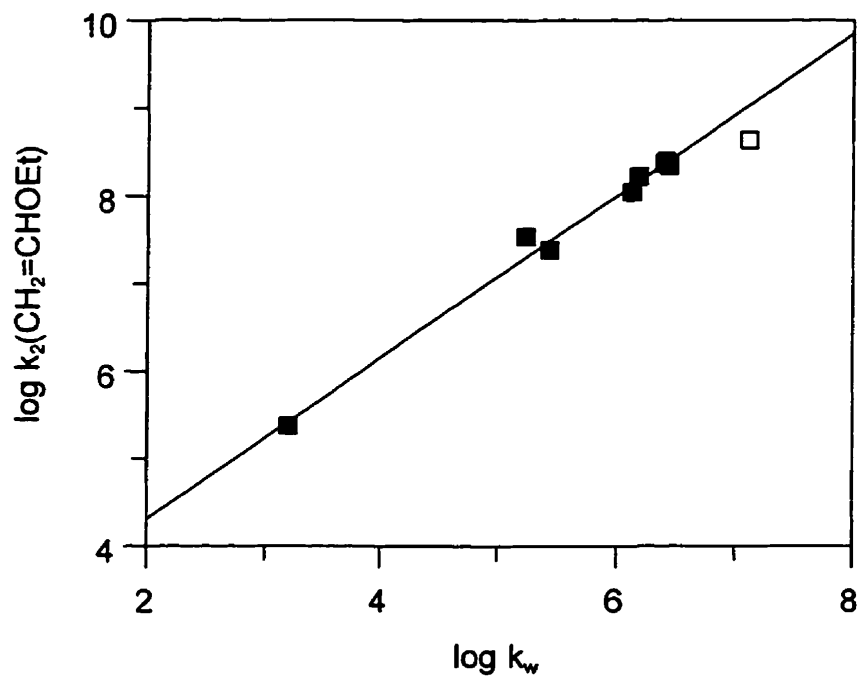
The electrophilic reactivity of nitrenium ions **44** toward the π -nucleophile ethyl vinyl ether was also investigated. The second-order rate constants $k_2(\text{CH}_2=\text{CHOEt})$, and the ratio of $k_2(\text{CH}_2=\text{CHOEt})/k_w$ are listed in Table 11. From these data, a quite different reactivity pattern is observed, as compared to that for azide ion and deoxyguanosine. While the latter react with most nitrenium ions at or near diffusion limit, it appears that rate constants for the trapping of nitrenium ions by ethyl vinyl ether are dependent on the kinetic stability of the nitrenium ions. In fact as demonstrated in Figure 20, the values of $\log k_2(\text{CH}_2=\text{CHOEt})$ correlate very well with the values of $\log k_w$. The plot is linear with a slope close to 1 (0.92), implying an almost constant selectivity of the series of 4-biphenylnitrenium ions toward ethyl vinyl ether. Indeed, the values of $\log k_2(\text{CH}_2=\text{CHOEt})/k_w$ for all nitrenium ions but the 3'-chloro one are close to 2.

Mayr and coworkers observed constant selectivity relationships in the addition of diarylcarbenium ions to terminal double bonds.⁶⁷ The relative reactivity of π -nucleophiles is independent of the electrophilicity of the carbenium ions over a reactivity range of at least eight orders of magnitude. As for ethyl vinyl ether, they had only reported its rate constants of reaction with two diarylcarbenium ions: $(p\text{-ClC}_6\text{H}_4)_2\text{CH}^+$ and $(p\text{-MeC}_6\text{H}_4)_2\text{CH}^+$. The rate constants for these two cations differ by about two orders of magnitude, but their selectivities $k_2(\text{CH}_2=\text{CHOEt})/k_2(\text{H}_2\text{O})$ are about same (~ 1 , see Table 3). This represents a comparison of two bimolecular rate constants, both measured in 100% acetonitrile. If it is assumed that the same is true in 100% water, then the selectivity $k_2(\text{CH}_2=\text{CHOEt})/k_w$ is $\approx 10^{-2}$, where k_w is now expressed in unit of s^{-1} , as is the case in Table 10. It can thus be seen that the selectivity of diarylcarbenium ions toward ethyl vinyl ether is much lower than that of 4-biphenylnitrenium ions.

Table 11. Absolute rate constants for X-substituted-4-biphenylnitrenium ions **44** reacting with ethyl vinyl ether in 20% acetonitrile:water at zero ionic strength.

X	$k_2(\text{CH}_2=\text{CHOEt}), \text{M}^{-1}\text{s}^{-1}$	$\log [k_2(\text{CH}_2=\text{CHOEt})/k_w]$
4'-MeO	2.37×10^5	2.17
2,6-Me ₂	3.4×10^7	2.29
4'-Me	2.41×10^7	1.94
4'-F	1.10×10^8	1.92
3'-Me	1.65×10^8	2.04
3'-MeO	2.35×10^8	1.98
4'-Cl	2.48×10^8	1.99
None	2.2×10^8	1.91
3'-Cl	4.27×10^8	1.51

Figure 20. The correlation of $\log k_2(\text{CH}_2=\text{CHOEt})$ and $\log k_w$ for 4-biphenylnitrenium ions **44**. The open square represents the rate constant for the 3'-Cl derivative.



1.5. Nitrenium Ions and Carcinogenicity of Aromatic Amines

Aromatic amine carcinogenesis is the result of bioactivation to the ultimate carcinogenic form and then dissociation of the reactive species to give a nitrenium ion. Although the carcinogenic potential of the parent amines and amides is affected in a large part by the metabolic activation process, the reactivity and selectivity of the nitrenium ion toward biological nucleophiles such as guanine will be a determining factor. It is known that single aromatic or nonconjugated ring systems are usually weak carcinogens.¹ This may be related to the very short aqueous lifetimes of the corresponding nitrenium ions so that the trapping of these nitrenium ions by nonsolvent nucleophiles is very inefficient. On the other hand, aromatic amines and amides consisting of two or more conjugated or fused aromatic rings, such as 2-fluorenylamine and 4-biphenylamine and their amides, are potent carcinogens. The nitrenium ions derived from these amines and amides do show a high reactivity and selectivity toward guanine (as shown by the values of k_{dG} and k_{dG}/k_w).⁵⁰

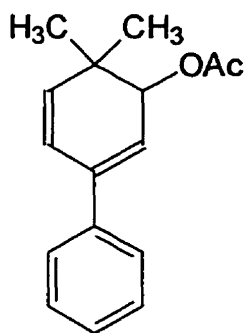
The Wild group reported that the mutagenicities of a series of aryl azides and heterocyclic azides are directly proportional to the stability of the nitrenium ions and inversely proportional to the electrophilicity of the exocyclic nitrogen.⁹⁴⁻⁹⁸ The data used in the correlations for the nitrenium ions were obtained from theoretical calculations.

We believe that the nitrenium ion reactivity and selectivity for biological nucleophiles such as dG should be an index in the correlation of the potential carcinogenicity with the structure of the parent amine. As to the 4-biphenyl series, it has been reported that 4'-fluoro-4-biphenylamine is a more potent carcinogen than the parent 4-biphenylamine.¹ Although this may be affected by other factors such as metabolic activation, the greater selectivity of 4'-fluoro-4-biphenylnitrenium ion for dG as compared to the parent, could be an important factor.

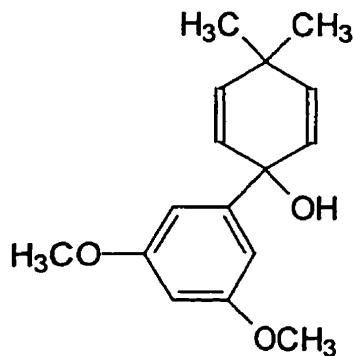
Section 2 Generation of 6,6-Dimethyl-3-phenylcyclohexadienyl Cations and Comparison with the Carbenium Form of 4-Biphenylnitrenium Ions

2.1. Preparation of precursors

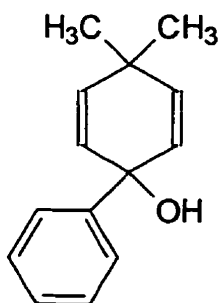
Cyclohexadienyl cations **45** have been generated from four precursors in either the ground state or the excited state: from 6,6-dimethyl-3-phenylcyclohexa-2,4-dien-1-yl acetate (**46**), from 4,4-dimethyl-1-(3',5'-dimethoxyphenyl)cyclohexa-2,5-dien-1-ol (**47**), and from the isomeric alcohols 4,4-dimethyl-1-phenylcyclohexa-2,5-dien-1-ol (**61**) and 6,6-dimethyl-3-phenylcyclohexa-2,4-dien-1-ol (**62**).



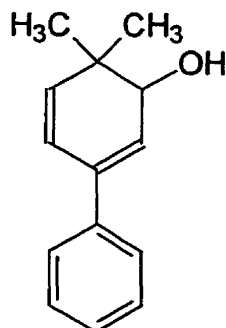
46



47



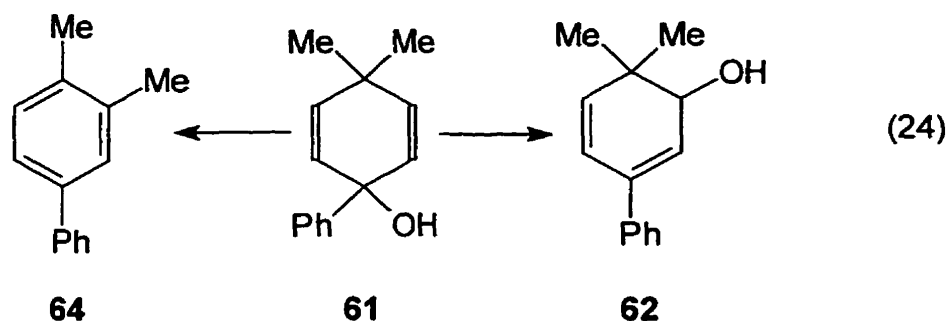
61



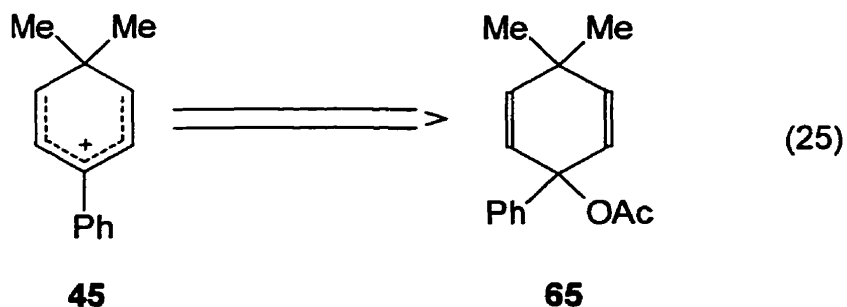
62

The alcohols **47** and **61** were prepared from 4,4-dimethylcyclohexa-2,5-dien-1-one (**63**) by reactions with 3,5-dimethoxyphenyl lithium⁹⁹ and phenyl lithium, respectively. The dienone **63** can be readily obtained by dehydrogenation of 4,4-dimethylcyclohexenone with 2,3-dichloro-4,5-dicyano-1,4-benzoquinone (DDQ)¹⁰⁰ (Scheme 12).

The alcohol **61** is not very stable and it slowly isomerizes to the more thermodynamically stable conjugated alcohol 6,6-dimethyl-3-phenylcyclohexa-2,4-dien-1-ol (**62**). Also formed in this reaction is the biphenyl **64** (eq. 24). Chromatographic separation of the mixture provides both products.

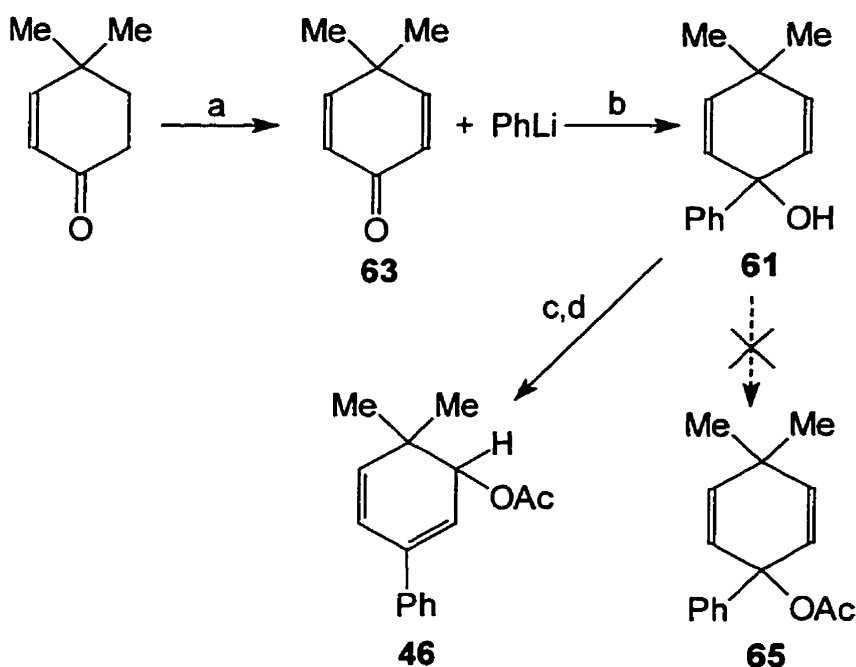


Since acetates have often been employed as precursors in the LFP generation of diaryl and triarylcation ions by photoheterolysis,^{57,90,101} we attempted to prepare 4,4-dimethyl-1-phenylcyclohexa-2,5-dien-1-yl acetate (**65**) as the precursor of the cation **45**.



It was expected that deprotonation of the alcohol **61** with NaH followed by the addition of acetic anhydride would give the acetate **65**. However, the final product turned out to be exclusively (>95%) the acetate **46** derived from the conjugated alcohol **62** (Scheme 12). The structural assignment of **46** were based on the comparison of its ^1H NMR spectra with those of **61** and **62**, particularly the close match of its ^1H chemical shifts and coupling pattern of the protons in the cyclohexadienyl ring with those of the alcohol **62**, as shown in Figures 21-23. Judging from the situation with the parent alcohols, **46** is likely more stable than the acetate **65** and the isomerization to this more stable form could not be prevented.

Scheme 12



a. DDQ, dioxane, reflux, overnight;

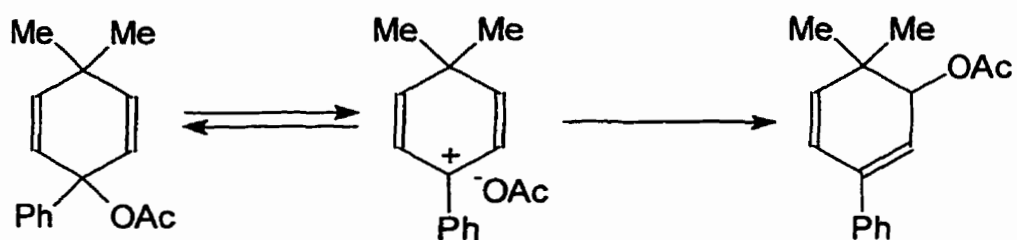
b. hexanes, -78°C ; K_2CO_3 (aq.);

c. NaH, THF, 40°C , 2 hr; d. Acetic anhydride, -78°C .

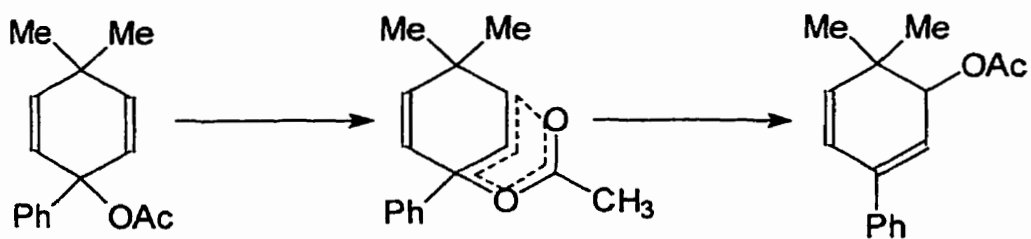
No attempt was made to investigate the mechanism of the acetate isomerization. Two possibilities are shown in Scheme 13. Mechanism A involves the ionization of the acetate **65** to generate a tight ion pair. This ion pair then undergoes internal return with rearrangement to yield the acetate **46**. Mechanism B involves a [3,3]-sigmatropic rearrangement in which two oxygen atoms are present in the reacting system.

Scheme 13

Mechanism A:



Mechanism B:



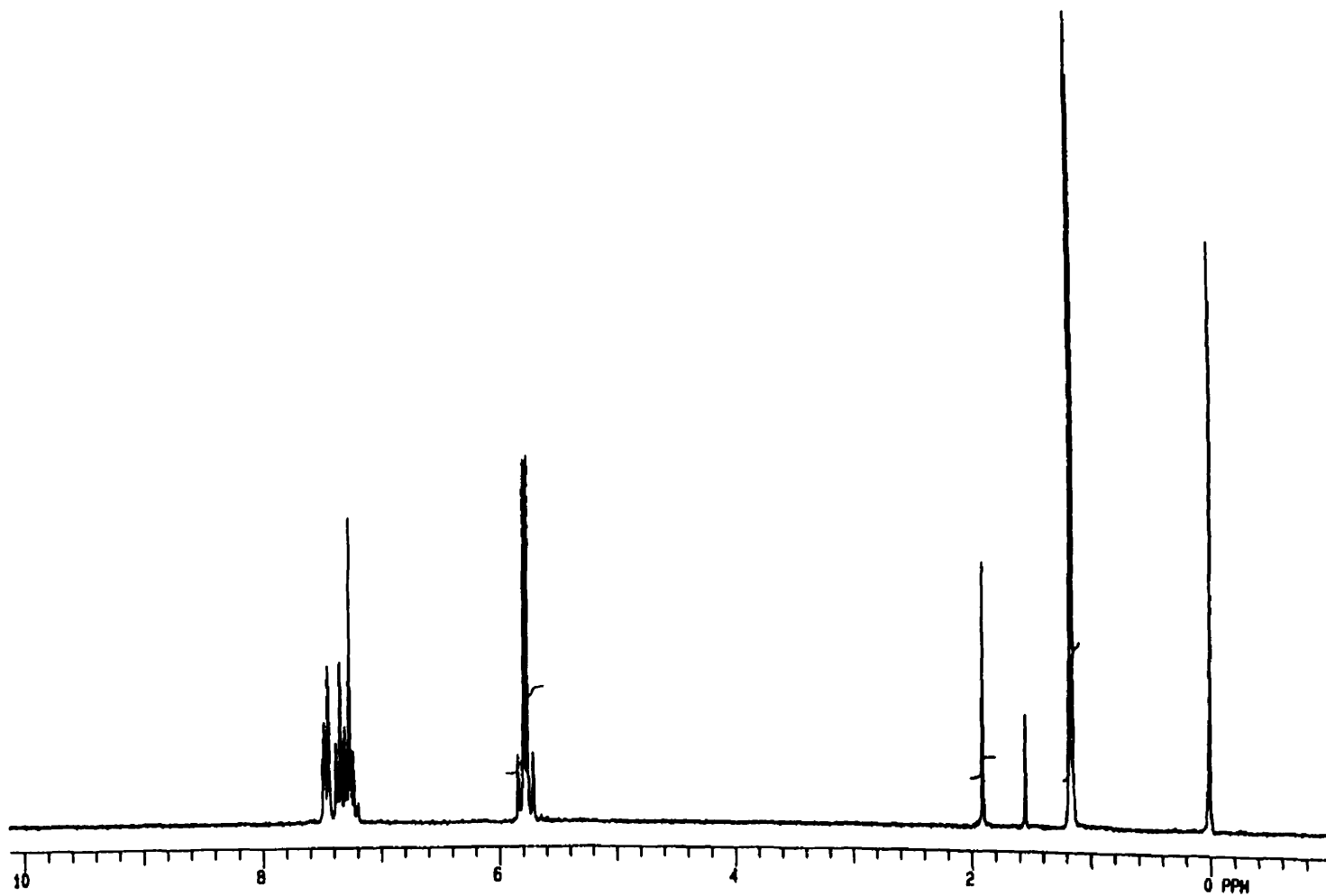


Figure 21. The ^1H NMR of 4,4-dimethyl-1-phenylcyclohexa-2,5-dien-1-ol (**61**).

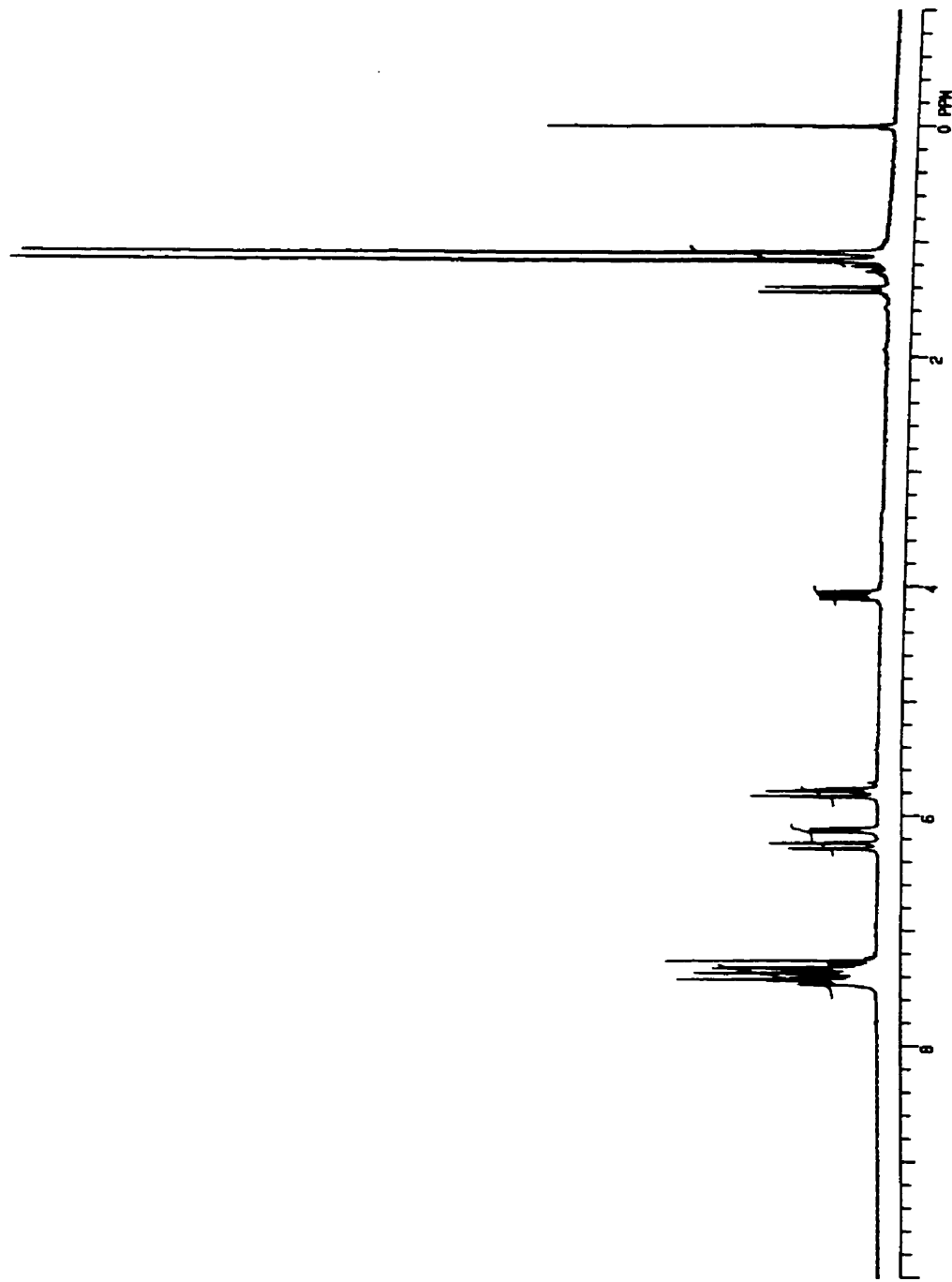


Figure 22. The ^1H NMR of 6,6-dimethyl-3-phenylcyclohexa-2,4-dien-1-ol (62).

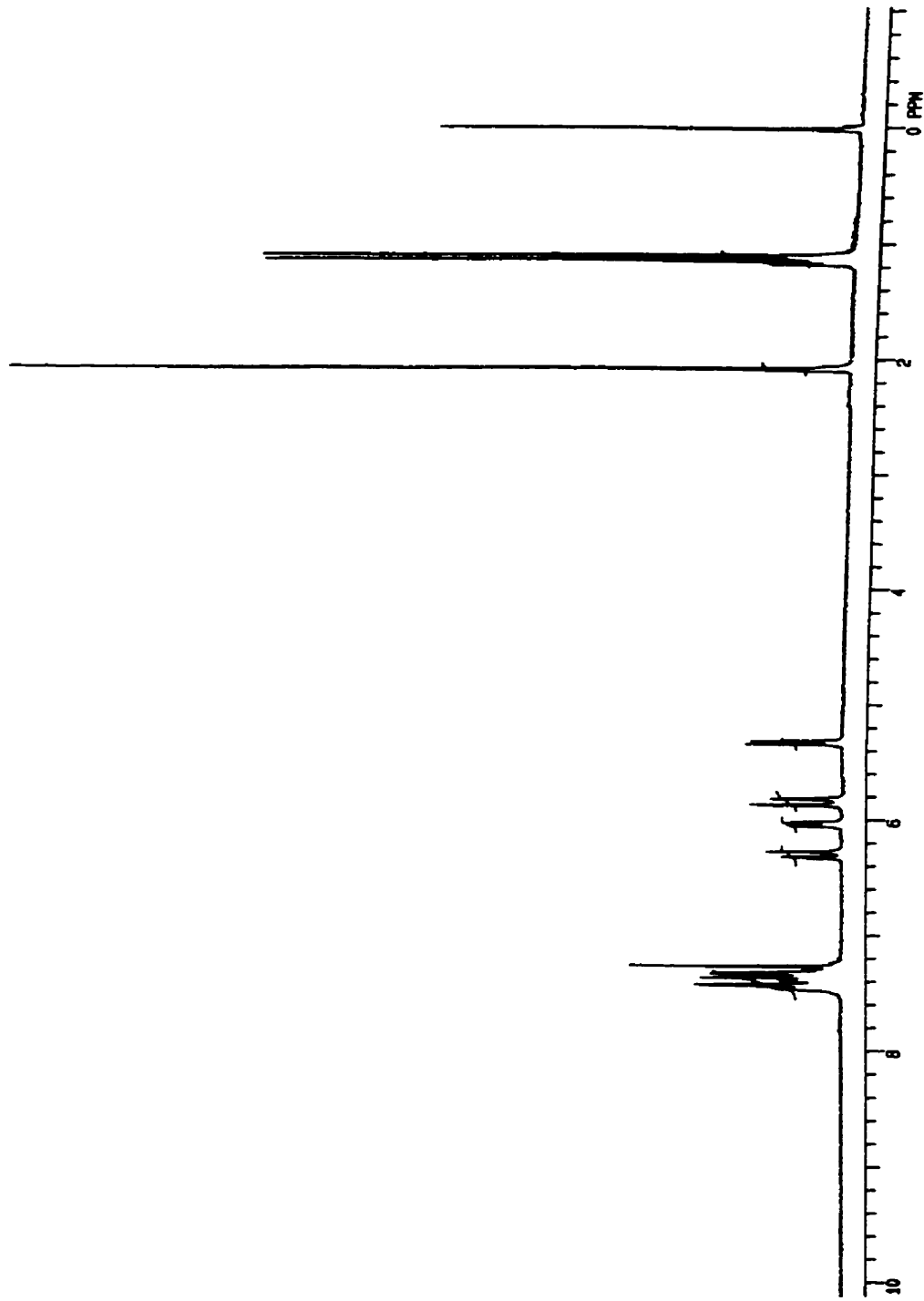
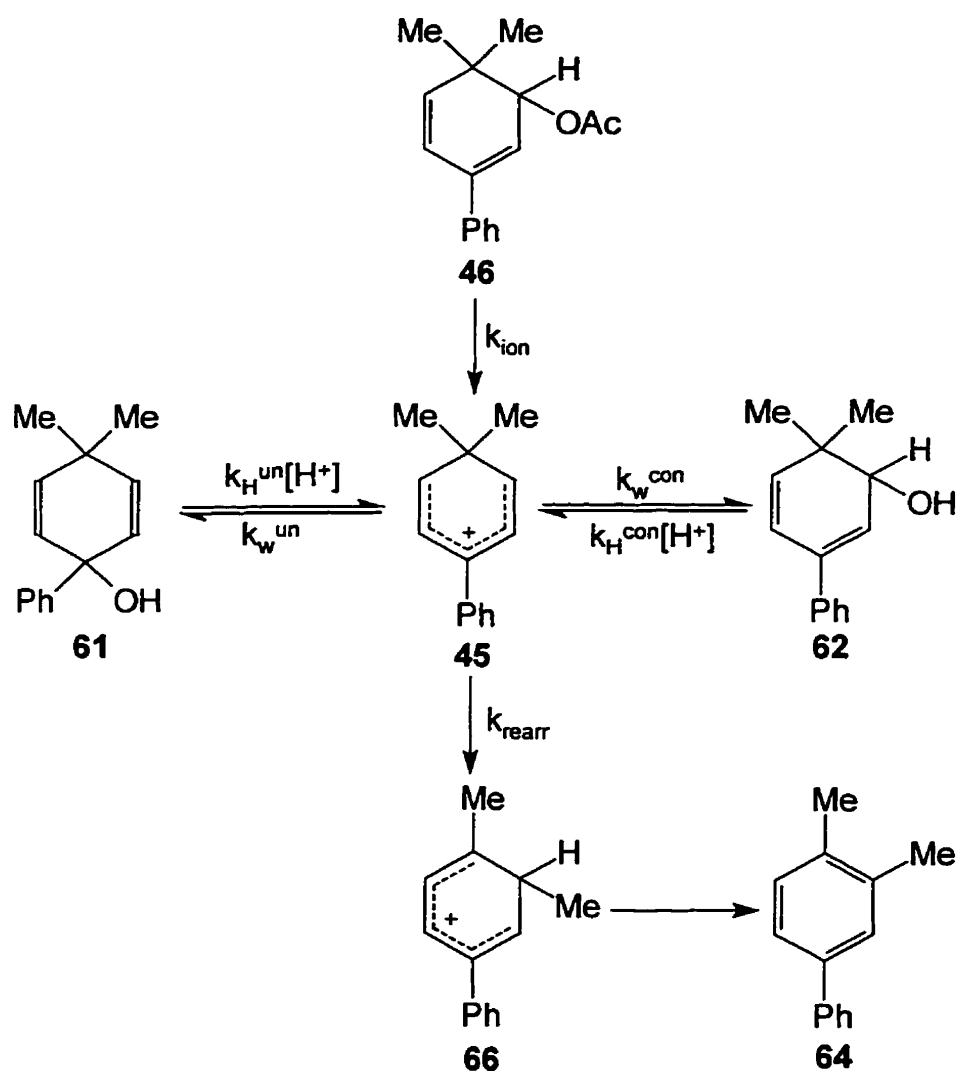


Figure 23. The ^1H NMR of 6,6-dimethyl-3-phenylcyclohexa-2,4-dien-1-yl acetate (**46**).

2.2. Formation of the 6,6-Dimethyl-3-phenylcyclohexadienyl Cation in Aqueous Solutions

Before attempting LFP studies, we examined the aqueous solution chemistry of the cation **45**. As will be demonstrated, this could be generated in the ground state as a steady-state intermediate,¹⁰² either in the solvolysis of the acetate **46** or from the isomeric alcohols **61** and **62** under acidic conditions (see Scheme 14).

Scheme 14



2.2.1. Solvolysis of the acetate 46

The acetate **46** proved to be relatively reactive in aqueous acetonitrile solutions, solvolyzing in 20% (by volume) acetonitrile with a rate constant k_{ion} of $1.34 \times 10^{-3} \text{ s}^{-1}$. The reaction was sensitive to solvent polarity. Using data obtained in four acetonitrile-water mixtures (10, 20, 30, and 40% acetonitrile), a plot of $\log k_{ion}$ versus the solvent Y parameter¹⁰³ was found to have a slope of 1.15 (Figure 24). This indicates that the solvolysis is proceeding in an S_N1 fashion, with the cation **45** as an intermediate.

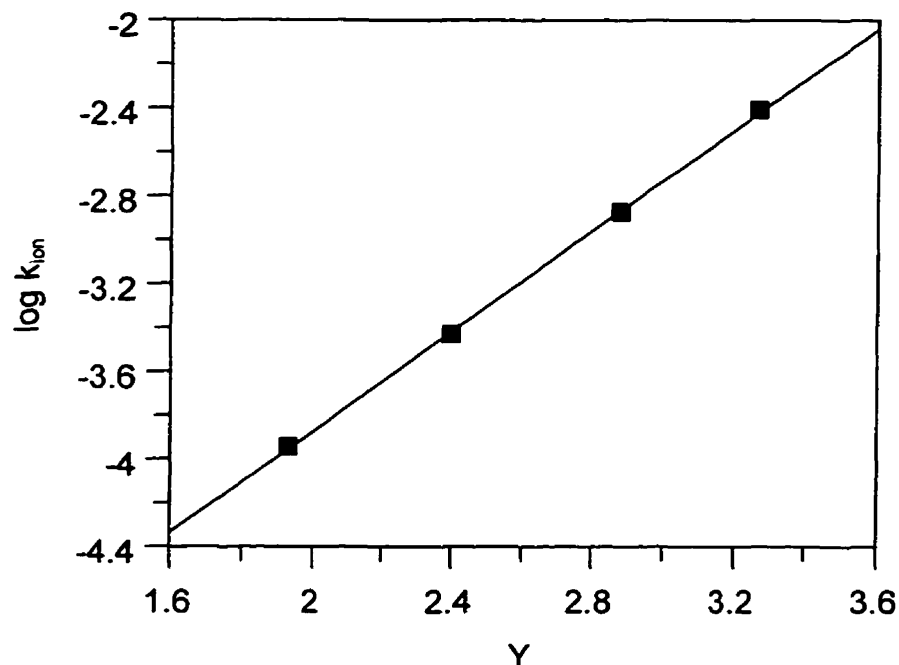
Product analysis was carried out with HPLC for the solvolysis in 20% acetonitrile. The solvent also contained 0.010 M Na_2HPO_4 -0.002 M NaH_2PO_4 , to provide a pH that was sufficiently basic to prevent further reactions. Three products were observed, with the conjugated alcohol **62** as the major product at $89.8 \pm 0.5\%$, the unconjugated alcohol **61** at $7.9 \pm 0.4\%$ and the rearranged product **64** at $2.3 \pm 0.4\%$. Since **61** and **62** are stable under these conditions, the rate constant ratios of eqs. 26-28 describe the partitioning of **45** into the three products. The assumption is made that methyl migration is rate-determining in the rearrangement reaction. That is, once the cation **66** forms it rapidly aromatizes by loss of proton.

$$\frac{k_w^{un}}{k_w^{un} + k_w^{con} + k_{rearr}} = 0.079 \quad (26)$$

$$\frac{k_w^{con}}{k_w^{un} + k_w^{con} + k_{rearr}} = 0.898 \quad (27)$$

$$\frac{k_{rearr}}{k_w^{un} + k_w^{con} + k_{rearr}} = 0.023 \quad (28)$$

Figure 24. The correlation of $\log k_{\text{ion}}$ of acetate **46** with the solvent polarity parameter Y .



2.2.2. Acid-catalyzed reactions of the alcohols **61** and **62**

Solutions of the alcohol **61** are unstable in weakly acidic solutions. Initial experiments involved UV spectroscopy, and the pertinent spectra are given in Figure 25. At wavelengths above 230 nm, ca. 10^{-4} M solutions of **61** are only weakly absorbing, as shown in curve (a). Addition of acid results in an absorbance increase, resulting eventually in a spectrum [curve (b)] that closely resembles that of **62**. Further changes then occur, resulting ultimately in a spectrum corresponding closely to that of **64** [curve (c)]. The two changes are separated by three orders of magnitude in rate, and thus each can be analyzed in terms of single exponential kinetics. Both follow the same kinetic pattern, a first-order dependence on H^+ concentration. Experiments in acetate buffers show no dependence on the concentration of the buffer. The first-order dependence in $[\text{H}^+]$ holds to solutions of pH ca. 7, where the rates become too slow to measure

conveniently. Values of k_H , the catalytic coefficient in H^+ , are given in eqs. 29 and 30.

$$k_H(A \rightarrow B) = k_H^{un} \left(\frac{k_w^{con} + k_{rearr}}{k_w^{un} + k_w^{con} + k_{rearr}} \right) = (6.8 \pm 0.4) \times 10^2 M^{-1} s^{-1} \quad (29)$$

$$k_H(B \rightarrow C) = k_H^{con} \left(\frac{k_{rearr}}{k_w^{con} + k_{rearr}} \right) = (7.1 \pm 0.3) \times 10^{-1} M^{-1} s^{-1} \quad (30)$$

To understand better the chemistry behind these changes, the reaction was followed with HPLC. Figure 27 illustrates results for times representing the faster reaction. The starting alcohol **61** decreases in a first order reaction, with a rate constant that is within experimental error the same as that obtained from the UV change in the same solution. Two products appear, the isomeric alcohol **62** and the rearrangement product **64** in a ratio of $[62]:[64] = 43 \pm 4$. The HPLC peak for **61** does not completely disappear even at times corresponding to 20 half-lives of the faster kinetic process. The ratio $[61]:[62]$ is approximately 0.003 at this stage, but there is uncertainty in this number. This is due to the small amount of **61** that is present, coupled with its HPLC sensitivity being only *ca.* 1/3 of that of **62** at the monitoring wavelength. At much longer times, the alcohol **62** disappears along with the small amount of **61**. The rate constant for this process is identical to that obtained for the slow kinetic phase observed spectrally. At times corresponding to 10 half-lives of this kinetic stage, the only substrate present is the biphenyl **64**.

These results point to a mechanism (Scheme 14) whereby **61** undergoes an H^+ -catalyzed ionization to the cation **45**, which then converts to the isomer **62** and a small amount of **64**. The ratio $[62]:[64] = 43$ is within experimental error the same as the ratio of **39** obtained in the solvolysis of the acetate precursor **46**. This demonstrates that a common intermediate **45** is involved in both reactions. At the completion of the faster kinetic process, the two alcohols have achieved

equilibrium. The equilibrium concentration of **61** (ca. 0.3%) is however sufficiently small that it can be ignored in the kinetic analysis. Therefore, with the assumption of a steady-state in **45**, the observed rate constant for the fast kinetic process is given by the term containing the microscopic rate constants in eq. 29 above. The ratio in brackets in this expression is the fraction of the cation **45** that reacts to form **61** and **64**. This fraction is calculated as 0.92 from the product analysis involving the acetate **46** [add eq. 27 and 28 above]. Thus, k_H^{un} is obtained as $7.4 \times 10^2 \text{ M}^{-1}\text{s}^{-1}$. This number is slightly larger than the observed value of k_H because of the 8% of **45** that returns to the alcohol.

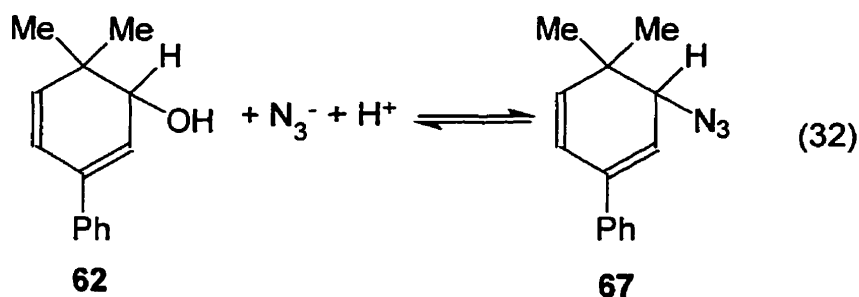
At the completion of the faster kinetic phase, the solution contains ca. 98% of **62**. This explains the similarity in the UV spectrum at this stage to that of this material. An H^+ -catalyzed ionization of **62** to form **45** does occur, and eventually **64** forms as the only species present. The observed rate constant is given by the expression that contains the microscopic rate constants in eq. 30. The term in brackets in this equation represents the fraction of **45** that undergoes methyl migration in competition with the addition of water to form **62**. Values of this fraction are available from two independent product analysis; 0.025 from the experiments with **46** and 0.023 from the experiments with **61**. Using the average, k_H^{con} is calculated as $29 \text{ M}^{-1}\text{s}^{-1}$. This number is much larger than the observed rate constant for the disappearance of **62**, since with this alcohol cation formation is largely reversible.

The equilibrium constant relating the two alcohols is given by a ratio of rate constants (eq. 31). This can now be calculated,

$$\frac{[\mathbf{62}]}{[\mathbf{61}]} = \frac{k_w^{con} k_H^{un}}{k_w^{un} k_H^{con}} \quad (31)$$

since the absolute values for k_H^{con} and k_H^{un} have been determined as outlined above, and the ratio $k_w^{\text{un}}:k_w^{\text{con}}$ is available from the products obtained with **46**. The value of $[\mathbf{62}]:[\mathbf{61}]$ is thus obtained as 2.9×10^2 . This is clearly consistent with the HPLC analysis that shows that there is only a small amount of **61** at equilibrium.

In an attempt to investigate the reaction of **45** with azide ion, the conjugate alcohol **62** was added to weakly acidic solutions (pH 5-6) containing sodium azide. This results in a decrease in the area of the peak for **62** in the HPLC and a new peak growing in at the same rate as **62** decays. Although the new product proved to be too unstable to be isolated for structural characterization, we believe that it is the azide-substituted adduct **67** (eq. 32). This is based on the observation that a UV spectrum recorded as the compound elutes from the HPLC is essentially the same as that of **62**, indicating that the conjugate system remains unchanged. In addition the quantitative HPLC analyses also show that at any given time, the area of the new product is within experimental error the same as the area of **62** which has been lost.



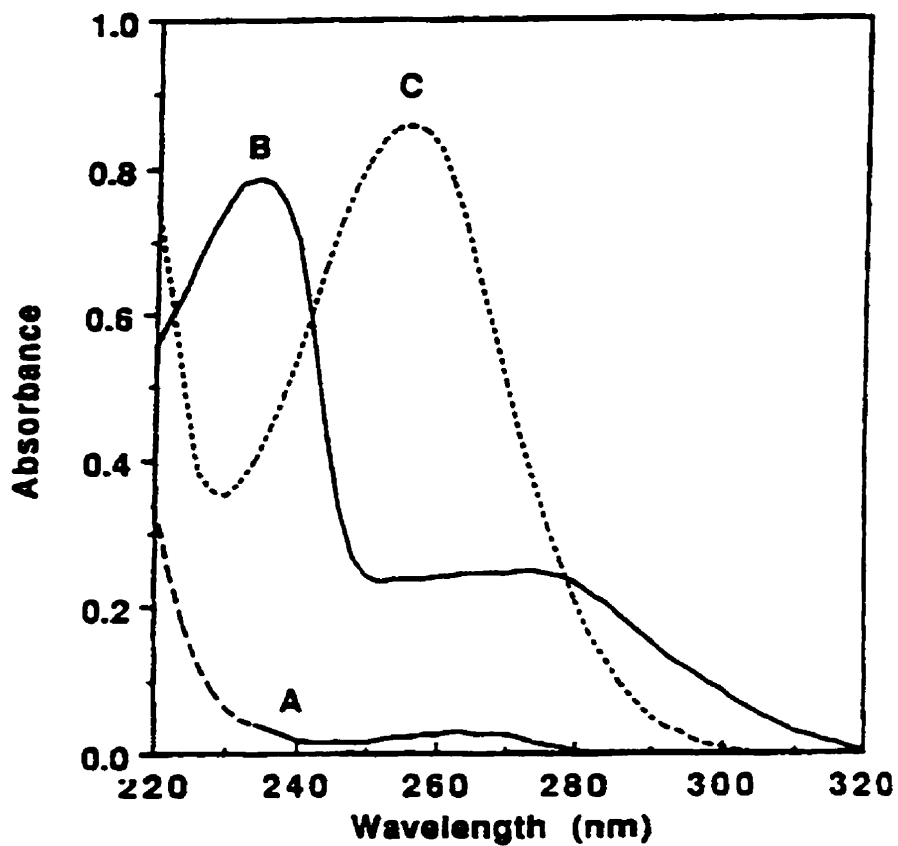


Figure 25. UV spectra observed with 4,4-dimethyl-1-phenylcyclohexa-2,5-dien-1-ol (**61**) (8×10^{-5} M) in acetic acid buffers (pH 5-6) in 20% acetonitrile:water. Curve (A) is the spectrum of the starting material, curve (B) is the spectrum after the initial kinetic phase, and curve (C) is the final spectrum.

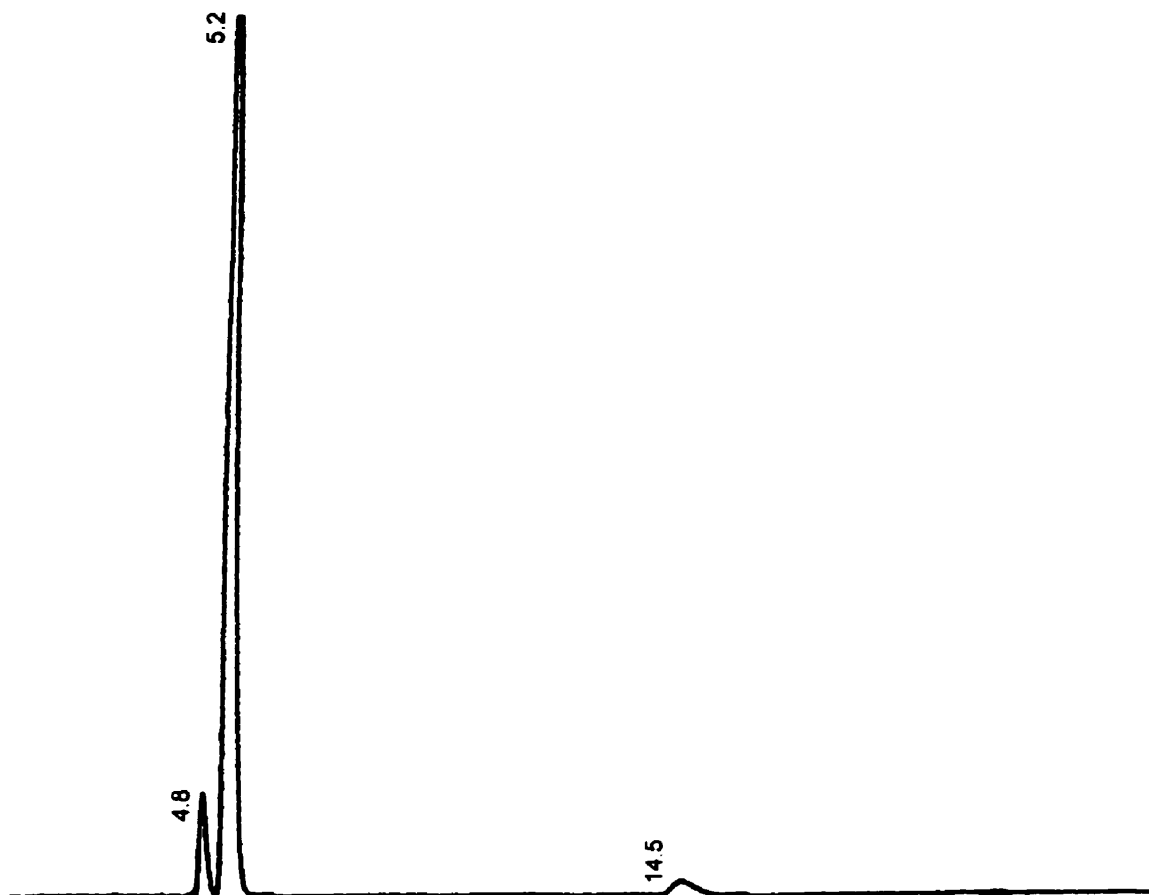


Figure 26. HPLC Chromatogram and product identifications for acid catalyzed reactions of the unconjugated alcohol **61** (initially 2×10^{-4} M in acetic acid buffer (pH 6.2, [NaOAc] = 0.02 M, [HOAc] = 0.002 M) in 20% acetonitrile. Retention times: 4.8 min. (**61**), 5.2 min. (**62**), 14.5 min. (3,4-dimethylbiphenyl, **64**).

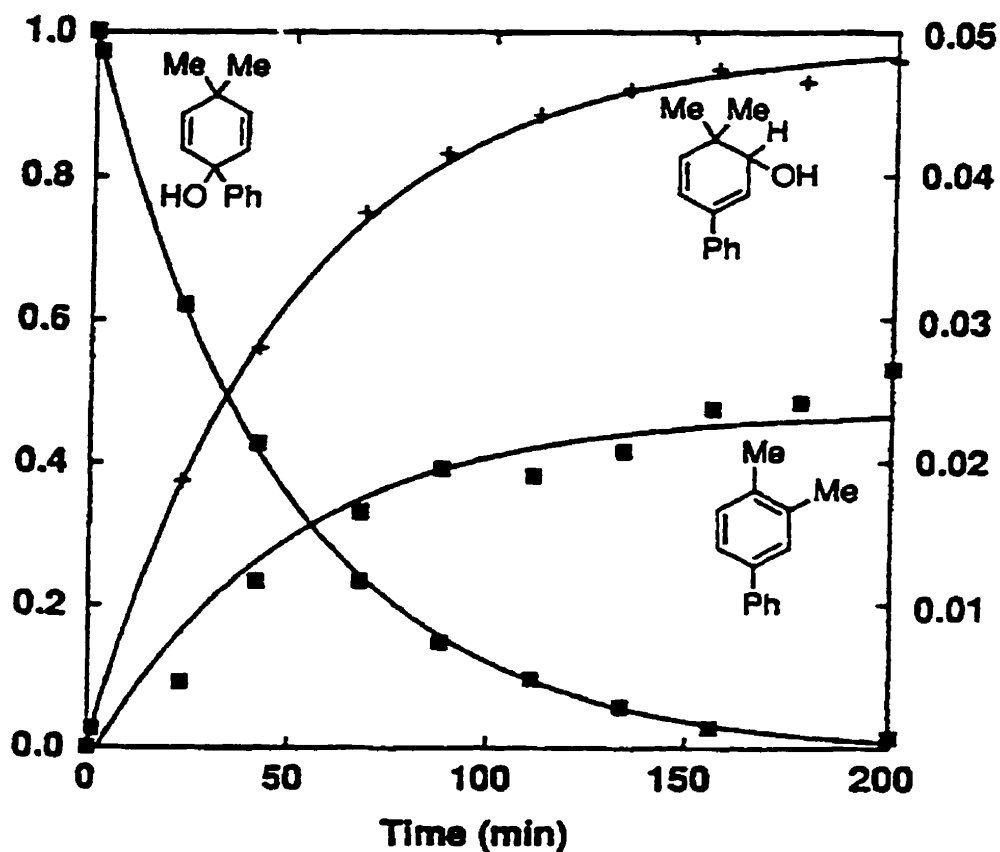


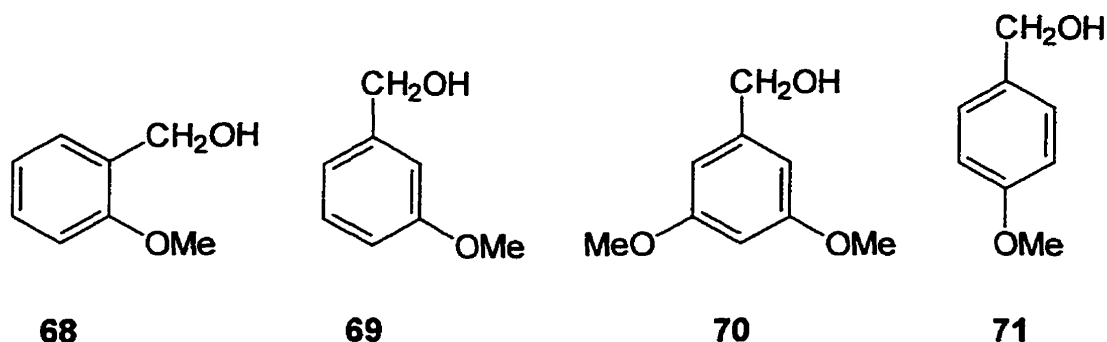
Figure 27. Fraction of starting material **61**, and the two products **62** and **64** for a solution of the unconjugated alcohol **61** (initially 2×10^{-4} M in acetic acid buffer (pH 6.2, $[\text{NaOAc}] = 0.02$ M, $[\text{HOAc}] = 0.002$ M) in 20% acetonitrile. Points for **61** and **62** refer to lefthand axis. Points for **64** refer to righthand axis.

2.3. Generation of a 6,6-Dimethyl-3-phenylcyclohexadienyl Cation by Laser Flash Photolysis

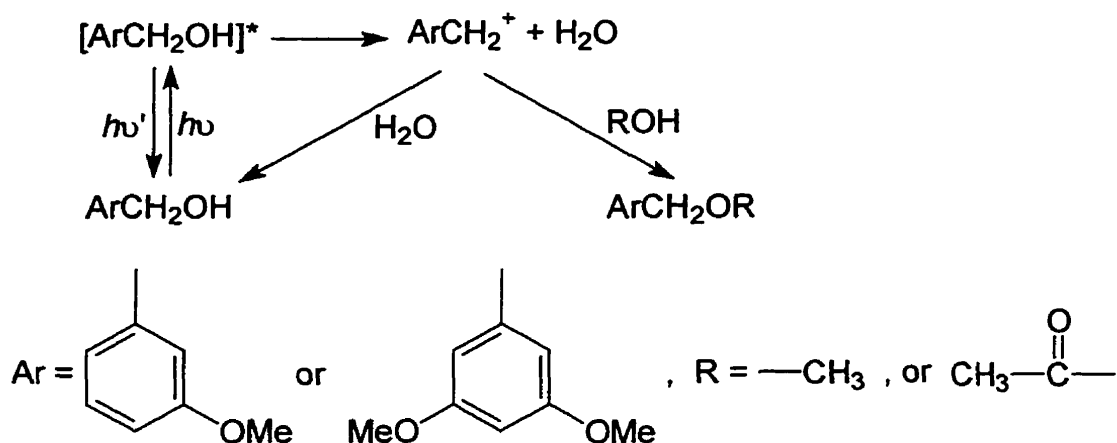
2.3.1. Laser flash photolysis of the alcohol 47

In an attempt to directly observe the cation and to obtain the absolute values for the k_w terms, we initially sought to generate the cation **45** using flash photolysis, employing the acetate **46** as the precursor. These experiments proved unsuccessful, since irradiation of **46** in 20% acetonitrile:water failed to give either a transient in flash photolysis experiments or products on steady irradiation that were consistent with a cation intermediate. One possible reason for the failure of the generation of **45** from **46** by flash photolysis is the ground state solvolytic lability of the latter. Calculated from its k_{ion} , the lifetime of **46** in 20% aqueous acetonitrile is only ca. 12 minutes.

We then turned to alcohol precursors, which have seen use in generations of aryl carbocations by photolysis.¹⁰⁴⁻¹⁰⁷ Although hydroxide is a poor leaving group in the ground state, it can be an excellent leaving group in the excited state when the appropriate chromophore and solvent system are used.^{108,109, 110} Wan and coworkers reported that, on excitation to the singlet excited state, *ortho* and *meta* methoxy-substituted benzyl alcohols underwent proton-assisted loss of hydroxide to give the corresponding benzyl cations.¹¹¹ They observed that *ortho* and *meta* methoxy-substituted benzyl alcohols **68-70** underwent efficient photosolvolytic in aqueous methanol or acetic acid solutions to give the corresponding methyl ether or acetate (Scheme 15). On the other hand, photolysis of the *para* methoxy-substituted compound **71** under similar conditions resulted in recovery of 90% or more of the starting material; methyl ethers and acetates were not observed.



Scheme 15



The results were explained by the “meta effect”, a term which was first suggested by Zimmerman and Sandel in their classic work on the photosolvolysis of methoxybenzyl acetates in aqueous dioxane.^{113,114} In this work it was observed that 3-methoxybenzyl acetate and 3,5-methoxybenzyl acetate photosolvololyze efficiently to the corresponding benzyl alcohol via benzyl cation intermediates, while 4-methoxybenzyl acetate gave predominantly benzyl radical-derived products. Based on experimental observations and theoretical calculations, Zimmerman suggested that in the singlet excited state electron donors transmit charge to the *meta* position rather than *para* while electron-withdrawing groups selectively withdraw electron density from the *meta* site. Therefore a *m*-methoxy

group usually leads to higher yields of benzylic cations than a p-methoxy substituent under photochemical conditions.

McClelland and coworkers reported observation of the meta effect in the generation of diaryl cations by laser flash photolysis with acetates as precursors.⁹⁰ While signals due to both cation and radical were typically observed with most acetates precursors, photolysis of 3,4'-dimethoxydiphenyl acetate gave a large cation signal with little radical. This effect was so pronounced that cation was even observed with the alcohol as the precursor, while other diarylmethanols lacking the m-methoxy substituent gave only a radical signal.

Our experiments provided another example of the meta effect. Both the parent alcohol **61** and the 3',5'-dimethoxy-substituted compound **47** were subject to laser flash photolysis in 20% acetonitrile:water. As shown in Figure 28, with **47** as the precursor, two absorbing species were observed, one absorbing in the 400-500 nm region with the absorption maximum at 440 nm, and a second one at 300-350 nm. The transient at higher wavelength decays with excellent exponential kinetics, as shown in Figure 29; the absorbance at lower wavelength shows little decay at times up to 50 μ s. With **61** as the precursor, only the absorbance at lower wavelength was observed.

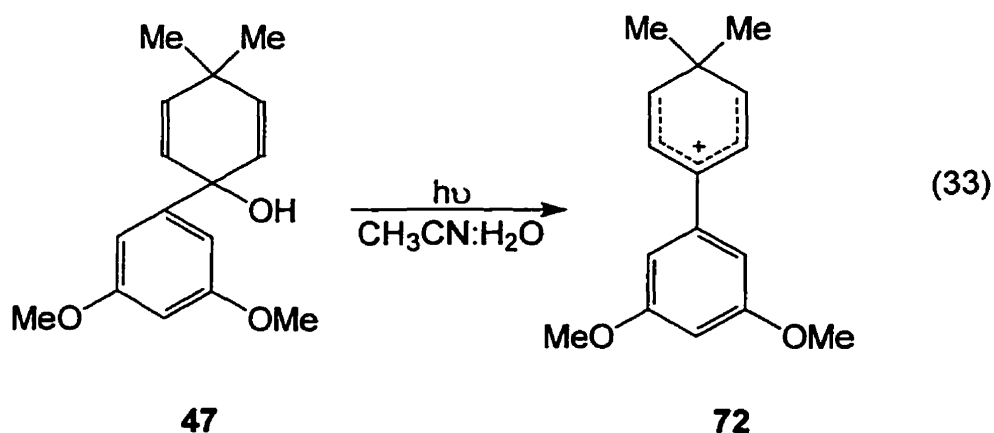


Figure 28. Transient absorption spectra obtained by 248-nm irradiation of 0.2 mM alcohol 47 in 20% acetonitrile:water.

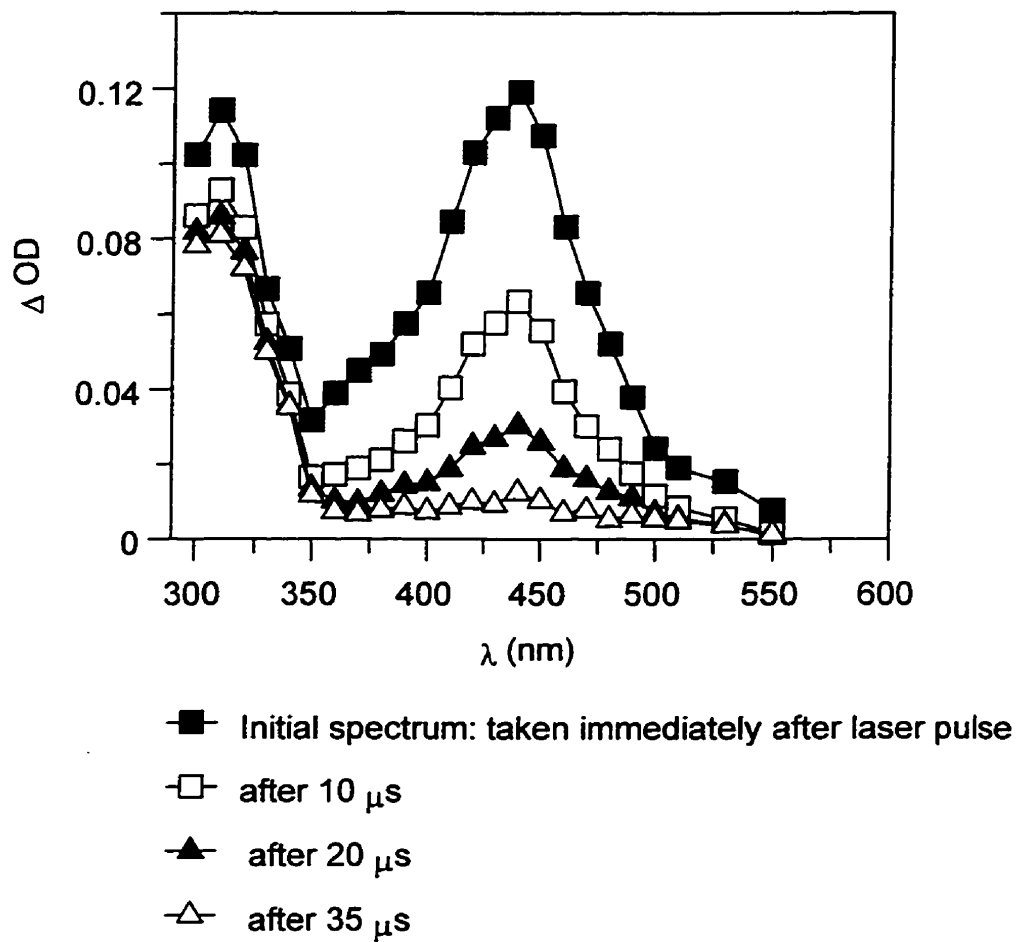


Figure 29. The change of optical density at 440 nm as a function of time upon irradiation of the alcohol **47** at 248 nm in 20% acetonitrile:water.

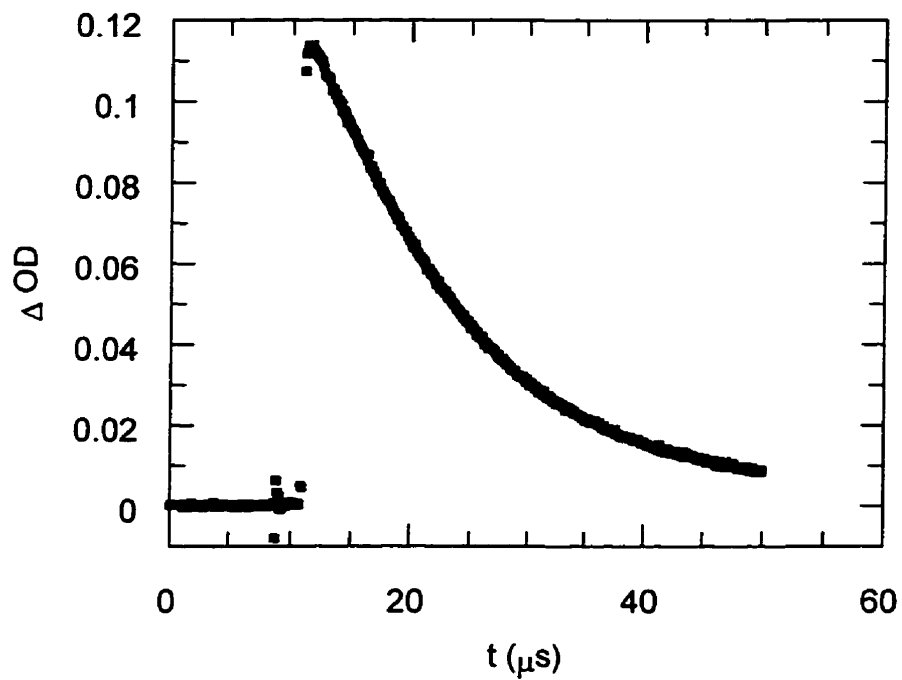


Figure 30. The dependence of the observed rate constant for decay of the transient at 440 nm as a function of the concentration of sodium azide.

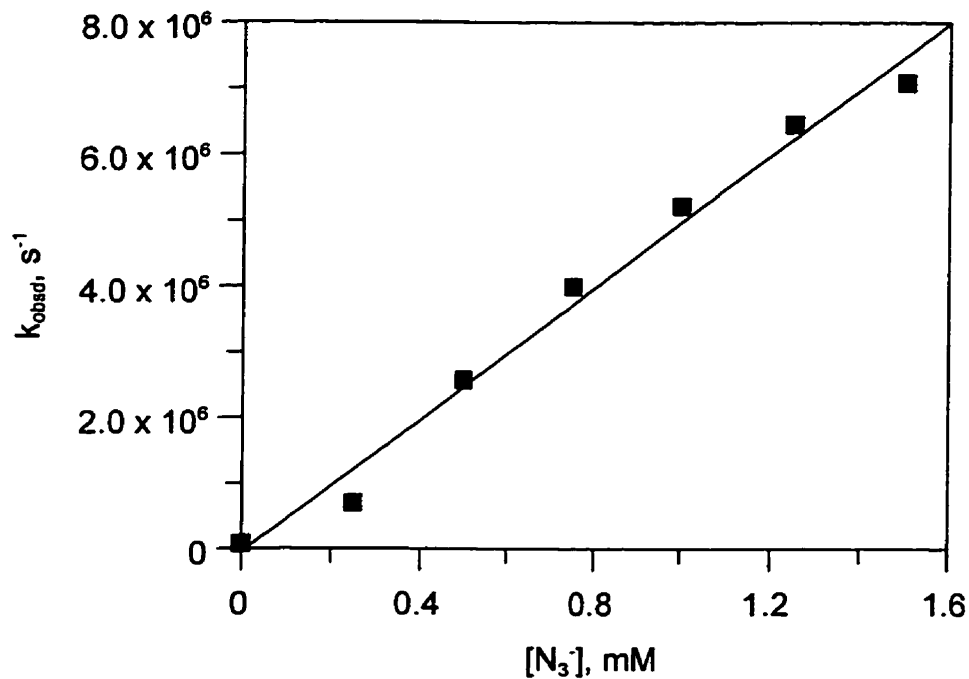


Table 12. Observed rate constants for decay of the transient at 440 nm generated upon irradiation of alcohol **47** in 20% acetonitrile:water in the presence of azide ion.

[N ₃ ⁻], 10 ⁻³ M	k _{obsd} , s ⁻¹	Slope, M ⁻¹ s ⁻¹
0.00	6.92 × 10 ⁴	5.03 × 10 ⁹
0.25	6.90 × 10 ⁵	
0.50	2.57 × 10 ⁶	
0.75	3.99 × 10 ⁶	
1.00	5.22 × 10 ⁶	
1.25	6.45 × 10 ⁶	
1.50	7.08 × 10 ⁶	

We have not assigned the absorbance at lower wavelength observed with both precursors. However the decaying species observed with **47** at higher wavelength can be assigned to the cation **72** (eq. 33). This is clearly seen by the behavior of this species in the presence of azide ion. As shown in Figure 30, the transient was quenched by azide ion, with a linear relationship between the observed decay rate constants and the concentration of azide ion. The second-order rate constant k_{az} was obtained as $5.0 \times 10^9 \text{ M}^{-1}\text{s}^{-1}$ (Table 12). This is characteristic of a carbocation intermediate. (The other possibility for this transient is a cation radical obtained by photoionization of the electron-rich 3,5-dimethoxyphenyl system. This however can be ruled out, since the absorption spectrum of such a cation would be very different from the one that is observed).¹¹⁴

2.3.2. Comparison with 4-biphenylnitrenium ion

It is interesting to note that the transient spectrum of the cyclohexadienyl cation **72** is very similar to those of the 4-biphenylnitrenium ions. This cation is however somewhat more stable than its nitrenium ion analog.

For comparison purposes, the values of k_w and k_{az} for selected 4-biphenylnitrenium ions and triarylmethyl cations⁸⁵ are listed in Table 13 along with those for **72**. It is worth noting that meta-methoxy substituent(s) do not have a large effect on the solvent reactivity of these cations, as shown by the fact that the k_w values for both m-methoxy substituted nitrenium ions and triarylmethyl cations are about the same as those of the parent cations. Therefore, although we are unable to generate the parent cyclohexadienyl cation **45** by LFP, we may assume that the reactivity of **45** is about the same as that of **72**.

Table 13. The values of k_w and k_{az} for the cyclohexadienyl cation **72**, and *meta*-methoxy-substituted 4-biphenylnitrenium ions and triphenylmethyl cations.

Cation	k_w, s^{-1}	$k_{az}, M^{-1}s^{-1}$
4,4-Dimethyl-1-(3',5'-dimethoxyphenyl)-cyclohexadienyl cation (72)	6.92×10^4	5.03×10^9
4-Biphenylnitrenium ion	2.7×10^6	9.6×10^9
3',5'-Dimethoxy-4-biphenylnitrenium ion	2.55×10^6	7.78×10^9
3'-Methoxy-4-biphenylnitrenium ion	2.46×10^6	7.85×10^9
Triphenylmethyl cation ^a	1.6×10^5	4.1×10^9
3-Methoxytriphenylmethyl cation ^a	1.7×10^5	4.0×10^9

^a Ref. 85.

With the assumption that k_w for **45** is the same as that for **72**, it is possible to calculate all the absolute rate constants for the reactions of the former cation. This is done by recognizing that the decay rate constant obtained by laser flash photolysis is the sum of all the rate constant for the reactions of the cations, or that

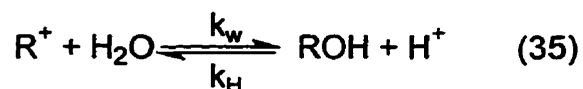
$$k_{\text{obsd}} = 6.92 \times 10^4 \text{ s}^{-1} = k_w^{\text{un}} + k_w^{\text{con}} + k_{\text{rearr}} \quad (34)$$

Since the fractional contributions of each rate constant are known (eqs 26-28), the absolute rate constants can be calculated. These are given in Table 14, along with other related parameters shown in Scheme 14.

Table 14. Absolute rate constants and equilibrium constants for reactions of the cyclohexadienyl cation **45**.

Constants	Value
k_H^{un}	$7.4 \times 10^2 \text{ M}^{-1}\text{s}^{-1}$
k_w^{un}	$5.6 \times 10^3 \text{ s}^{-1}$
$\text{p}K_R^{\text{un}}$	-0.88
k_H^{con}	$29 \text{ M}^{-1}\text{s}^{-1}$
k_w^{con}	$6.2 \times 10^4 \text{ s}^{-1}$
$\text{p}K_R^{\text{con}}$	-3.3
$K_{\text{eq}} (61 \rightleftharpoons 62)$	2.9×10^2
k_{rearr}	$1.5 \times 10^3 \text{ s}^{-1}$

The pK_R values refer to the pseudo acid-base equilibria:



Both alcohols **61** and **62** are relatively easily ionized to cations. For comparison purpose, the triphenylmethyl cation, with $pK_R = -6.63$, is less easily ionized than either **61** or **62**.

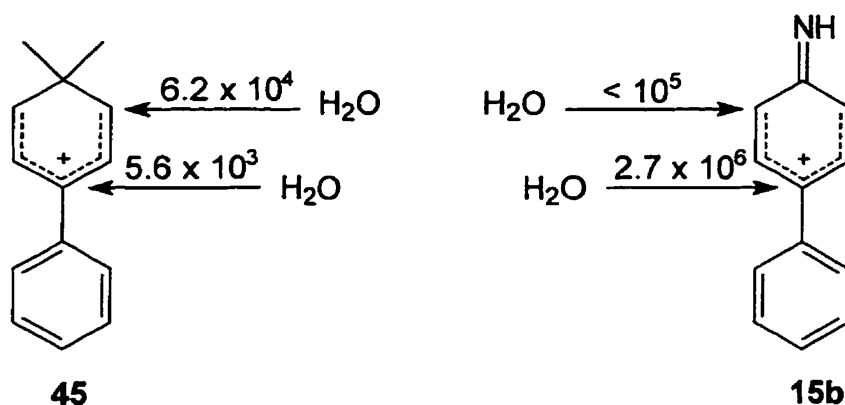


Figure 31. Comparison of rate constants (s^{-1} , 20-25°C) for the addition of water to cyclohexadienyl cations.

Figure 31 provides a comparison of absolute reactivities of **45** and the 4-biphenylnitrenium ion **15b** with water. With the latter there is no addition of water to the carbon *ortho* to the nitrogen, and the rate constant given in Figure 32 is the upper limit based on the assumption that 5% yield of the product would have been observed.

Overall, **45** is more stable kinetically than **15b** by a factor of 30. The higher reactivity of **15b** may come from the electron-withdrawing effect of the imino group that makes the cation less stable.

As can be seen in Figure 31, the two cations differ significantly in the site preference of water addition. With **45** the addition to the carbon adjacent to the *gem*-dimethyl group is kinetically preferred, favored by an order of magnitude over the reaction at the position *para* to the methyl groups. This site has also been shown experimentally to be thermodynamically favored (see Table 14). With the nitrenium ion, however, the *para* position is kinetically favored sufficiently so that no product derived from water addition to the *ortho* site is obtained.

With the imino system, the thermodynamic preference is not experimentally known, but theoretical calculations suggest that the thermodynamic product is also the one obtained by water addition at the carbon next to the nitrogen.¹⁰² As shown in Figure 32, AM1 calculations on the isomerization of alcohols **61** and **62** give results that also show thermodynamic preference for **62** over **61**, in fact within a factor of two of the experimental value. With the imino system the calculations show even greater preference for the adduct derived from water addition to the *ortho* position.

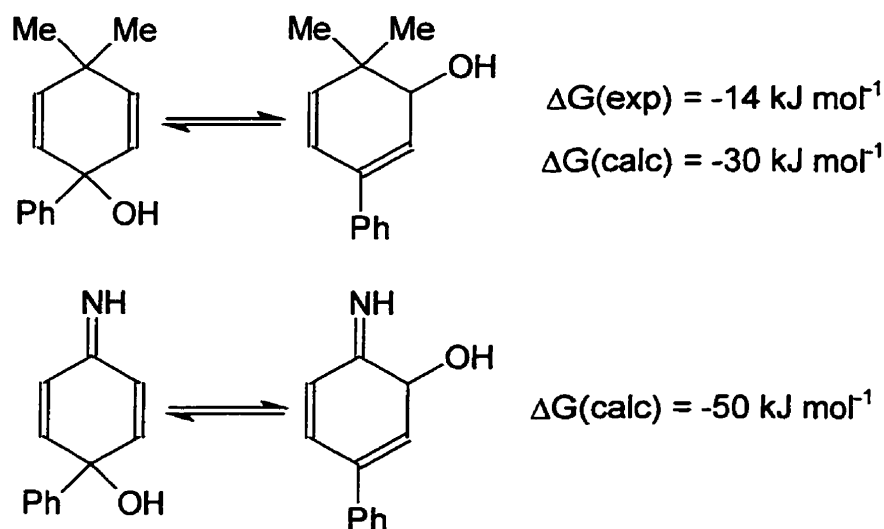
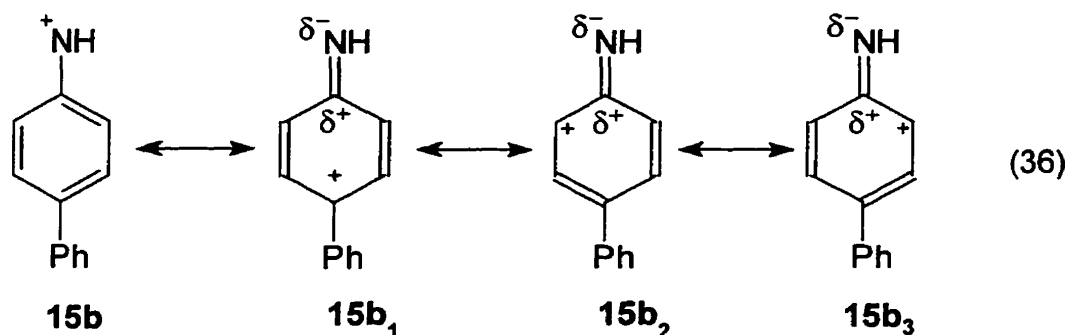


Figure 32. Free energy changes for the isomerization of cyclohexadienols. Calculated values are based on the AM1 method.

Thus for **15b** there is a strong kinetic preference for water addition to give the thermodynamically unstable product. This is not unusual since other arylnitrenium ions, including the parent cation, show a kinetic preference for reaction with water at the carbon *para* to the nitrogen.¹¹⁵ One simple explanation is that the electronegative nitrogen causes the positive charge to localize at the most distant *para* carbon. In other words the resonance contributor **15b₁**, in the nitrenium system is more important than the contributors **15b₂** and **15b₃**, where the positive charge is on the carbon adjacent to the electronegative atom (eq. 36). This explanation is obviously consistent with the fact that substituents in the phenyl ring attached at C4 of **15b** have a very pronounced effect on the rate constants for the reaction with water. The effect is demonstrated by the large values of the ρ and r^* parameters for **44a** (Table 7, Section 1).



As for the cyclohexadienyl cation **45**, a general LFP method has yet to be developed to generate a series of this type of cations with substituents in the phenyl ring so that the substituent effect on the water reactivity can be investigated. However, judging from the kinetic preference of the parent, the reaction with water should be less sensitive to the substituents because the reaction occurs at the carbon adjacent to the *gem*-dimethyl group which is remote from the phenyl ring, and thus the values of ρ and r^* can be expected to be smaller than that of the nitrenium ions **44a**.

Experimental

1. Materials

Reagents employed in the syntheses were purchased from the Aldrich Chemical company. 1-Bromo-3,5-dimethoxybenzene was prepared by Sandmeyer reaction from 3,5-dimethoxyaniline following the procedure of J. L. Hartwell.¹¹⁶ The crude product was purified by chromatography on a silica gel column eluted with 20% ethyl acetate-hexanes. This gave a white solid and was used without further purification. Tetrahydrofuran and diethyl ether were distilled from sodium suspension with benzophenone as indicator. HPLC grade acetonitrile and deionized water were used for LFP experiments. All aryl azides were purified by column chromatography and (or) recrystallization prior to use.

2. General Methods

2.1. Laser Flash Photolysis (LFP) Studies

Laser flash photolysis experiments were carried out at room temperature with about 20 ns pulses, typical 80 mJ, of 248 nm (KrF) or 308 nm (XeCl) monochromatic light from a Lumonics excimer 510 laser with optical detection system to monitor transients (Figure 33). The signals were digitized by a Tektronix SCD-1000 digitizer interfaced with a Tektronics DX 386 computer. The DX computer also prepared the raw experimental data for further processing. The changes in optical density were observed as changes in voltage. The optical density can be expressed as eq. 37, where OD is the optical density, V_0 is the

voltage obtained by the baseline compensator, V_p is the average voltage for prepulse signals, and $V_{(t)}$ is the voltage at each time interval.

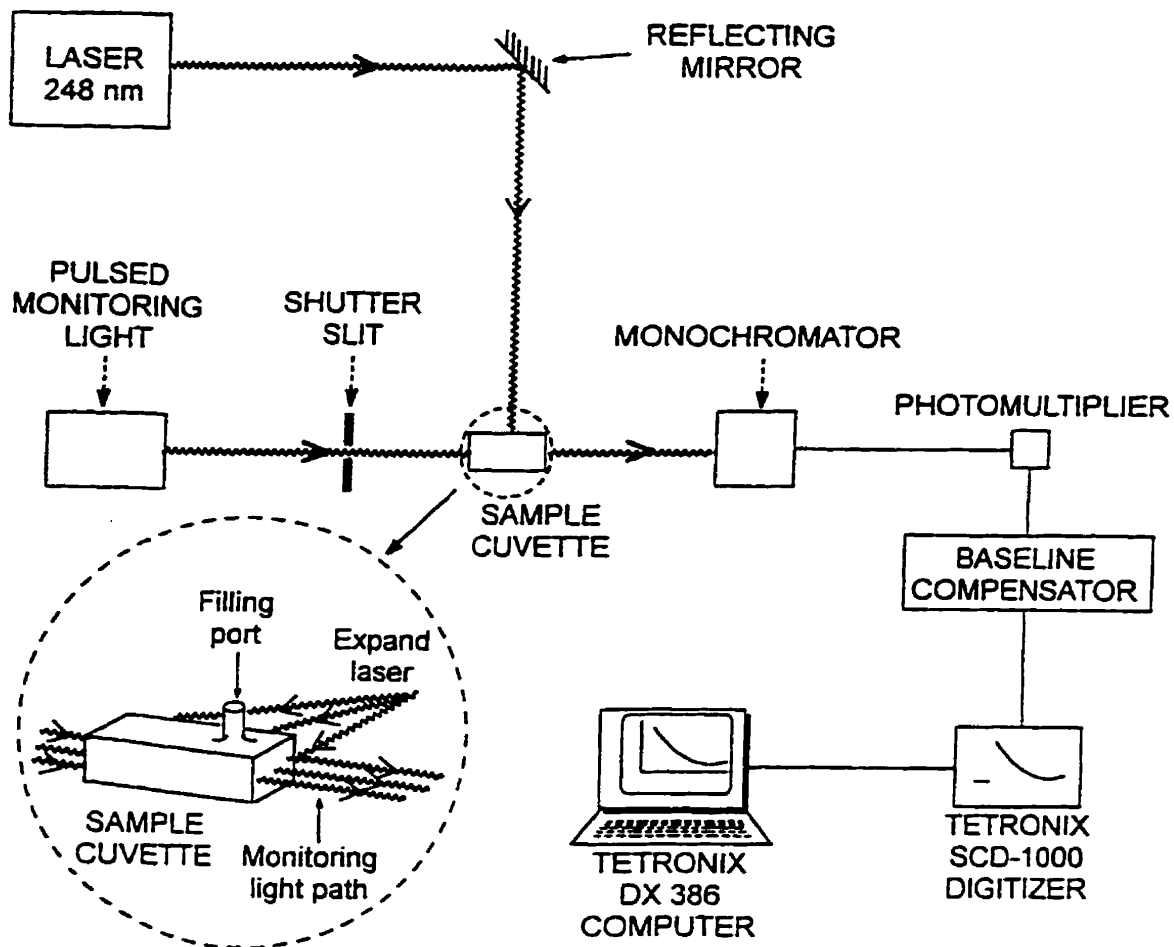
$$OD = \log_{10} \left[\frac{V_b - V_p}{V_b - V_{(t)}} \right] \quad (37)$$

Solutions used in laser flash photolysis were prepared by adding a small amount of a stock solution (~0.02 M) of substrates in acetonitrile to the solvent (prepared by mixing HPLC grade acetonitrile and deionized water in an appropriate ratio (v/v)). The final concentrations of the substrate solutions are in the range of $2-3 \times 10^{-5} \text{ M}^{-1}$.

Final data analysis, such as fitting of the traces and the construction of absorption spectra was conducted with the Grafit program. The absorption spectra are usually recorded by monitoring the signal between 300-600 nm at 10-nm intervals. The absorbance at each wavelength is the maximum optical density following the irradiation.

The first-order rate constants for the decay of the cations were usually measured at 460 nm or the wavelength with maximum absorbance. A typical trace of transient that decays with exponential kinetics is shown in Figure 34. To obtain the first-order rate constants for decay of the transient, the trace after the laser flash (Figure 35) were fitted according to equation $OD = a \exp(-kt) + b$, where OD is the optical density at the time (t), a is the difference of the optical densities between the maximum and minimum absorbance of the transient, and b is the minimum optical density. The rate constant for decay is obtained as k.

Figure 33. Schematic diagram of nanosecond laser flash photolysis apparatus.



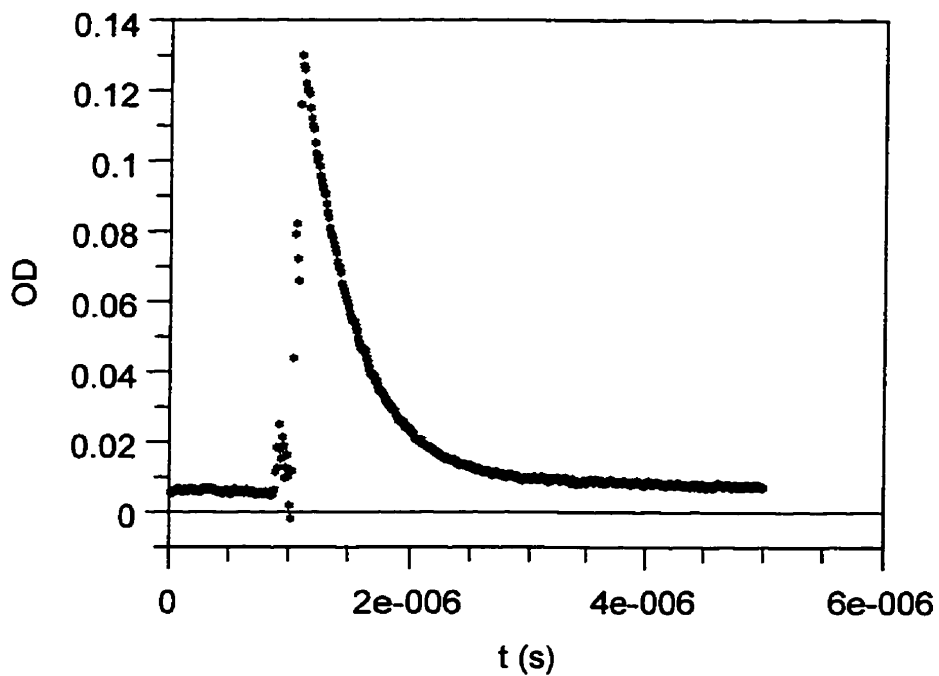


Figure 34. A typical trace of the signal recorded at 460 nm.

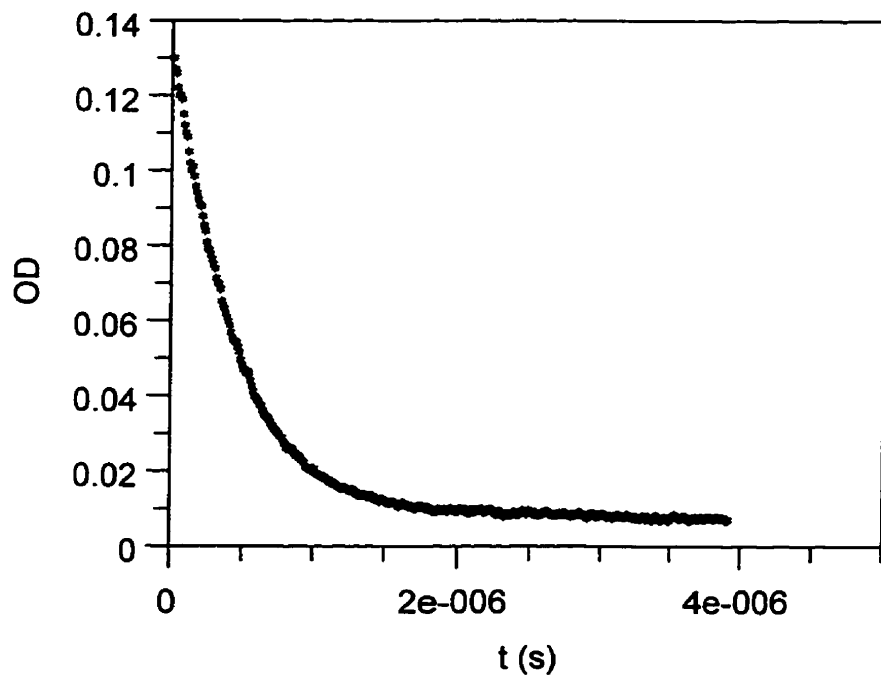


Figure 35. The trace of the transient, i.e. the signal after laser pulse signal.

2.2. HPLC

These experiments were performed with a Waters 600E system with UV detector. Conditions: 1×10 cm C18 column, flow rate = 2 ml min^{-1} , isocratic 30:70 methanol:water for 6 min followed by a linear gradient from 6-9 min to 15:85 methanol:water from 9-16 min, detector wavelength at 220 nm for 0-6 min followed by 235nm from 6-16 min. Retention times: 4.8 min (**61**), 5.2 min (**62**), 10.5 min (**46**), 13.8 min (**67**) and 14.5 min (**64**). Peak areas were converted into absolute quantities by use of response factors determined by injecting known amounts of the authentic samples of **46**, **61**, **62**, and **64**. Solutions of substrates of concentration $1\text{-}2 \times 10^{-4}$ M were placed in a constant temperature bath at 25°C . At appropriate times 0.080 ml were removed and injected directly to the HPLC.

2.3. UV Spectroscopic Studies

These experiments were performed with a Carey 2200 spectrometer thermostated at 25°C by injecting 0.003 ml of a stock solution of the substrate in acetonitrile into 3 ml of an appropriate solution in a UV cuvette. The final concentration of the substrate was 1×10^{-4} M. The data from the spectrometer were transferred directly to a computer, where the first-order rate constants were calculated by fitting the exponential equation to the traces of absorbance *versus* time, as described above.

2.4. NMR and Mass Spectroscopy

NMR spectra were obtained on Gemini 200 MHz or Varian XR-500 MHz spectrometers in deuterated chloroform or DMSO solvents. Chemical shifts are reported in parts per million, δ . Multiplicities are abbreviated as: s = singlet, d = doublet, t = triplet, and m = multiplet.

Mass spectra (both low resolution and high resolution) were obtained on a VG-70-2505 instrument.

3. Synthesis

3.1. Syntheses of 4-azidobiaryl compounds

The 4-azidobiaryls were prepared by the diazotization of the corresponding 4-aminobiaryls, followed by the addition of sodium azide. The 4-aminobiaryls were prepared by the coupling of appropriately substituted phenylboronic acids with 4-bromoaniline. The exceptions here were 4'-methoxy- and 4'-methyl-4-aminobiphenyl, which were prepared by the coupling of appropriately substituted phenylstannanes with 4-nitrophenyl triflate followed by the hydrogenation.

3.1.1. Preparation of aryltin compounds

General procedure. Tri-n-butyl-(4-methoxyphenyl)stannane. Aryltin compounds were prepared from the reactions of Bu_3SnCl and the Grignard reagents. Tri-n-butyltin bromide (5.7 ml, 20 mmol) was added dropwise to a solution of 4-methoxyphenylmagnesium bromide (20 mmol) prepared from 1-bromo-4-methoxybenzene and Mg turnings in 20 ml ether. The resulting mixture was stirred for 12 hrs. After treated with 50 ml of 5% aqueous ammonium chloride solution, the mixture was extracted with ether. The ether extract was washed with water twice, dried over MgSO_4 , and concentrated to give an oil. Chromatography on a silica gel column eluted with hexanes-ethyl acetate (20:1) afforded a colorless oil.

$^1\text{H NMR}$ (CDCl_3 , 200 MHz) δ 7.40-7.36 (d, $J = 8.0$ Hz, 2H), 6.93-6.89 (d, $J = 8.0$ Hz, 2H), 3.80 (s, 3H), 1.59-1.47 (m, 6H), 1.38-1.28 (m, 6H), 1.09-1.00 (t, $J = 8.2$ Hz, 6H), 0.94-0.87 (t, $J' = 7.2$ Hz, 9H). MS (EI, 70 eV): 341 ($[\text{M}-\text{C}_4\text{H}_9]^+$, 100), 285 ($[\text{M}-(\text{C}_4\text{H}_9)_2]^+$, 57), 227 ($[\text{M}-(\text{C}_4\text{H}_9)_3]^+$, 76).

Tri-n-butyl-(4-methylphenyl)stannane was prepared by the same procedure starting from 1-bromo-4-methylbenzene. The purified product is a

colorless oil. $^1\text{H NMR}$ (CDCl_3 , 200 MHz) δ 7.40-7.36 (d, $J = 8.0$ Hz, 2H), 7.19-7.15 (d, $J = 8.0$ Hz, 2H), 2.35 (s, 3H), 1.60-1.51 (m, 6H), 1.48-1.29 (m, 6H), 1.09-1.01 (t, $J = 8.2$ Hz, 6H), 0.94-0.87 (t, $J' = 7.2$ Hz, 9H). MS (EI, 70 eV): 325 ($[\text{M}-\text{C}_4\text{H}_9]^+$, 100), 269 ($[\text{M}-(\text{C}_4\text{H}_9)_2]^+$, 66), 211 ($[\text{M}-(\text{C}_4\text{H}_9)_3]^+$, 99).

3.1.2. Preparation of arylboronic acids

General procedure: 3-methylphenylboronic acid. Arylboronic acids were prepared by a modification of the method of Washburn and Levens, et al.* A solution of 3-methylphenylmagnesium bromide (0.1 mol) was prepared by reaction of 1-bromo-3-methylbenzene with magnesium turnings in 100 ml of anhydrous ether and stored in a 250 ml round-bottom flask under argon atmosphere. Methyl borate (11.2 ml, 0.1 mol) was distilled into a second round-bottom flask. Both solutions were pressure-transferred by argon flow simultaneously to 100 ml of vigorously stirred anhydrous ether in a 500 ml round-bottom flask maintained at -60°C to -70°C by a dry ice-acetone bath. The reactants were added within a 15-minute period and the mixture was stirred for an additional 30 minutes at -70°C . The mixture was then allowed to warm to 0°C and was stirred at that temperature for 1 hr. The mixture was then hydrolyzed by addition of 20 ml of water at 0°C and allowed to stand overnight.

The mixture was then neutralized with sulfuric acid. The organic layer was separated from the pasty aqueous phase and combined with 3 ether extracts of the latter. The ether was removed by distillation. As the head temperature approached 42°C , water was added from a funnel. Distillation was continued until the head temperature reached 100°C . While stirring was continued the cloudy aqueous mixture was cooled rapidly in an ice bath. This resulted in white, shiny crystals which were collected, washed with ice-water, and allowed to air dry. A second crop was isolated from the combined filtrates and washings by

concentration and cooling. The first and second crops came to constant weight after two days.

3-Methylphenylboronic acid had ^1H NMR (DMSO- d_6 , 200 MHz) δ 7.99 (s, 2H, OH), 7.61-7.59 (m, 2H), 7.24-7.21 (m, 2H), 2.31 (s, 3H).

The following boronic acids were prepared by the procedure described above and characterized by ^1H NMR taken in DMSO- d_6 . The hydroxyl proton has a typical chemical shift at ~ 8 .

4-Fluorophenylboronic acid: white crystals; ^1H NMR (DMSO- d_6 , 200 MHz) δ 8.11 (s, 2OH), 7.89-7.81 (m, 2H), 7.21-7.12 (m, 2H).

3-Methoxyphenylboronic acid: white crystals; ^1H NMR (DMSO- d_6 , 200 MHz) δ 8.06 (s, 2OH), 7.39-7.36 (m, 2H), 7.31-7.23 (t, $J = 8.0$ Hz, 1H), 6.89-6.85 (m, 1H).

4-Chlorophenylboronic acid: white crystals; ^1H NMR (DMSO- d_6 , 200 MHz) δ 8.19 (s, 2OH), 7.82-7.78 (d, $J = 8.4$ Hz, 2H), 7.43-7.39 (d, $J = 8.4$ Hz, 2H).

3-Chlorophenylboronic acid: white crystals; ^1H NMR (DMSO- d_6 , 200 MHz) δ 8.28 (s, 2OH), 7.80-7.71 (m, 2H), 7.50-7.35 (m, 2H).

4-(Trifluoromethyl)phenylboronic acid: white crystals; ^1H NMR (DMSO- d_6 , 200 MHz) δ 8.38 (s, 2OH), 8.02-7.98 (d, $J = 8.0$ Hz, 2H), 7.72-7.68 (d, $J = 8.0$ Hz, 2H).

3,5-Dimethoxyphenylboronic acid: white crystals; ^1H NMR (DMSO- d_6 , 200 MHz) δ 8.10 (s, 2OH), 7.00 (d, $J = 2.2$ Hz, 2H), 6.56 (t, $J = 2.2$ Hz, 1H).

4-(N,N-dimethylamino)phenylboronic acid: white crystals; ^1H NMR (DMSO- d_6 , 200 MHz) δ 7.62 (s, 2OH), 7.66-7.62 (d, $J = 8.0$ Hz, 2H), 6.68-6.64 (d, $J = 8.0$ Hz, 2H), 2.94 (s, 6H).

3.1.3. Synthesis of 4-aminobiaryls

(1) By the coupling of phenylstannanes with 4-nitrophenyl triflate.

4-Nitrophenyl trifluoromethanesulfonate (triflate). To a solution of 4-nitrophenol (1.39g, 10 mmol) in 6 ml of pyridine at 0°C was slowly added trifluoromethanesulfonic anhydride (1.85 ml, 3.10 g, 11 mmol). The mixture was stirred at 0°C for 5 min, then allowed to warm up to room temperature, and stirred at this temperature for 25 hrs. The resulting mixture was poured into water and extracted twice with ether. The ether extract was washed with water, 10% aqueous hydrochloric acid solution (twice), water, and a concentrated sodium chloride solution. After drying over MgSO₄, ether was removed to give a white solid. Recrystallization from hexanes afforded white, shiny plates.

¹H NMR (CDCl₃, 200 MHz) δ 8.40-8.35 (d, J = 9.2 Hz, 2H), 7.51-7.46 (d, J = 9.2 Hz, 2H).

General coupling procedure. 4'-Methoxy-4-nitrobiphenyl. To a solution of 4-nitrophenyl trifluoromethanesulfonate (0.54 g, 2 mmol) in 10 ml DMF was added tri-n-butyl-(4-methoxyphenyl)stannane (0.794 g, 2mmol), LiCl (0.254 g, 6 mmol), Pd(PPh₃)₂Cl₂ (29 mg, 0.04 mmol), and a few crystals of 2,6-di-*tert*-butyl-4-methylphenol. The resulting suspension was refluxed at 98°C for 4 hrs, cooled to room temperature, and treated with 1 ml of pyridine and 2 ml of pyridinium fluoride (1.4 M solution in THF, 2.8 mmol). The mixture was stirred at room temperature for 16 hrs. The mixture was then diluted with 20 ml of ether, stirred with Celite, and filtered. The solution was washed with water, 10% HCl, water, and a concentrated NaCl solution, dried over MgSO₄, and concentrated to give a yellow solid. Chromatography on a silica gel column eluted with hexanes-ethyl acetate (9:1) and recrystallization from hexanes gave rise to yellow needles.

¹H NMR (CDCl₃, 200 MHz) δ 8.30-8.26 (d, J = 8.8 Hz, 2H), 7.72-7.68 (d, J = 8.8 Hz, 2H), 7.61-7.57 (d, J = 8.8 Hz, 2H), 7.05-7.00 (d, J = 8.8 Hz, 2H), 3.88 (s, 3H).

4'-Methyl-4-nitrobiphenyl was prepared by the same procedure starting with tri-n-butyl-(4-methylphenyl)stannane. Recrystallization of the crude product yielded yellow needles; ¹H NMR (CDCl₃, 200 MHz) δ 8.31-8.27 (d, J = 9.0 Hz, 2H), 7.75-7.71 (d, J = 9.0 Hz, 2H), 7.56-7.52 (d, J = 9.0 Hz, 2H), 7.33-7.29 (d, J = 9.0 Hz, 2H), 2.43 (s, 3H).

Hydrogenation of 4-nitrobiphenyls. 4-Amino-4'-methoxybiphenyl. A solution of 4-methoxy-4'-nitrobiphenyl (0.115 g, 0.5 mmol) in 5 ml of ethanol was hydrogenated with 5% Pd on charcoal (11.5 mg) as catalyst. The catalyst was removed by filtration. Concentration of the filtrate afforded a white solid which was recrystallized from aqueous ethanol.

¹H NMR (CDCl₃, 200 MHz) δ 7.48-7.44 (d, J = 8.8 Hz, 2H), 7.39-7.35 (d, J' = 8.4 Hz, 2H), 6.97-6.92 (d, J = 8.8 Hz, 2H), 6.77-6.733 (d, J' = 8.4 Hz, 2H), 3.70 (s, NH₂), 3.84 (s, 3H).

4-Amino-4'-methylbiphenyl: white solid; ¹H NMR (CDCl₃, 200 MHz) δ 7.46-7.38 (m, 4H), 7.23-7.19 (d, J = 8.4 Hz, 2H), 6.78-6.73 (d, J = 8.4 Hz, 2H), 3.70 (s, NH₂), 2.38 (s, 3H).

(2) By the coupling of phenylboronic acid with 4-bromoaniline.

General procedure. 4-Amino-4'-fluorobiphenyl. A 50 ml-flask was charged with 0.35 g of Pd(PPh₃)₄ (0.3 mmol), 20 ml of benzene, 1.72 g of *p*-bromoaniline (10 mmol), and 10 ml of 2M aqueous Na₂CO₃ solution under argon, and then 10 mmol of 4-fluorophenylboronic acid in a minimum amount of 95% ethanol was added. The mixture was refluxed overnight under vigorous stirring. After the reaction was completed, the product was extracted with ether, washed with a saturated NaCl solution, and dried over Na₂SO₄. After removal of solvents, the crude product was further purified by column chromatography on silica gel eluting with ethyl acetate/hexanes followed by recrystallization in aqueous ethanol to give a white solid.

^1H NMR (CDCl_3 , 200 MHz) δ 7.52-7.44 (m, 2H), 7.38-7.34 (d, $J = 8.6$ Hz, 2H), 7.12-7.03 (m, 2H), 6.78-6.73 (d, $J = 8.6$ Hz, 2H), 3.72 (s, NH_2).

The following 4-aminobiphenyls were prepared by the procedure described above.

4-Amino-3'-methylbiphenyl: colorless liquid. ^1H NMR (CDCl_3 , 200 MHz) δ 7.44-7.28 (m, 5H), 7.12 (m, 1H), 6.79-6.75 (d, $J = 8.2$ Hz, 2H), 3.72 (s, NH_2), 2.40 (s, 3H).

4-Amino-3'-methoxybiphenyl: colorless liquid. ^1H NMR (CDCl_3 , 200 MHz) δ 7.43-7.39 (d, $J = 8.2$ Hz, 2H), 7.36-7.28 (t, $J' = 8.0$ Hz, 1H), 7.15-7.07 (m, 2H), 6.86-6.80 (m, 1H), 6.78-6.40 (d, $J = 8.2$ Hz, 2H), 3.86 (s, 3H), 3.74 (s, NH_2).

4-Amino-4'-chlorobiphenyl: white crystals. ^1H NMR (CDCl_3 , 200 MHz) δ 7.48-7.33 (m, 6H), 6.77-6.73 (d, $J = 8.6$ Hz, 2H), 3.75 (s, NH_2).

4-Amino-3'-chlorobiphenyl: colorless oil. ^1H NMR (CDCl_3 , 200 MHz) δ 7.46-7.10 (m, 6H), 6.78-6.74 (d, $J = 8.2$ Hz, 2H), 3.75 (s, NH_2).

4-Amino-4'-(trifluoromethyl)biphenyl: white crystals. ^1H NMR (CDCl_3 , 200 MHz) δ 7.64 (s, 4H), 7.46-7.42 (d, $J = 8.4$ Hz, 2H), 6.80-6.76 (d, $J = 8.4$ Hz, 2H), 3.80 (s, NH_2).

4-Amino-3',5'-dimethoxybiphenyl: white solid. ^1H NMR (CDCl_3 , 200 MHz) δ 7.43-7.39 (d, $J = 8.6$ Hz, 2H), 6.77-6.73 (d, $J = 8.6$ Hz, 2H), 6.69-6.68 (d, $J' = 2.2$ Hz, 2H), 6.42-6.40 (t, $J' = 2.2$ Hz, 1H).

4-Amino-4'-(N,N-dimethylamino)biphenyl: white solid. ^1H NMR (200 MHz, CDCl_3) δ 7.44-7.40 (2H, d, $J = 8.6$ Hz), 7.38-7.34 (2H, d, $J = 8.6$ Hz), 6.81-6.77 (2H, d, $J = 8.6$ Hz), 6.76-6.71 (2H, d, $J = 8.6$ Hz), 3.66 (s, NH_2), 2.97 (6H, s).

4-Amino-3,5-dimethylbiphenyl was prepared from phenylboronic acid and 4-bromo-2,6-dimethylaniline. It is a white solid. ^1H NMR (CDCl_3 , 200 MHz) δ 7.56-7.52 (d, $J = 8.2$ Hz, 2H), 7.43-7.35 (t, $J = 8.2$ Hz, 2H), 7.30-7.22 (t, $J = 8.2$ Hz, 1H), 7.21 (s, 2H), 3.75 (s, NH_2), 2.27 (s, 6H).

3.1.4. Synthesis of 4-azidobiaryls

General procedure. 4-Azido-4'-methoxybiphenyl. The 4-amino-4'-methoxybiphenyl (10 mmol) was dissolved in 40 ml of glacial acetic acid containing 10 ml of concentrated sulfuric acid. The solution was cooled to below 5°C in an ice bath and diazotized with a solution of 0.76 g of NaNO₂ (11 mmol) in 7 ml of distilled water. After one hour of stirring, 100 ml of ice-water was added. Enough urea was added to destroy the excess nitrous acid, and 0.5 gm of Norit was then added. The cold suspension was stirred for 15 minutes and was then rapidly filtered into a flask immersed in an ice bath. The clear, yellow filtrate was treated with 1.34 g of NaN₃ (20 mmol) in 10 ml of water at 0°C. Nitrogen was immediately evolved, the solution became turbid and a light tan precipitate formed in a few minutes. The mixture was kept in the ice-bath and stirred for one hour after the addition of NaN₃ was complete, and was then allowed to warm to room temperature and stand overnight. The precipitate was filtered, washed first with 10% Na₂CO₃ and then with water. The crude product was purified by column chromatography on silica gel eluted with ethyl acetate/hexanes and was recrystallized in hexanes to give pale yellow crystals.

¹H NMR (500 MHz, CDCl₃) δ 7.52-7.50 (2H, d, J = 8.5 Hz), 7.48-7.46 (2H, d, J = 8.5 Hz), 7.06-7.04 (2H, d, J = 8.5 Hz), 6.96-6.94 (2H, d, J = 8.5 Hz), 3.83 (3H, s); HRMS (EI, 70eV): m/z 225.0891, C₁₃H₁₁N₃O requires 225.0902, after loss of N₂, 197.0837, C₁₃H₁₁NO requires 197.0841.

The following azides were prepared by the procedure described above and characterized with 500 MHz ¹H NMR and high resolution mass spectroscopy.

4-Azido-4'-methylbiphenyl: pale yellow crystals; ¹H NMR (500 MHz, CDCl₃) δ 7.55-7.53 (2H, d, J = 8.5 Hz), 7.45-7.43 (2H, d, J = 8.5 Hz), 7.24-7.22 (2H, d, J = 8.5 Hz), 7.07-7.05 (2H, d, J = 8.5 Hz), 2.37 (3H, s); HRMS (EI, 70ev): m/z 209.0951, C₁₃H₁₁N₃ requires 209.0953.

4-Azido-4'-fluorobiphenyl: pale yellow crystals; ^1H NMR (500 MHz, CDCl_3) δ 7.51-7.47 (4H, m), 7.12-7.06 (4H, m); HRMS (EI, 70ev): m/e 213.0694, $\text{C}_{12}\text{H}_8\text{N}_3\text{F}$ requires 213.0702.

4-Azido-3'-methylbiphenyl: light yellow oil; ^1H NMR (500 MHz, CDCl_3) δ 7.56-7.54 (2H, d, $J = 8.5$ Hz), 7.36-7.3 (3H, m), 7.16-7.14 (1H, m), 7.08-7.06 (2H, d, $J = 8.5$ Hz); HRMS (EI, 70ev): m/z 209.0957, $\text{C}_{12}\text{H}_8\text{N}_3\text{Cl}$ requires 209.0953.

4-Azido-3'-methoxybiphenyl: light yellow oil; ^1H NMR (500 MHz, CDCl_3) δ 7.60-7.58 (2H, d, $J = 8.5$ Hz), 7.39-7.35 (1H, t, $J = 8.5$ Hz), 7.18-7.08 (3H, m), 6.94-6.90 (1H, m), 3.88 (3H, s); HRMS (EI, 70ev): m/z 225.0897, $\text{C}_{13}\text{H}_{11}\text{N}_3\text{O}$ requires 225.0902.

4-Azido-4'-chlorobiphenyl: pale yellow crystals; ^1H NMR (500 MHz, CDCl_3) δ 7.53-7.51 (2H, d, $J = 8.5$ Hz), 7.47-7.45 (2H, d, $J = 8.5$ Hz), 7.39-7.37 (2H, d, $J = 8.5$ Hz), 7.09-7.07 (2H, d, $J = 8.5$ Hz); HRMS (EI, 70ev): m/z 229.0409, $\text{C}_{12}\text{H}_8\text{N}_3\text{Cl}$ requires 229.0407.

4-Azido-3'-chlorobiphenyl: light yellow crystals; ^1H NMR (500 MHz, CDCl_3) δ 7.54-7.52 (3H, m), 7.42-7.4 (1H, m), 7.36-7.33 (1H, t, $J = 8.0$ Hz), 7.31-7.29 (1H, m), 7.09-7.07 (2H, d, $J = 8.5$ Hz); HRMS (EI, 70ev): m/z 229.0411, $\text{C}_{12}\text{H}_8\text{N}_3\text{Cl}$ requires 229.0407.

4-Azido-4'-trifluoromethylbiphenyl: light yellow crystals; ^1H NMR (500 MHz, CDCl_3) δ 7.68-7.66 (2H, d, $J = 8.5$ Hz), 7.65-7.63 (2H, d, $J = 8.5$ Hz), 7.58-7.56 (2H, d, $J = 8.5$ Hz), 7.12-7.10 (2H, d, $J = 8.5$ Hz); HRMS (EI, 70ev): m/z 263.0668, $\text{C}_{13}\text{H}_8\text{N}_3\text{F}_3$ requires 263.0670.

4-Azido-3',5'-dimethoxybiphenyl: light yellow oil; ^1H NMR (200 MHz, CDCl_3) δ 7.59-7.55 (2H, d, $J = 8.6$ Hz), 7.11-7.07 (2H, d, $J = 8.6$ Hz), 6.70-6.69 (2H, d, $J' = 2.2$ Hz), 6.48-6.46 (1H, t, $J' = 2.2$ Hz); HRMS (EI, 70ev): m/z 255.1015, $\text{C}_{14}\text{H}_{13}\text{N}_3\text{O}_2$ requires 255.1008.

4-Azido-4'-(N,N-dimethylamino)biphenyl: yellow crystals; ^1H NMR (500 MHz, CDCl_3) δ 7.61-7.56 (2H, d, $J = 8.8$ Hz), 7.54-7.49 (2H, d, $J = 8.8$ Hz), 7.12-

7.08 (2H, d, J = 8.8 Hz), 6.87-6.82 (2H, d, J = 8.8 Hz), 3.04 (6H, s); HRMS (EI, 70ev): m/z 238.1222, C₁₄H₁₄N₄ requires 238.1218.

4-Azido-3,5-dimethylbiphenyl: pale yellow crystals; ¹H NMR (500 MHz, CDCl₃) δ 7.53-7.51 (2H, m), 7.41-7.37 (2H, m), 7.33-7.30 (1H, m), 7.225 (2H, s), 2.41 (6H, s); HRMS (EI, 70ev): m/z 223.1107, C₁₄H₁₃N₃ requires 223.1109.

3.2. Synthesis of 4,4-dimethyl-1-phenyl-2,5-cyclohexadienol (61), and compounds derived from 61

4,4-Dimethylcyclohexa-2,5-dienone (63). To a solution of 2,3-dichloro-4,5-dicyanobenzoquinone (10g, 0.045 mol) in 70 ml of purified dioxane under the protection of argon was added 4,4-dimethylcyclohex-2-enone (5 ml, 4.6 g, 0.038 mol). The resulting mixture was refluxed at 95-100°C for 24 hrs. After cooling to room temperature, the 2,3-dichloro-4,5-dicyanodihydrobenzoquinone solid formed from the reaction was filtered off and washed by large amount of pentane. The combined supernatants were dried over MgSO₄ and concentrated to yield an oil. Chromatography (flash column, silica gel, and ethyl acetate-hexanes 30:70) afforded the product as a colorless oil.

¹H NMR (CDCl₃, 200 MHz) δ 6.86-6.81(d, J = 10.0 Hz, 2H), 6.22-6.17 (d, J = 10.0 Hz, 2H), 1.26 (s, 6H).

4,4-Dimethyl-1-phenylcyclohexa-2,5-dien-1-ol (61). 4,4-Dimethylcyclohexa-2,5-dienone (1.22 g, 10.0 mmol) in 10 ml of THF was added dropwise at -78°C to phenyl lithium (10.08 mmol) in hexanes under an Argon atmosphere. After stirring at -78°C for 30 minutes, the flask was allowed to warm to room temperature and stirred at this temperature for a further hour. The mixture was then hydrolyzed with aqueous K₂CO₃ and extracted with ether. The ether extract was dried over MgSO₄, and concentrated to yield an oil. Chromatography on a silica gel column eluted with 15% ethyl acetate-85% hexane gave 1.32 g of **61** as a viscous oil, which solidified to a waxy solid on complete removal of solvent.

^1H NMR (500 MHz, CDCl_3) δ 7.55-7.45 (m, 2H), 7.4-7.2 (m, 3H), 5.82 (d, $J = 8$ Hz, 2H), 5.76 (d, $J = 8$ Hz, 2H), 1.93 (s, OH), 1.18 (s, 3H), 1.16 (s, 3H). HRMS (EI, 70 eV): m/z , 200.1200, $\text{C}_{14}\text{H}_{16}\text{O}$ requires 200.1201.

Isolation of 6,6-dimethyl-3-phenylcyclohexa-2,4-dienol (62) and 3,4-dimethylbiphenyl (64). When 4,4-dimethyl-1-phenylcyclohexa-2,5-dienol (61) contains trace amount of solvents (hexanes and/or ethyl acetate), it slowly isomerizes to the conjugate alcohol 62, and loses water to form 64. Thus after standing for several days a mixture of the three compounds was obtained. These could be separated by chromatography on silica gel with 15% ethyl acetate-85% hexanes: 64 elutes first as a colorless liquid, followed by 61, and then 62 elutes as a sticky oil.

62: ^1H NMR (CDCl_3 , 200 MHz) δ 7.5-7.3 (m, 5H), 6.52 (dd, $J = 8$ Hz and $J' = 1$ Hz, 1H), 6.24 (dd, $J'' = 3$ Hz and $J' = 1$ Hz, 1H), 5.82 (d, $J = 8$ Hz), 4.08 (dd, $J''' = 7$ Hz, and $J'' = 3$ Hz, 1 H), 1.7 (d, $J''' = 7$ Hz, OH), 1.19 (s, 3H), 1.11 (s, 3H). HRMS (EI, 70 eV) m/z , 200.1205, $\text{C}_{14}\text{H}_{16}\text{O}$ requires 200.1201.

64: ^1H NMR (CDCl_3 , 200 MHz) δ 7.8-7.6 (m, 8H), 2.15 (s, 3H), 2.13 (s, 3H). HRMS (EI, 70 eV): m/z , 182.1902, $\text{C}_{14}\text{H}_{14}$ requires 182.1906.

6,6-Dimethyl-3-phenylcyclohexa-2,4-dienyl acetate (46). Sodium hydride (0.4 g of 60% dispersion in oil, 10.5 mmol) was washed three times with dry hexanes, and after evaporation of hexanes under vacuum, 2 ml of dry THF was then added. To the resulting suspension was slowly added a solution of 61 (2.0 g, 10.0 mmol) in 10 ml of dry THF. After stirring at 40°C for 2 hrs, the mixture was cooled in dry ice-acetone bath and acetic anhydride (10.6 mmol) in 5 ml of dry THF was slowly added. The resulting mixture was then allowed to warm to room temperature and stirred for half an hour. Aqueous K_2CO_3 was then added and the mixture was extracted with ether. The organic layer was dried over CaCl_2 and solvent was removed. Chromatography of the crude product on a silica gel column eluted with 20% ethyl acetate- 80% hexanes gave 1.24 g of 46 as a colorless oil.

^1H NMR (CDCl_3 , 200 MHz) δ 7.5-7.3 (m, 5H), 6.32 (dd, $J = 8$ Hz, $J' = 1$ Hz, 1H), 6.05 (dd, $J'' = 3$ Hz, $J' = 1$ Hz, 1H), 5.84 (d, $J = 8$ Hz, 1H), 5.32 (d, $J'' = 3$ Hz, 1H). HRMS (EI, 70 eV): m/z , 242.1309, $\text{C}_{16}\text{H}_{18}\text{O}_2$ requires 242.1307.

4,4-Dimethyl-1-(3',5'-dimethoxyphenyl)cyclohexa-2,5-dien-1-ol (47). *n*-Butyl lithium (2.5M solution in hexanes, 2 ml, 5 mmol) was slowly added at -78°C to a solution of 1-bromo-3,5-dimethoxybenzene (1.1g, 5 mmol) in 25 ml of dry THF under the protection of argon. After stirring for half an hour, 4,4-dimethylcyclohexa-2,5-dienone (0.61 g, 5.0 mmol) in 5 ml of dry THF was added dropwise to the mixture. The resulting mixture was stirred at -78°C for 30 minutes, then was allowed to warm up to room temperature, at which point it was stirred for a further half hour. Aqueous K_2CO_3 was then added, the organic layer was separated, and dried over MgSO_4 . After removal of the solvent, chromatography on silica gel with 15% ethyl acetate-85% hexane gave 1 g of **47** as a viscous oil.

^1H NMR (CDCl_3 , 200 MHz) δ 6.63 (d, $J = 2.2$ Hz, 2H), 6.34 (t, $J = 2.2$ Hz, 1H), 5.83-5.78 (d, $J' = 10$ Hz, 2H), 5.74-5.69 (d, $J' = 10$ Hz, 2H), 3.78 (s, 6H), 1.93 (s, OH), 1.15 (s, 3H), 1.13 (s, 3H). HRMS (EI, 70 eV): m/z , 260.1414, $\text{C}_{16}\text{H}_{20}\text{O}$ requires 260.1412.

4. LFP Measurements of Second-order Rate Constants for Reactions of Nitrenium Ions with Added Nucleophiles

For the trapping studies with azide ion and ethyl vinyl ether, the irradiation wavelength of laser was set at 248 nm, whereas it was set at 308 nm for the study of guanine derivatives since these compounds absorb at 248 nm. The first-order rate constants for the decay of the nitrenium ions were measured at 460 nm in the presence of 5-6 concentrations of nucleophiles, over the range of $0-1.5 \times 10^{-3}$ M for sodium azide, and 0-0.5 M for ethyl vinyl ether. Sodium azide was added to the substrate solution as 0.1 M solution in deionized water and ethyl vinyl ether was added as 0.5 M solution in 20% aqueous acetonitrile. Good linear relationships were observed between the observed rate constants for decay (k_{obsd}) and the concentrations of added nucleophiles. The data fit the equation $k_{\text{obsd}} = k_0 + k_{\text{nu}}[\text{Nu}]$. Linear least-squares analysis by the Grafit program gives the second-order rate constants k_{Nu} . The plots of k_{obsd} vs. nucleophile concentrations and observed rate constants for decay are given in the following figures and tables.

4.1. Trapping of nitrenium ions by azide ion.

Figure 36. Relationship between the observed first-order rate constants for the decay of 4'-methoxy-4-biphenylnitrenium ion and the concentration of azide ion.

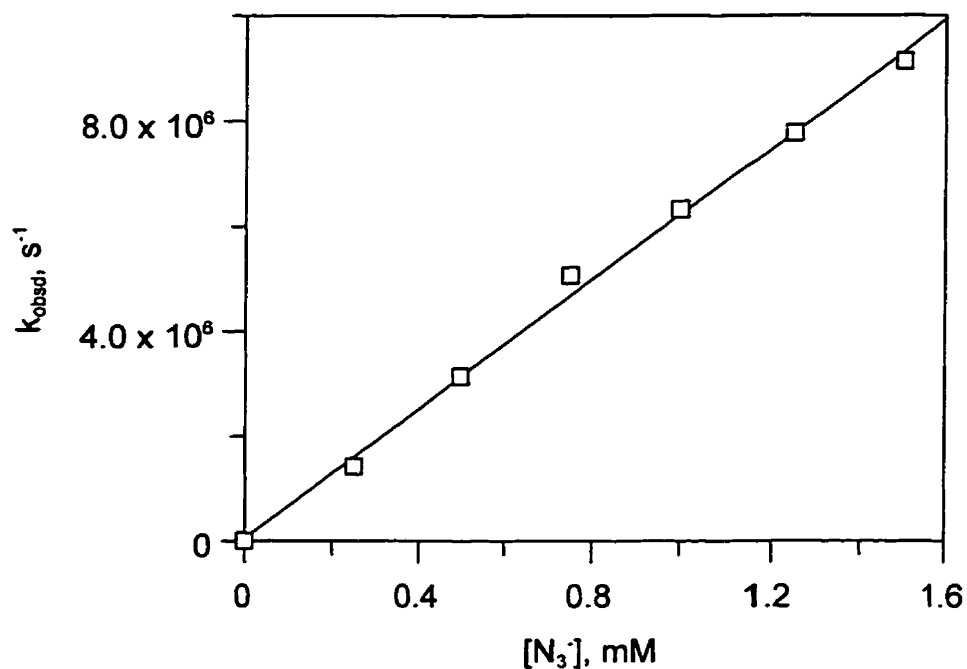


Table 15. Observed first-order rate constants for the decay of 4'-methoxy-4-biphenylnitrenium ion in the presence of azide ion.

$[\text{N}_3^-], 10^{-3}\text{M}$	$k_{\text{obsd}}, \text{s}^{-1}$	Slope, $\text{M}^{-1}\text{s}^{-1}$
0.00	2.00×10^3	6.18×10^9
0.25	1.41×10^6	
0.50	3.14×10^6	
0.75	5.07×10^6	
1.00	6.32×10^6	
1.25	7.77×10^6	
1.50	9.13×10^6	

Figure 37. Relationship between the observed first-order rate constants for the decay of 4'-methyl-4-biphenylnitrenium ion and the concentration of azide ion.

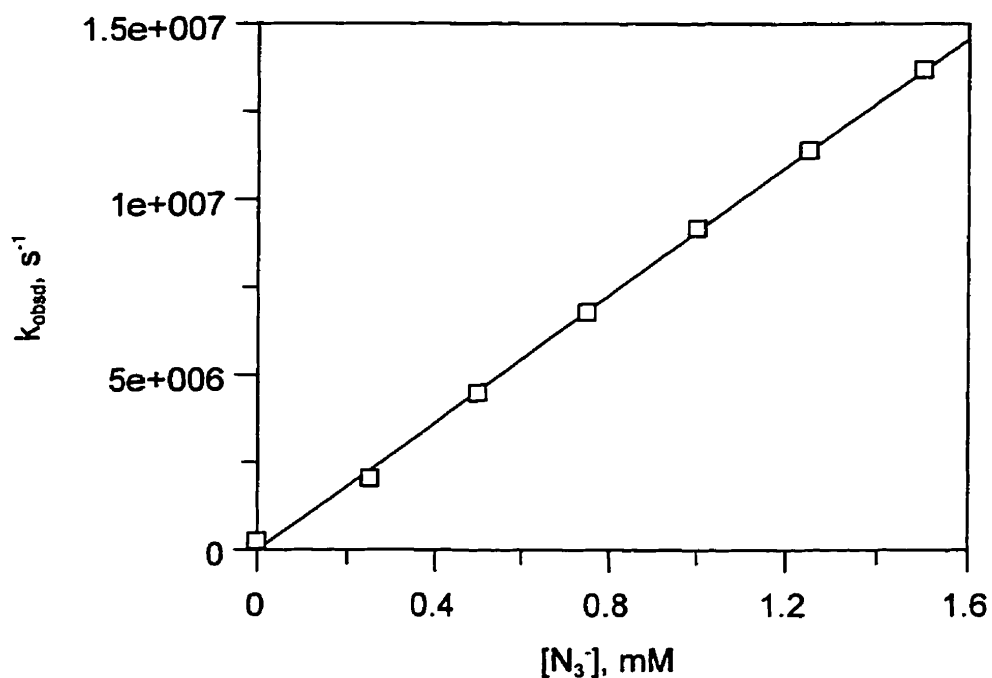


Table 16. Observed first-order rate constants for the decay of 4'-methyl-4-biphenylnitrenium ion in the presence of azide ion.

[N ₃], 10 ⁻³ M	k _{obsd} , s ⁻¹	Slope, M ⁻¹ s ⁻¹
0.00	2.44 × 10 ⁵	9.11 × 10 ⁹
0.25	2.04 × 10 ⁶	
0.50	4.48 × 10 ⁶	
0.75	6.79 × 10 ⁶	
1.00	9.18 × 10 ⁶	
1.25	1.14 × 10 ⁷	
1.50	1.37 × 10 ⁷	

Figure 38. Relationship between the observed first-order rate constants for the decay of 4'-fluoro-4-biphenylnitrenium ion and the concentration of azide ion.

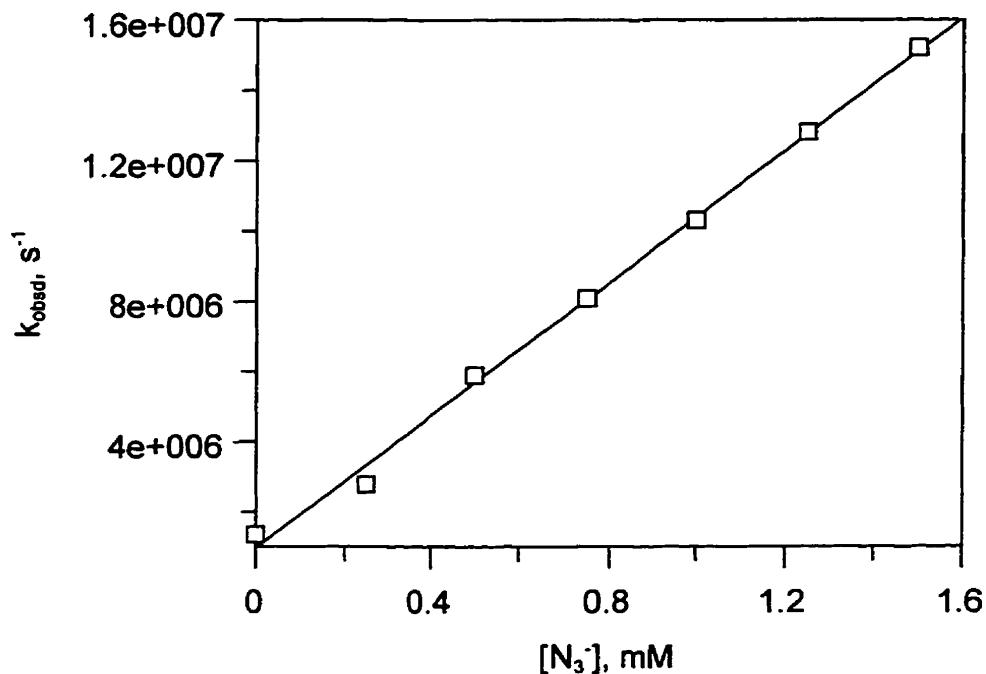


Table 17. Observed first-order rate constants for the decay of 4'-fluoro-4-biphenylnitrenium ion in the presence of azide ion.

[N ₃ ⁻], 10 ⁻³ M	k _{obsd} , s ⁻¹	Slope, M ⁻¹ s ⁻¹
0.00	1.34 × 10 ⁶	9.43 × 10 ⁹
0.25	2.77 × 10 ⁶	
0.50	5.88 × 10 ⁶	
0.75	8.07 × 10 ⁶	
1.00	1.03 × 10 ⁷	
1.25	1.28 × 10 ⁷	
1.50	1.52 × 10 ⁷	

Figure 39. Relationship between the observed first-order rate constants for the decay of 3'-methyl-4-biphenylnitrenium ion and the concentration of azide ion.

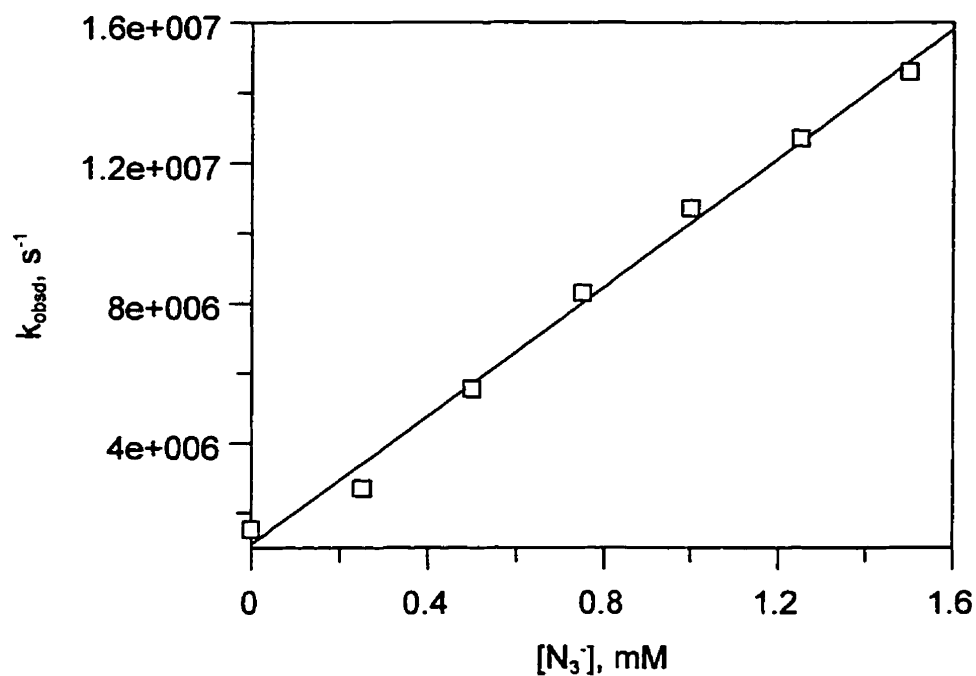


Table 18. Observed first-order rate constants for the decay of 3'-methyl-4-biphenylnitrenium ion in the presence of azide ion.

[N ₃ ⁻], 10 ⁻³ M	k _{obsd} , s ⁻¹	Slope, M ⁻¹ s ⁻¹
0.00	1.52 × 10 ⁶	9.20 × 10 ⁹
0.25	2.69 × 10 ⁶	
0.50	5.54 × 10 ⁶	
0.75	8.28 × 10 ⁶	
1.00	1.07 × 10 ⁷	
1.25	1.27 × 10 ⁷	
1.50	1.46 × 10 ⁷	

Figure 40. Relationship between the observed first-order rate constants for the decay of 3'-methoxy-4-biphenylnitrenium ion and the concentration of azide ion.

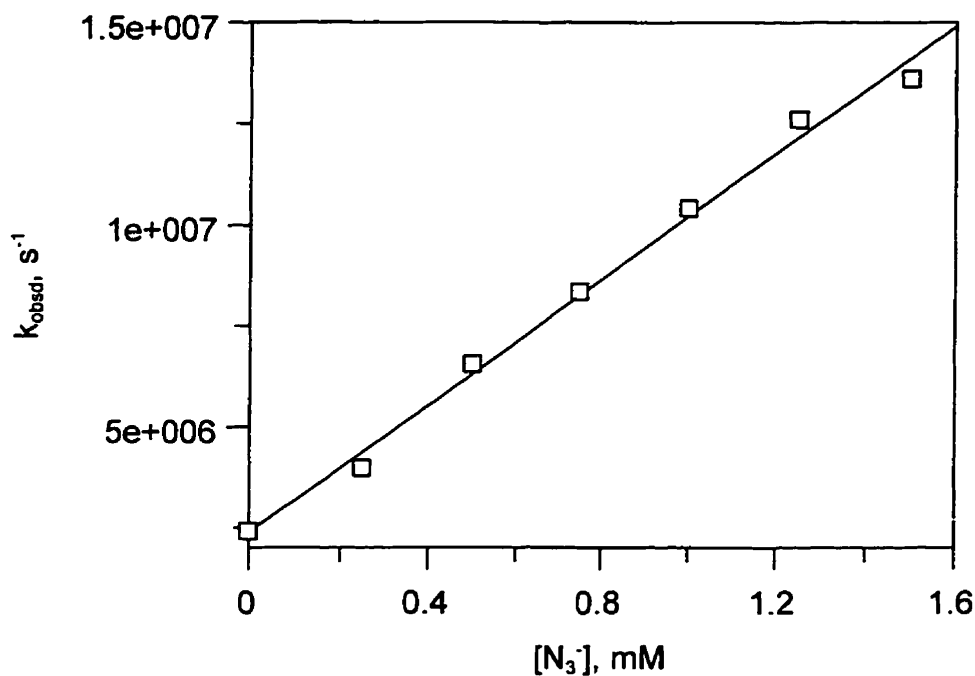


Table 19. Observed first-order rate constants for the decay of 3'-methoxy-4-biphenylnitrenium ion in the presence of azide ion.

[N ₃ ⁻], 10 ⁻³ M	k _{obsd} , s ⁻¹	Slope, M ⁻¹ s ⁻¹
0.090	2.40 × 10 ⁶	7.82 × 10 ⁹
0.25	3.96 × 10 ⁶	
0.50	6.55 × 10 ⁶	
0.75	8.35 × 10 ⁶	
1.00	1.04 × 10 ⁷	
1.25	1.26 × 10 ⁷	
1.50	1.36 × 10 ⁷	

Figure 41. Relationship between the observed first-order rate constants for the decay of 4'-chloro-4-biphenylnitrenium ion and the concentration of azide ion.

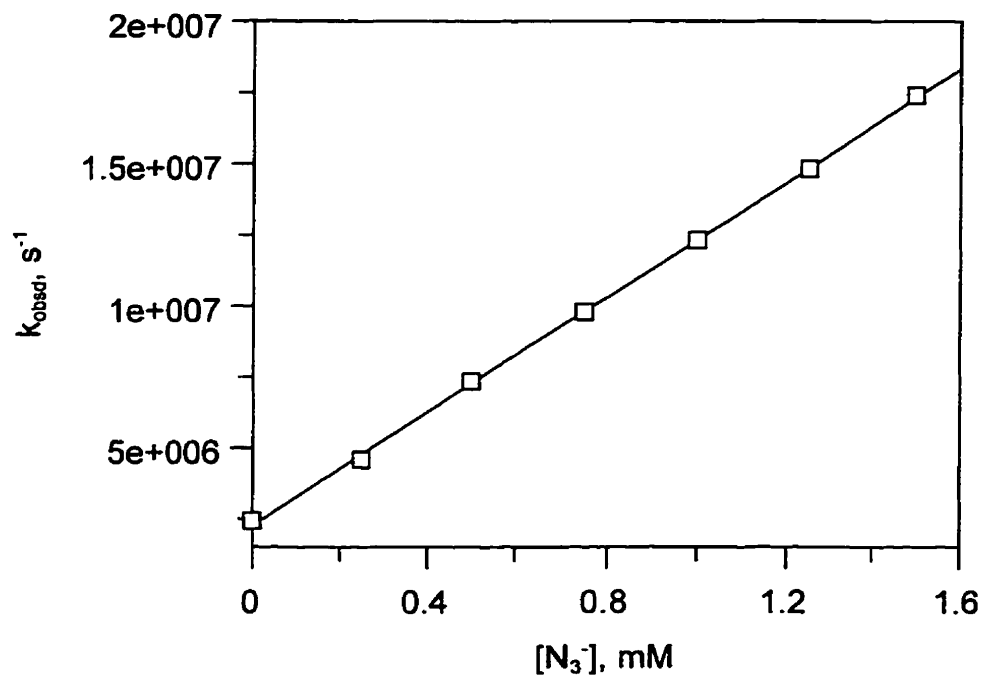


Table 20. Observed first-order rate constants for the decay of 4'-chloro-4-biphenylnitrenium ion in the presence of azide ion.

[N ₃ ⁻], 10 ⁻³ M	k _{obsd} , s ⁻¹	Slope, M ⁻¹ s ⁻¹
0.00	2.42 × 10 ⁶	1.01 × 10 ¹⁰
0.25	4.57 × 10 ⁶	
0.50	7.34 × 10 ⁶	
0.75	9.78 × 10 ⁶	
1.00	1.23 × 10 ⁷	
1.25	1.48 × 10 ⁷	
1.50	1.74 × 10 ⁷	

Figure 42. Relationship between the observed first-order rate constants for the decay of 3'-chloro-4-biphenylnitrenium ion and the concentration of azide ion.

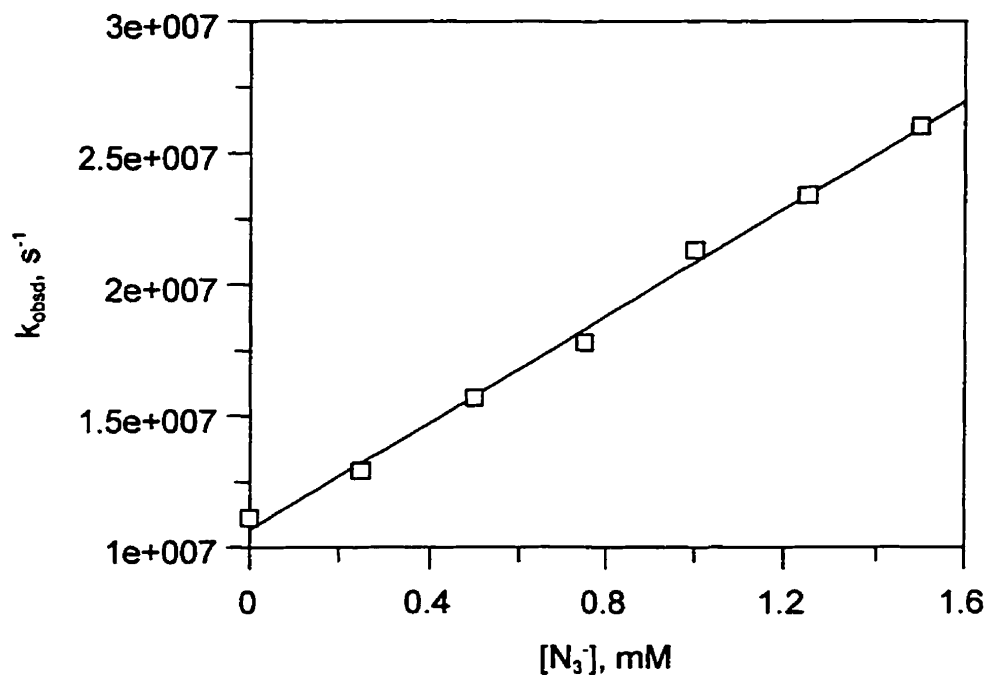


Table 21. Observed first-order rate constants for the decay of 3'-chloro-4-biphenylnitrenium ion in the presence of azide ion.

[N ₃ ⁻], 10 ⁻³ M	k _{obsd} , s ⁻¹	Slope, M ⁻¹ s ⁻¹
0.00	1.11 × 10 ⁷	1.02 × 10 ¹⁰
0.25	1.29 × 10 ⁷	
0.50	1.57 × 10 ⁷	
0.75	1.78 × 10 ⁷	
1.00	2.13 × 10 ⁷	
1.25	2.34 × 10 ⁷	
1.50	2.6 × 10 ⁷	

Figure 43. Relationship between the observed first-order rate constants for the decay of 3',5'-dimethoxy-4-biphenylnitrenium ion and the concentration of azide ion.

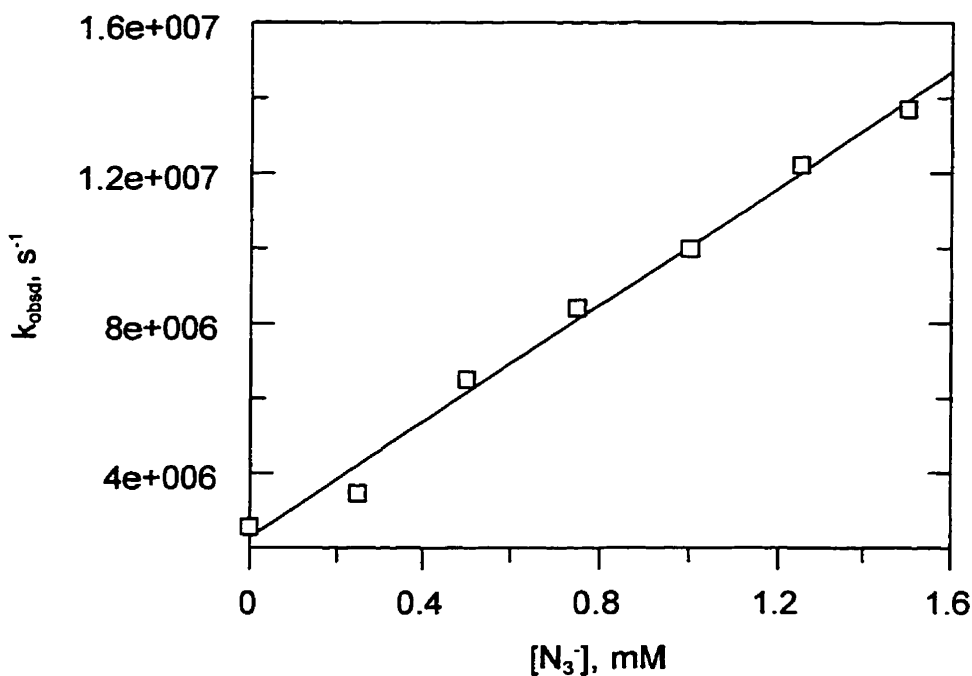


Table 22. Observed first-order rate constants for the decay of 3',5'-dimethoxy-4-biphenylnitrenium ion in the presence of azide ion.

[N ₃ ⁻], 10 ⁻³ M	k _{obsd} , s ⁻¹	Slope, M ⁻¹ s ⁻¹
0.00	2.55 × 10 ⁶	7.78 × 10 ⁹
0.25	3.45 × 10 ⁶	
0.50	6.49 × 10 ⁶	
0.75	8.40 × 10 ⁶	
1.00	9.98 × 10 ⁶	
1.25	1.22 × 10 ⁷	
1.50	1.37 × 10 ⁷	

Figure 44. Relationship between the observed first-order rate constants for the decay of 2,6-dimethyl-4-biphenylnitrenium ion and the concentration of azide ion.

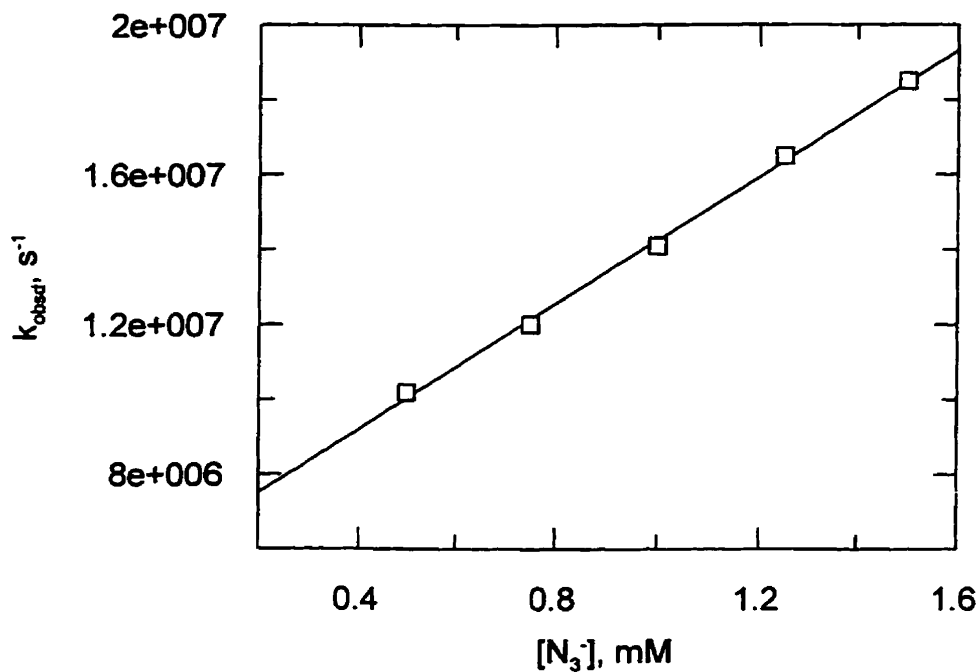


Table 23. Observed first-order rate constants for the decay of 2,6-dimethyl-4-biphenylnitrenium ion in the presence of azide ion.

[N ₃ ⁻], 10 ⁻³ M	k _{obsd} , s ⁻¹	Slope, M ⁻¹ s ⁻¹
0.00	1.48 × 10 ⁵	8.44 × 10 ⁹
0.50	1.02 × 10 ⁷	
0.75	1.20 × 10 ⁷	
1.00	1.41 × 10 ⁷	
1.25	1.65 × 10 ⁷	
1.50	1.85 × 10 ⁷	

4.2. Trapping of nitrenium ions by ethyl vinyl ether.

Figure 45. Relationship between the observed first-order rate constants for the decay of 4'-methoxy-4-biphenylnitrenium ion and the concentration of ethyl vinyl ether.

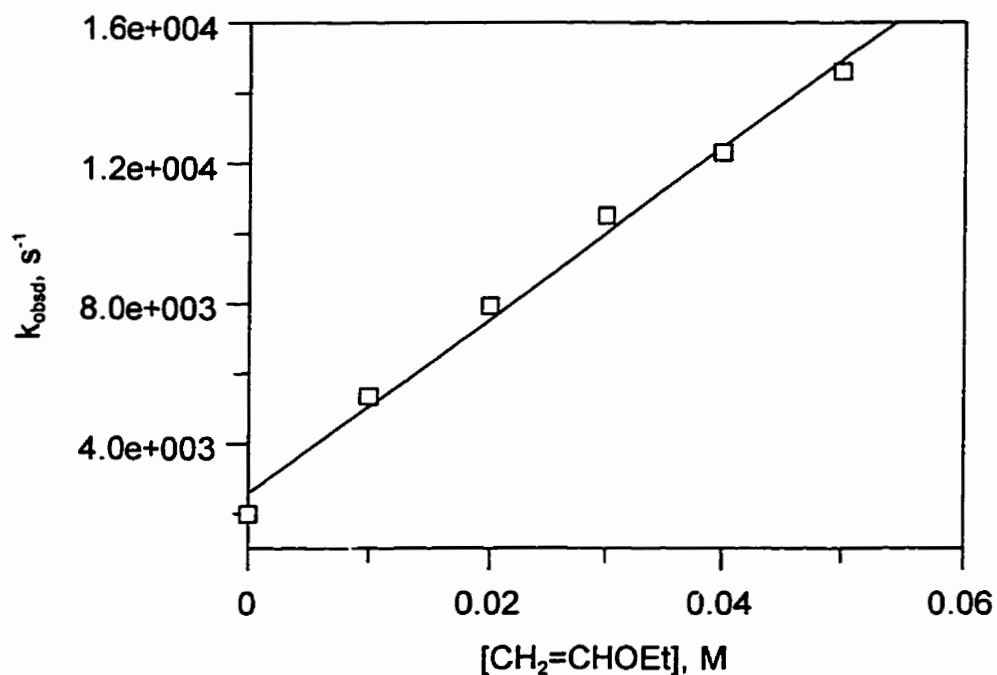


Table 24. Observed first-order rate constants for the decay of 4'-methoxy-4-biphenylnitrenium ion in the presence of ethyl vinyl ether.

[CH ₂ =CHOEt], M	k _{obsd} , s ⁻¹	Slope, M ⁻¹ s ⁻¹
0.00	1.97 × 10 ³	2.47 × 10 ⁵
0.01	5.34 × 10 ³	
0.02	7.92 × 10 ³	
0.03	1.05 × 10 ⁴	
0.04	1.23 × 10 ⁴	
0.05	1.46 × 10 ⁴	

Figure 46. Relationship between the observed first-order rate constants for the decay of 4'-methyl-4-biphenylnitrenium ion and the concentration of ethyl vinyl ether.

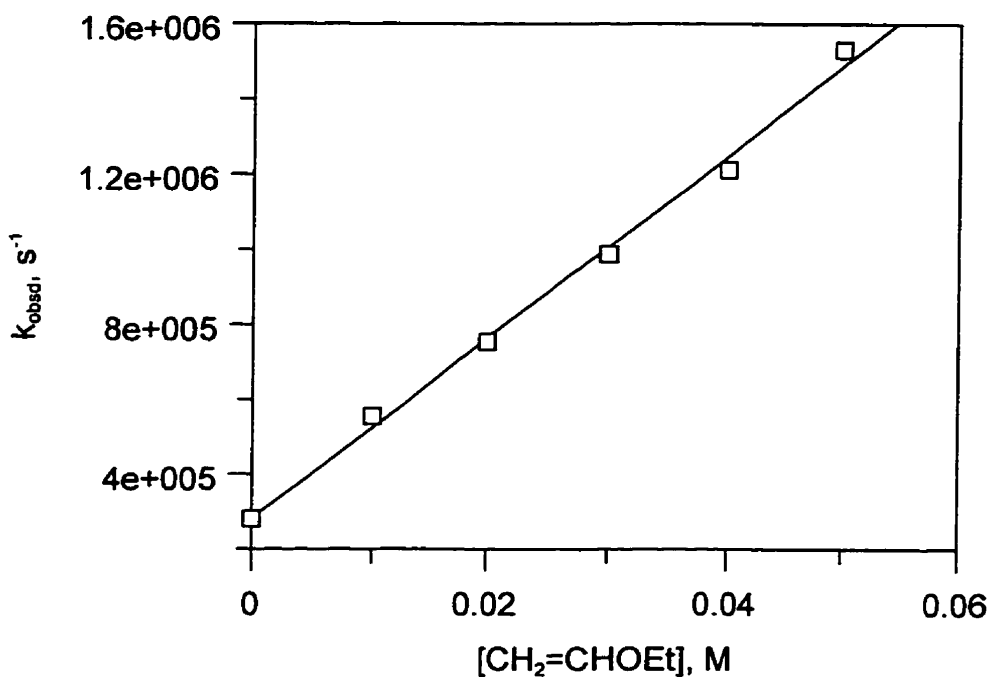


Table 25. Observed first-order rate constants for the decay of 4'-methyl-4-biphenylnitrenium ion in the presence of ethyl vinyl ether.

[CH ₂ =CHOEt], M	k _{obsd} , s ⁻¹	Slope, M ⁻¹ s ⁻¹
0.00	2.80 × 10 ⁵	2.41 × 10 ⁷
0.01	5.54 × 10 ⁵	
0.02	7.54 × 10 ⁵	
0.03	9.87 × 10 ⁵	
0.04	1.21 × 10 ⁶	
0.05	1.53 × 10 ⁶	

Figure 47. Relationship between the observed first-order rate constants for the decay of 4'-fluoro-4-biphenylnitrenium ion and the concentration of ethyl vinyl ether.

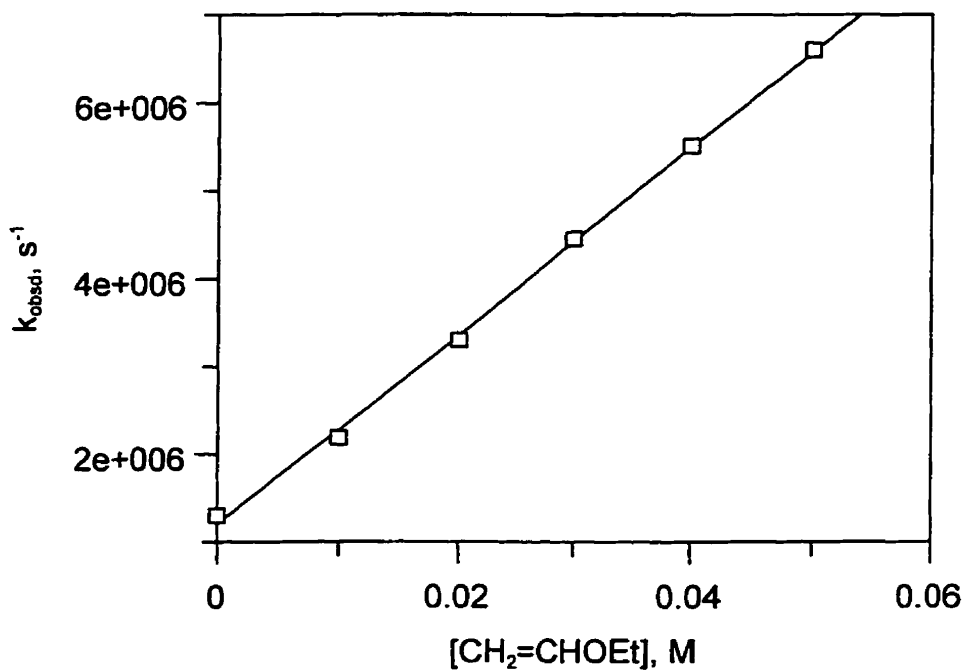


Table 26. Observed first-order rate constants for the decay of 4'-fluoro-4-biphenylnitrenium ion in the presence of ethyl vinyl ether.

[CH ₂ =CHOEt], M	k _{obsd} , s ⁻¹	Slope, M ⁻¹ s ⁻¹
0.00	1.30 × 10 ⁶	1.07 × 10 ⁸
0.01	2.19 × 10 ⁶	
0.02	3.30 × 10 ⁶	
0.03	4.45 × 10 ⁶	
0.04	5.51 × 10 ⁶	
0.05	6.60 × 10 ⁶	

Figure 48. Relationship between the observed first-order rate constants for the decay of 3'-methyl-4-biphenylnitrenium ion and the concentration of ethyl vinyl ether.

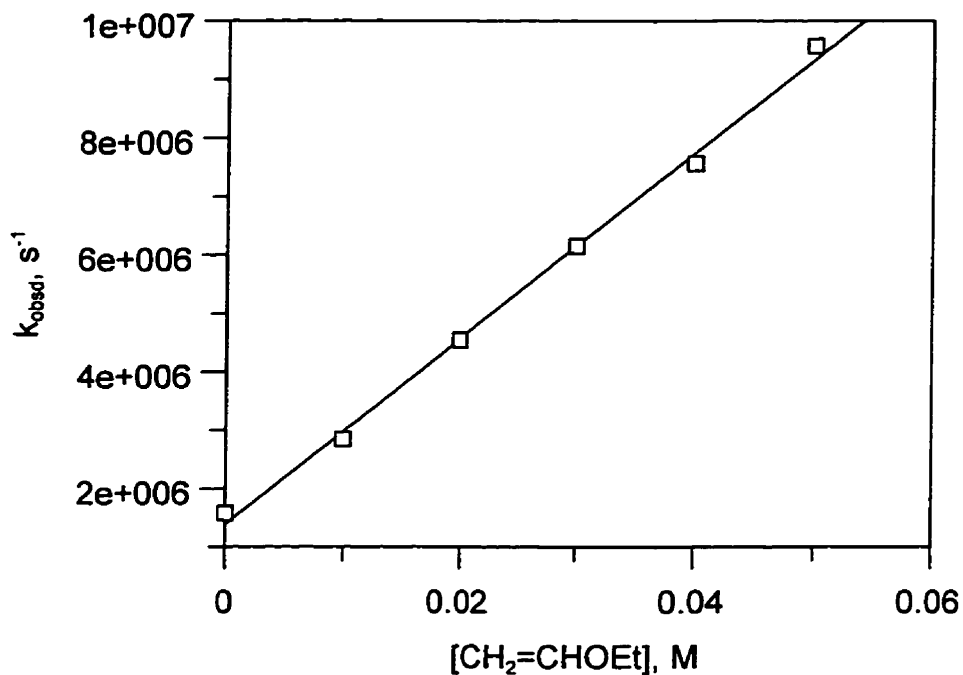


Table 27. Observed first-order rate constants for the decay of 3'-methyl-4-biphenylnitrenium ion in the presence of ethyl vinyl ether.

[CH ₂ =CHOEt], M	k _{obsd} , s ⁻¹	Slope, M ⁻¹ s ⁻¹
0.00	1.57 x 10 ⁶	1.59 x 10 ⁸
0.01	2.84 x 10 ⁶	
0.02	4.54 x 10 ⁶	
0.03	6.15 x 10 ⁶	
0.04	7.56 x 10 ⁶	
0.05	9.56 x 10 ⁶	

Figure 49. Relationship between the observed first-order rate constants for the decay of 3'-methoxy-4-biphenylnitrenium ion and the concentration of ethyl vinyl ether.

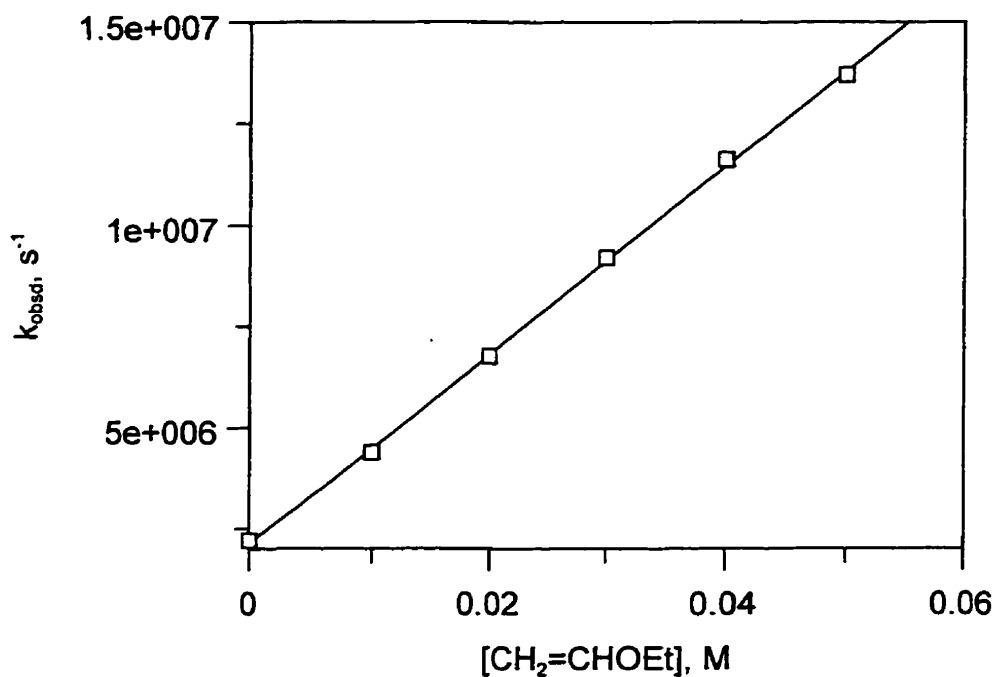


Table 28. Observed first-order rate constants for the decay of 3'-methoxy-4-biphenylnitrenium ion in the presence of ethyl vinyl ether.

[CH ₂ =CHOEt], M	k _{obsd} , s ⁻¹	Slope, M ⁻¹ s ⁻¹
0.00	2.20 × 10 ⁶	2.33 × 10 ⁸
0.01	4.37 × 10 ⁶	
0.02	6.76 × 10 ⁶	
0.03	9.19 × 10 ⁶	
0.04	1.16 × 10 ⁷	
0.05	1.37 × 10 ⁷	

Figure 50. Relationship between the observed first-order rate constants for the decay of 4'-chloro-4-biphenylnitrenium ion and the concentration of ethyl vinyl ether.

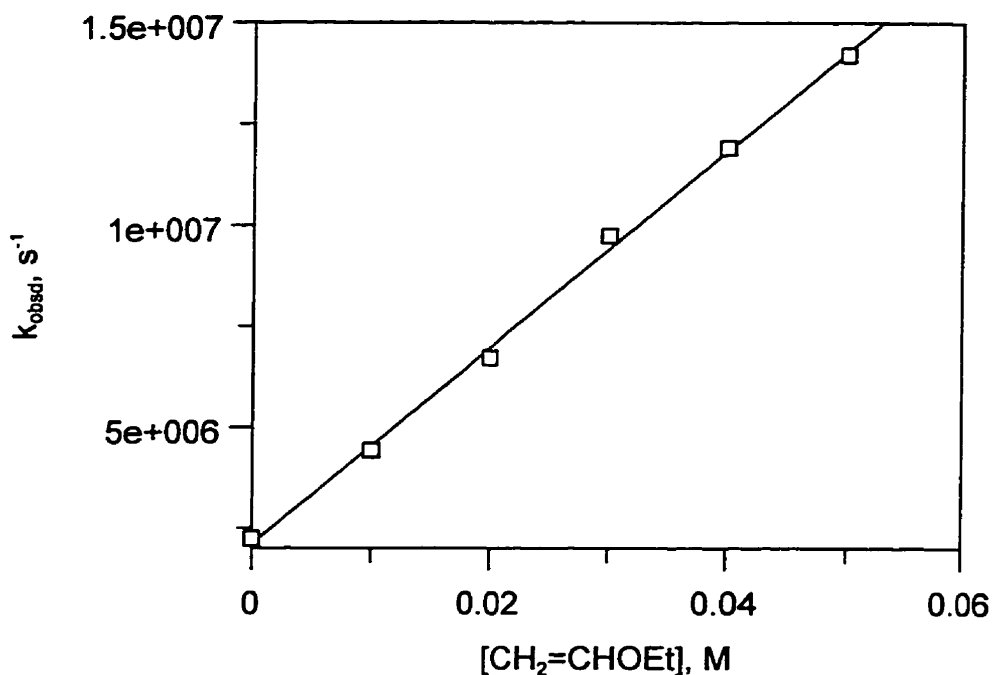


Table 29. Observed first-order rate constants for the decay of 4'-chloro-4-biphenylnitrenium ion in the presence of ethyl vinyl ether.

[CH ₂ =CHOEt], M	k _{obsd} , s ⁻¹	Slope, M ⁻¹ s ⁻¹
0	2.23 × 10 ⁶	2.44 × 10 ⁸
0.01	4.42 × 10 ⁶	
0.02	6.71 × 10 ⁶	
0.03	9.73 × 10 ⁶	
0.04	1.19 × 10 ⁷	
0.05	1.42 × 10 ⁷	

Figure 51. Relationship between the observed first-order rate constants for the decay of 3'-chloro-4-biphenylnitrenium ion and the concentration of ethyl vinyl ether.

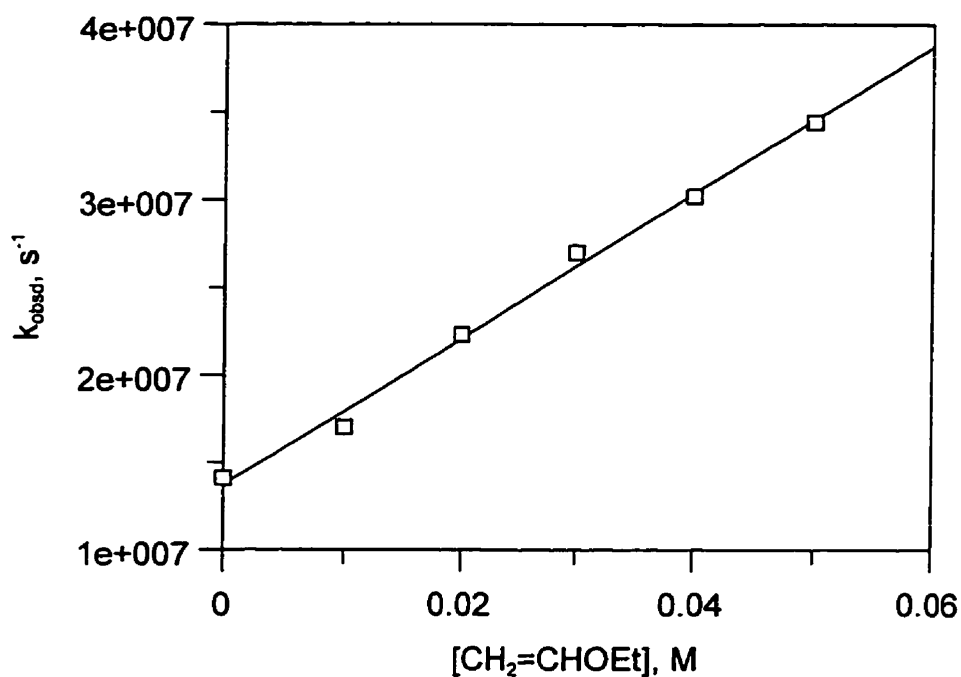


Table 30. Observed first-order rate constants for the decay of 3'-chloro-4-biphenylnitrenium ion in the presence of ethyl vinyl ether.

[CH ₂ =CHOEt], M	k _{obsd} , s ⁻¹	Slope, M ⁻¹ s ⁻¹
0.00	1.41 × 10 ⁷	4.17 × 10 ⁸
0.01	1.70 × 10 ⁷	
0.02	2.23 × 10 ⁷	
0.03	2.70 × 10 ⁷	
0.04	3.02 × 10 ⁷	
0.05	3.44 × 10 ⁷	

Figure 52. Relationship between the observed first-order rate constants for the decay of 2,6-dimethyl-4-biphenylnitrenium ion and the concentration of ethyl vinyl ether.

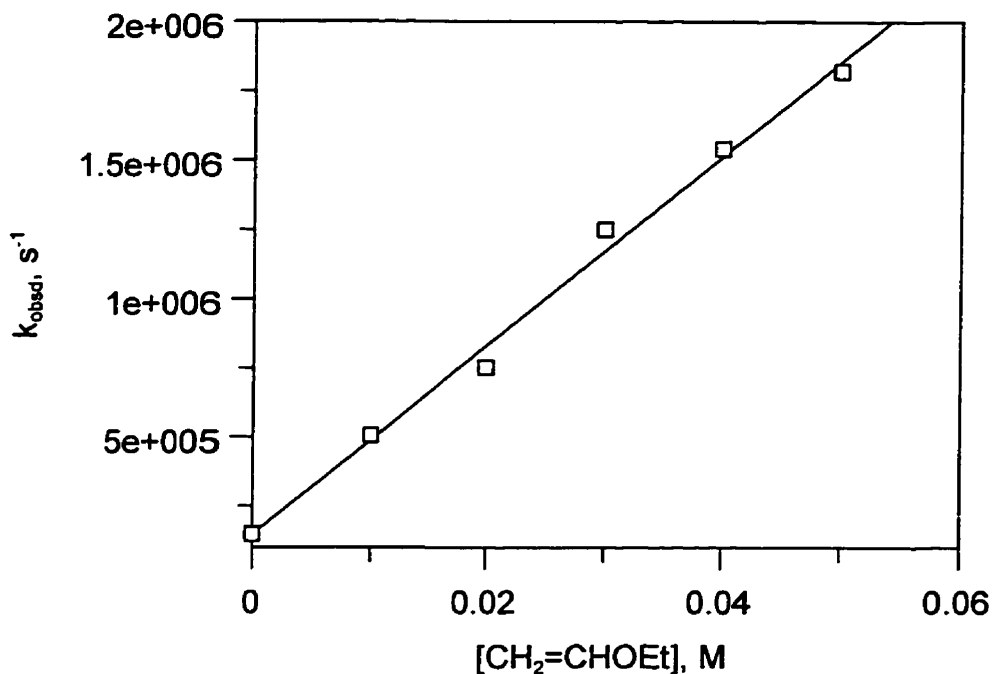


Table 31. Observed first-order rate constants for the decay of 2,6-dimethyl-4-biphenylnitrenium ion in the presence of ethyl vinyl ether.

[CH ₂ =CHOEt], M	k _{obsd} , s ⁻¹	Slope, M ⁻¹ s ⁻¹
0.00	1.47 × 10 ⁵	3.42 × 10 ⁷
0.01	5.06 × 10 ⁵	
0.02	7.52 × 10 ⁵	
0.03	1.25 × 10 ⁶	
0.04	1.54 × 10 ⁶	
0.05	1.82 × 10 ⁶	

REFERENCES

1. Garner, R. C.; Martin, C. N.; Clayson, D. B. In *Chemical Carcinogens (ACS Monograph, No. 182)*, Searle C. E., Ed.; American Chemical Society; Washington, D. C., 2nd ed. **1984**, Vol. 1, pp 175-276.
2. Kadlubar, F. F.; Beland, F. A. In *Polycyclichydrocarbons and Carcinogenesis*; ACS Symposium Series 283; American Chemical Society: Washington, D. C., **1985**, pp 341-370.
3. Kriek, E.; Westra J. G. In *Chemical Carcinogens and DNA*, Grover, P. L., Ed.; CRC; Boca Raton, Florida; **1979**, Vol. II, pp 1-28.
4. Miller, E. C.; Miller, J. A. *Cancer*, **1981**, *47*, 2327-2345.
5. Schut, H. A. J.; Castonguay, A. *Drug Metab. Rev.* **1984**, *15*, 753-839.
6. Abramovitch, R. A.; Jeyaraman, R. In *Azides and Nitrenes: Reactivity and Utility*, Scriven, E. F. V., Ed.; Academic; Orlando, FL., **1984**; pp 297-357.
7. Abramovitch, R. A. In *Organic Reactive Intermediates*, McManus, S. P., Ed.; Academic; New York and London; **1973**, pp 181-184.
8. Gassman, P. G. *Acc. Chem. Res.* **1970**, *3*, 26-33.
9. Simonova, T. P.; Nefedov, V. D.; Toropova, M. A.; Kirillov, N. F. *Russ. Chem. Rev.* **1992**, *61*, 584-599.
10. Heller, H. E.; Hughes, E. D.; Ingold, C. K. *Nature* **1951**, *168*, 909-910.
11. Cramer, C. J.; Dulles, F. J.; Storer, J. W.; Worthington, S. E. *Chem. Phys. Lett.* **1994**, *218*, 387-394.

12. Peyerimhoff, S. D.; Buenker, R. J. *Chem. Phys.* **1979**, *42*, 167-176.
13. Gibson, S. T.; Greene, J. P.; Berkowitz, J. J. *Chem. Phys.* **1985**, *83*, 4319-4328.
14. Ford, G. P.; Scribner, J. D. *J. Am. Chem. Soc.* **1981**, *103*, 4283-4291.
15. Falvey, D. E.; Cramer, C. J. *Tetrahedron Lett.* **1992**, *33*, 1705-1708.
16. Ford, G. P.; Herman, P. S. *J. Mol. Struct. (THEOCHEM)* **1991**, *236*, 269-282.
17. Glover, S. A.; Scott, A. P. *Tetrahedron* **1989**, *45*, 1763-1776.
18. Li, Y.; Abramovitch, R. A.; Houk, K. N. *J. Org. Chem.* **1989**, *54*, 2911-2914.
19. Cramer, C. J.; Dulles, F. J.; Falvey, D. E. *J. Am. Chem. Soc.* **1994**, *116*, 9787-9788.
20. Srivastava, S.; Falvey, D. E. *J. Am. Chem. Soc.* **1995**, *117*, 10186-10193.
21. Okamoto, T.; Shudo, K.; Ohta, T. *J. Am. Chem. Soc.* **1975**, *97*, 7184-7185.
22. Sone, T.; Tokudo, T.; Sakai, T.; Shinkai, S.; Manabe, O. *J. Chem. Soc., Perkin Trans II*, **1981**, 298-302.
23. Sone, T.; Hamamoto, K.; Seiji, Y.; Shinkai, S.; Manabe, O. *J. Chem. Soc., Perkin Trans II*, **1981**, 1596-1598.
24. Gassman, P. G.; Campbell, G. A.; Frederick, R. C. *J. Am. Chem. Soc.* **1972**, *94*, 3884-3890.
25. Gassman, P. G.; Campell, G. A. *J. Am. Chem. Soc.* **1972**, *94*, 3891-3896.
26. Takeuchi, H.; Takano, K.; Koyoma, K. *J. Chem. Soc., Chem. Commun.* **1982**, 1254-1256.
27. Takeuchi, H.; Koyoma, K. *J. Chem. Soc., Perkin Trans. I* **1982**, 1269-1273.

28. Takeuchi, H.; Ihara, R. *J. Chem. Soc., Chem. Commun.* **1983**, 175-177.
29. Takeuchi, H.; Takano, K. *J. Chem. Soc., Chem. Commun.* **1983**, 447-449.
30. Abramovitch, R. A.; Hawi, A.; Rodrigues, J. A. R.; Trombetta, T. R. *J. Chem. Soc., Chem. Commun.* **1986**, 283-284.
31. Takeuchi, H.; Hirayama, S.; Mitani, M.; Koyoma, K. *J. Chem. Soc., Perkin Trans. I* **1988**, 521-527.
32. Fishbein, J. C.; McClelland, R. A. *J. Am Chem. Soc.* **1987**, *109*, 2824-2825.
Bolton, J. L.; McClelland, R. A. *J. Am Chem. Soc.* **1989**, *111*, 8172-8181.
33. Novak, M.; Kahley, M. J.; Eiger, E.; Helmick, J. S.; Peters, H. E. *J. Am Chem. Soc.* **1993**, *115*, 9453-9460.
34. Miller, J. A. *Cancer Res.* **1970**, *30*, 559.
35. Frederick, C. B.; Mays, J. B.; Ziegler, D. M.; Guengerich, F. P.; Kadlubar, F. F. *Cancer Res.* **1982**, *42*, 2671.
36. Debaun, J. R.; Miller, E. C.; and Miller, J. A. *Cancer Res.* **1970**, *30*, 577-595.
37. Lotlikar, P. D.; Scribner, J. D.; Miller, J. A.; Miller, E. C. *Life Sci.* **1966**, *5*, 1263-1269.
38. Miller, J. A.; Miller, E. C. *Progr. Exptl. Tumor Res.* **1969**, *11*, 273-301.
39. Beland, F. A.; Kadlubar, F. F. In *Carcinogenesis and Mutagenesis*, Handbook of Experimental Pathology, Cooper, C. S. & Grover, P. L., Ed.; Springer; Heidelberg; **1990**, Vol. 94/I, pp267-325.
40. Famulok, M.; Boche, G. *Angew. Chem. Int. Ed. Engl.* **1989**, *28*, 468-469.
41. Novak, M.; Martin, K. A.; Heinrich, J. L. *J. Org. Chem.* **1989**, *54*, 5430-5431.

42. Scribner, J. D.; Miller, J. A.; Miller, E. C. *Cancer Res.* **1970**, *30*, 1570-1579.
43. Underwood, G. A.; Kirsch, R. B. *J. Chem. Soc., Chem. Comm.* **1985**, 136-138.
44. Underwood, G. A.; Price, M. F.; Shapiro, R. *Carcinogenesis* **1988**, *9*, 1817-1821.
45. Gassman, P. G.; Granrud, J. E. *J. Am. Chem. Soc.* **1984**, *106*, 1498-1499.
46. Novak, M.; Pelecanou, M.; Roy, A. K.; Andronico, A. F.; Plourde, F. M.; Olefirowicz, T. M.; Curtin, T. J. *J. Am. Chem. Soc.* **1984**, *106*, 5623-5631.
47. Fishbein, J. C.; McClelland, R. A. *J. Chem. Comm., Perkin Trans. 2* **1995**, 663-671.
48. Novak, M.; Kahley, M. J.; Lin, J.; Kennedy, S. A.; James, T. G. *J. Org. Chem.* **1995**, *60*, 8294-8304.
49. Panda, M.; Novak, M.; Magonski, J. *J. Am. Chem. Soc.* **1989**, *111*, 4524-4525.
50. Novak, M.; Kennedy, S. A. *J. Am. Chem. Soc.* **1995**, *117*, 574-575.
51. Davidse, P. A.; Kahley, M. J.; McClelland, R. A.; Novak, M. *J. Am. Chem. Soc.* **1994**, *116*, 4513-4514.
52. Olah, G.; Surya Prakash, G. K.; Arvanaghi, M. *J. Am. Chem. Soc.* **1980**, *102*, 6640-6641.
53. Olah, G. A.; Donovan, D. J. *J. Org. Chem.* **1978**, *43*, 1743-1750.
54. Svanholm, U.; Parker, V. D. *J. Am. Chem. Soc.* **1974**, *96*, 1234-1236.
55. Serve, D. *J. Am. Chem. Soc.* **1975**, *97*, 432-434.
56. Riecker, A.; Reiser, B. *Tetrahedron Lett.* **1990**, *31*, 5013.
57. McClelland, R. A. *Tetrahedron*, **1996**, *52*, 6823-6858.

58. McClelland, R. A.; Kahley, M. J.; Davidse, P. A. *J. Phys. Org. Chem.* **1996**, *9*, 355-360.
59. Anderson, G. B.; Falvey, D. E. *J. Am Chem. Soc.* **1993**, *115*, 9870-9871.
60. Robbins, R. J.; Yang, L. L.-N.; Anderson, G. B.; Falvey, D. E. *J. Am Chem. Soc.* **1995**, *117*, 6544-6552.
61. McClelland, R. A.; Davidse, P. A.; Hadzialic, G. *J. Am Chem. Soc.* **1995**, *117*, 4173-4174.
62. Novak, M.; Kahley, M. J.; Lin, J.; Kennedy, S. A.; Swanegan, L. A. *J. Am. Chem. Soc.* **1994**, *116*, 11626-11627.
63. Richard, J. P.; Jencks, W. P. *J. Am. Chem. Soc.* **1982**, *104*, 4689.
64. Richard, J. P.; Rothenberg, M. E.; Jencks, W. P. *J. Am. Chem. Soc.* **1984**, *106*, 1361.
65. Richard, J. P.; Lin, S. S.; Buccigros, J. M.; Amyes, T. L. *J. Am. Chem. Soc.* **1996**, *117*, 12603.
66. McClelland, R. A.; Kahley, M. J., unpublished results.
67. Mayr, H.; Patz, M. *Angew. Chem. Int. Ed. Engl.* **1994**, *33*, 938-957. Bartl, J.; Steenken, S.; Mayr, H. *J. Am. Chem. Soc.* **1991**, *113*, 7710-7716.
68. Mayr, H. *Angew. Chem., Int. Ed. Engl.* **1990**, *29*, 1371-1384.
69. Sukhai, P.; McClelland, R. A. *J. Chem. Soc., Perkin Trans. 2* **1996**, 1529-1530.
70. McClelland, R. A.; Cozens, F. L.; Steenken, S.; Amyes, T. L.; Richard, J. P. *J. Chem. Soc., Perkin Trans. 2*, **1993**, 1717.

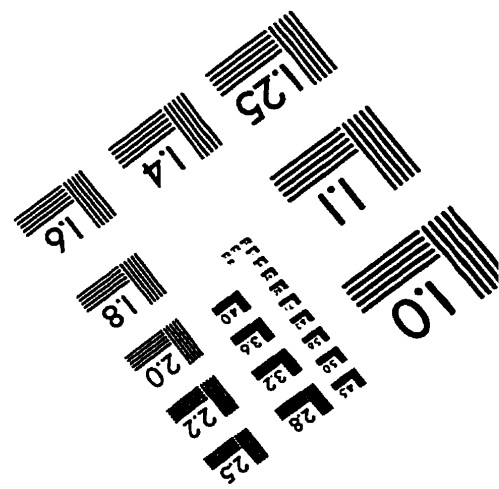
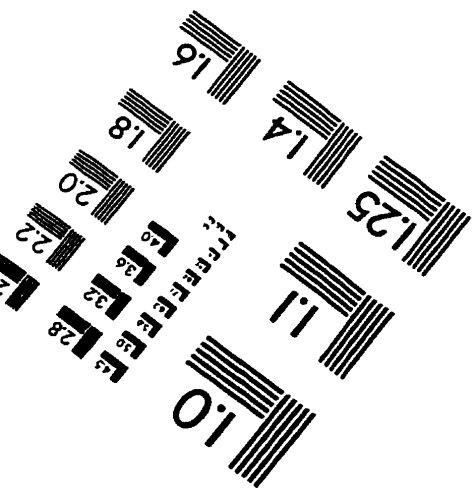
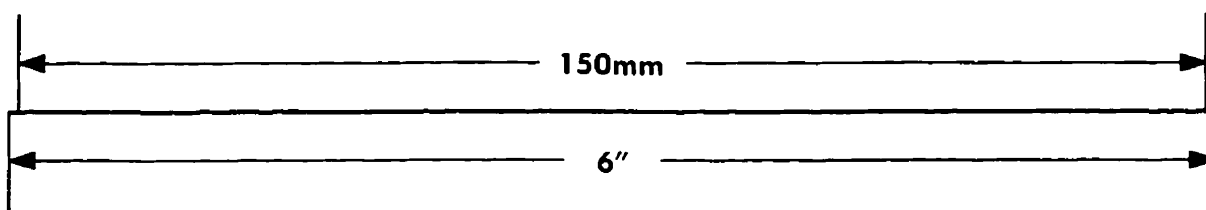
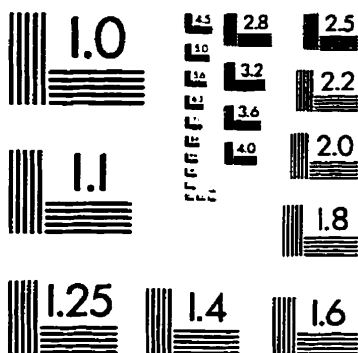
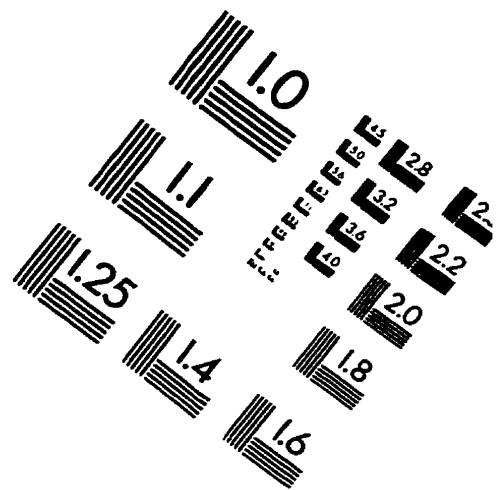
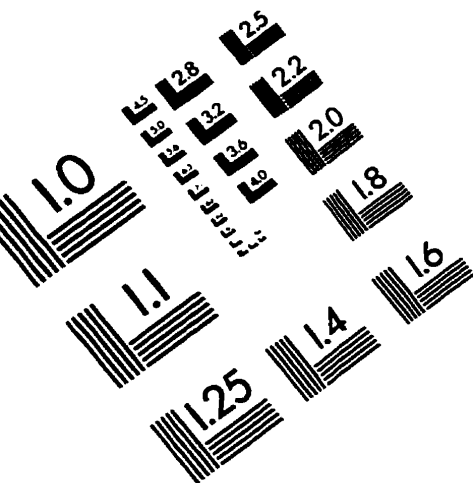
71. Manthivanan, N.; Cozens, F.; McClelland, R. A.; Steenken, S. *J. Am. Chem. Soc.* **1992**, *114*, 2198.
72. McClelland, R. A.; Kahley, M. J.; Davidse, P. A.; Hadzialic, G. *J. Am. Chem. Soc.* **1996**, *118*, 4794-4803.
73. Kashin, A. N.; Bumagina, I. G.; Bumagin, N. A.; Beletshaya, I. B. *Zh. Org. Khim.* **1981**, *17*, 21.
74. Echavarren, A. M.; Stille, J. K. *J. Am. Chem. Soc.* **1987**, *109*, 5478-5486.
75. Negishi, E.; King, A. O.; Okukado, N. *J. Org. Chem.* **1977**, 1821-1823.
76. Miyaura, N.; Yanagi, T.; Suzuki, A. *Synth. Commun.* **1981**, *11*, 513-519.
77. Miller, R. B.; Dugar, S. *Organometallics* **1984**, *3*, 1261-1263.
78. Washburn, R. M.; Levens, E.; Albright, C. F.; Billig, F. A.; Cernak, E. S. *Adv. Chem. Ser.* **1959**, *No. 23*, 102.
79. Hawkins, R. T.; Lennarz, W. J.; Snyder, H. R. *J. Am. Chem. Soc.* **1960**, *82*, 3053-3058.
80. Smith, P. S.; Brown, B. B. *J. Am. Chem. Soc.* **1951**, *73*, 2438-2441.
81. Gurst, J. E. In *The Chemistry of the Azido Group*, Patai, S., Ed.; Interscience Publishers; **1971**, pp199-200.
82. Schuster, G. B.; Platz, M. S. *Adv. Photochem.* **1992**, *17*, 143.
83. Bartl, J.; Steenken, S.; Mayr, H.; McClelland, R. A. *J. Am. Chem. Soc.* **1990**, *112*, 6918.
84. McClelland, R. A.; Chan, C.; Cozens, F.; Modro, A.; Steenken, S. *Angew. Chem., Int. Ed. Eng.* **1991**, *30*, 1337.

85. McClelland, R. A.; Kanagasabapathy, V. M.; Banait, N. S.; Steenken, S. J. *Am. Chem. Soc.* **1989**, *111*, 3966-3972.
86. Cozens, F. L.; Mathivanan, N.; McClelland, R. A.; Steenken, S. J. *Chem. Soc., Perkin Trans. 2*, **1992**, 2083.
87. Yukawa, Y.; Tsuno, Y.; Sawada, M. *Bull. Chem. Soc. Jpn.* **1966**, *39*, 2274.
88. Brown, H. C.; Kelly, D. P.; Periasamy, M. *Proc. Natl. Acad. Sci. U.S.A.* **77**, *1980*, 6956-6960.
89. McClelland, R. A.; Kanagasabapathy, V. M.; Banait, N. S.; Steenken, S. J. *Am. Chem. Soc.* **1991**, *113*, 1009-1014.
90. McClelland, R. A.; Kanagasabapathy, V. M.; Banait, N. S.; Steenken, S. J. *Am. Chem. Soc.* **1988**, *110*, 6913-6914.
91. Alonso, E. O.; Johnston, L. J.; Scaiano, J. S.; Toscano, V. G. *J. Am. Chem. Soc.* **1990**, *112*, 1270-1271.
92. Humphreys, W. R.; Kadlubar, F. F.; Guengerich, F. P. *Proc. Natl. Acad. Sci. USA*, **1992**, *89*, 8278-8282.
93. Kennedy, S. A.; Novak, M.; Kolb, B. A. *J. Am. Chem. Soc.* **1997**, *119*, 7654-7664.
94. Wild, D.; Dirr, A. *Carcinogenesis*, **1988**, *9*, 869-871.
95. Wild, D.; Dirr, A.; Fasshaur, I.; Henschler, D. *Carcinogenesis*, **1989**, *10*, 335-341.
96. Wild, D.; Dirr, A. *Mutagenesis*, **1989**, *4*, 446-452.
97. Wild, D. *Environ. Health Perspect.* **1990**, *88*, 27-31.
98. Sabbioni, G.; Wild, D. *Carcinogenesis*, **1992**, *13*, 709-713.

99. Buhle, J. D. *J. Org. Chem.* **1973**, *38*, 904-906.
100. Zimmerman, H. E.; Hackett, P.; Juers, D. J.; McCall, J. M.; Schroder, B. *J. Am. Chem.* **1971**, *93*, 3653-3661.
101. McClelland, R. A.; Banait, N.; Steenken, S. *J. Am. Chem. Soc.* **1986**, *108*, 7023-7027.
102. McClelland, R. A.; Ren, D.; Ghobrial, D; Gadosy, T. A. *J. Chem. Soc., Perkin Trans. 2*, **1997**, 451-456.
103. Bunton, C. A.; Mhala, M. M.; Moffat, J. R. *J. Org. Chem.* **1984**, *49*, 3637-3639.
104. McClelland, R. A.; Banait N; Steenken, S. *J. Am. Chem. Soc.* **1989**, *111*, 2929-2935.
105. Mecklenberg, S. L.; Hilinski, E. F. *J. Am. Chem. Soc.* **1989**, *111*, 5471.
106. Cozens, F. L.; Li, J.; McClelland, R. A.; Steenken, S. *Angew. Chem., Int. Ed. Engl.* **1992**, *31*, 743.
107. McClelland, R. A.; Cozens, F. L.; Li, J.; Steenken, S. *J. Chem. Soc., Perkin Trans 2*, **1996**, 1531-1543.
108. Li, J. Ph. D. Thesis, University of Toronto, **1994**.
109. Wan, P.; Krogh, E. *J. Am. Chem. Soc.* **1989**, *111*, 4877.
110. Wan, P.; Krogh, E. Ckak, B. *J. Am. Chem. Soc.* **1988**, *110*, 4073.
111. Turro, N. J.; Wan, P. *J. Photochem.* **1985**, *28*, 93-103.
112. Zimmerman, H. E.; Sandel, V. R. *J. Am. Chem. Soc.* **1963**, *85*, 915-922.
113. Zimmerman, H. E. *J. Am. Chem. Soc.* **1995**, *117*, 8988-8991.

114. O'Neil, P; Steenken, S.; Schulte-Frohlinde, D. *J. Phys. Chem.* **1975**, *79*, 2773.
115. Fishbein, J. C.; McClelland, R. A. *Can. J. Chem.* **1996**, *74*, 1321, and references therein.
116. Hartwell, J. L. *Organic Syntheses Coll. Vol. III*, 185.

IMAGE EVALUATION TEST TARGET (QA-3)



APPLIED IMAGE . Inc
1653 East Main Street
Rochester, NY 14609 USA
Phone: 716/482-0300
Fax: 716/288-5989

© 1993, Applied Image, Inc., All Rights Reserved